Technische Universität München
School of Life Sciences
Lehrstuhl für Grünlandlehre

The transfer of the ^{18}O signal from meteoric water to cellulose in a grassland ecosystem – an evaluation with a process-based model

Regina Theresia Hirl

Vollständiger Abdruck der von der promotionsführenden Einrichtung TUM School of Life Sciences der Technischen Universität München zur Erlangung des akademischen Grades eines

Doktors der Naturwissenschaften

genehmigten Dissertation.

Vorsitzender:		Prof. Dr. Dr. h.c. Hans Pretzsch
Prüfer der Dissertation:	1.	Prof. Dr. Johannes Schnyder
	2.	Prof. Dr. Anja Rammig

Die Dissertation wurde am 29.01.2021 bei der Technischen Universität München eingereicht und durch die promotionsführende Einrichtung TUM School of Life Sciences am 05.05.2021 angenommen.

Summary

Aims. The stable oxygen isotope composition of cellulose ($\delta^{18}O_{cellulose}$) integrates important physiological and environmental information that can aid to understand better the response of plant water use efficiency to climate change. As yet, limited knowledge of the drivers of the isotopic composition of leaf water and cellulose in crop and grassland vegetation has restricted our ability to predict and interpret $\delta^{18}O_{cellulose}$. The aim of this work was to evaluate current theories in their ability to explain how physiological traits and climate variability drive variation of the $\delta^{18}O$ of all relevant water pools in a grassland ecosystem and of cellulose in leaf samples. Specifically, the objective was to establish a comprehensive modelling framework for predicting isotopic signals in a grassland ecosystem.

Materials and Methods. The physically-based ^{18}O-enabled soil-vegetation-atmosphere transfer model MuSICA was parameterised for a drought-prone grazed grassland ecosystem. Model predictions of ecosystem $\delta^{18}O$ signals in soil, source and leaf water pools ($\delta^{18}O_{soil}$, $\delta^{18}O_{source}$ and $\delta^{18}O_{leaf}$), and the ^{18}O enrichment of leaf water above source water ($\Delta^{18}O_{leaf}$), were compared with fortnightly observations made throughout seven consecutive growing seasons (2006–2012). For predicting $\delta^{18}O_{cellulose}$, a new allocation-and-growth-model was developed and added to MuSICA to predict, in an assimilation- and allocation-weighted fashion, the incorporation of photo-assimilates into leaf cellulose, and the associated $\delta^{18}O_{cellulose}$ signal and its enrichment above source water ($\Delta^{18}O_{cellulose}$). Model predictions of carbon dynamics (metabolic pool turnover, shoot/root allocation) were validated with results from ^{13}C-tracer-based studies at the same pasture site.

Results and Discussion. The model produced realistic $\delta^{18}O$ variations of the water pools, suggesting that it captured well the various ecohydrological features (including soil water content and root water uptake dynamics) of the grassland ecosystem. Observed isotope data of soil and source water and model predictions indicated that root water uptake relied mainly on shallow soil water (top 20 cm), irrespective of the water status of the topsoil. $\Delta^{18}O_{leaf}$ was affected by both soil water content and air relative humidity, and model simulations indicated that the effect of dry soil was mediated by drought-induced stomatal closure. Cellulose ^{18}O signals were simulated based on the predictions of $\delta^{18}O_{source}$ and $\delta^{18}O_{leaf}$, and using the new allocation-and-growth model. Model predictions of $\delta^{18}O_{cellulose}$ and $\Delta^{18}O_{cellulose}$ agreed well with the observed data. The observed relationship between $\Delta^{18}O_{cellulose}$ and relative humidity, air temperature and canopy conductance was only reproduced by the model if the attenuation factor ($p_{ex}\,p_x$) was related to relative humidity and if biochemical fractionation (ε_{bio}) was assumed temperature-sensitive. Canopy conductance was negatively related to $\Delta^{18}O_{cellulose}$ and $\delta^{18}O_{cellulose}$. To verify coherence in the model's predictions, the same model was subsequently applied to predict the hydrogen isotope composition ($\delta^{2}H$) of the water pools of the studied grassland and the carbon isotope photosynthetic discrimination inferred from leaf cellulose ($\Delta^{13}C_{cellulose}$). The extra constraint brought about by $\Delta^{13}C_{cellulose}$ data strongly suggested seasonal changes in stomatal conductance and photosynthetic parameters, that had little ef-

fect on the predicted $\Delta^{18}O_{cellulose}$. Finally, the model was successfully tested for its ability to predict decadal-scale variation in $\delta^{18}O_{cellulose}$ in aboveground biomass samples from the Park Grass Experiment.

Conclusions. This work highlights the usefulness of mechanistic ^{18}O-enabled modelling for explorations and quantitative analyses of the ecohydrology of ecosystems. The relation between canopy conductance and cellulose-^{18}O underlines the value of $\delta^{18}O_{cellulose}$ to understand climate change-induced alterations in water-use efficiency of grassland, which eventually may allow us to make predictions on future behaviour of grassland vegetation. The revealed gaps in present-day mechanistic understanding of the link between leaf water and cellulose ^{18}O signals, specifically the mechanisms underlying the temperature-sensitivity of ε_{bio} and the humidity-sensitivity of $p_{ex}\, p_x$, should guide future theoretical and experimental studies.

Zusammenfassung

Zielsetzung. Die stabile Sauerstoffisotopensignatur der Cellulose ($\delta^{18}O_{cellulose}$) enthält bedeutende Informationen über die pflanzliche Physiologie und die Umwelt und kann damit zu einem besseren Verständnis der Reaktion der Wassernutzungseffizienz auf den Klimawandel beitragen. Die Vorhersage und Interpretation von $\delta^{18}O_{cellulose}$ wurde bislang durch das begrenzte Verständnis der Faktoren, welche einen Einfluss auf die Isotopensignaturen von Blattwasser und Cellulose in Feldfrüchten und in Graslandvegetation ausüben, erschwert. Ziel dieser Arbeit war es, zu bewerten, inwiefern anhand der gegenwärtigen Theorie der Einfluss physiologischer Merkmale und klimatischer Variation auf die Variation der Sauerstoffisotopensignaturen in allen relevanten Wasserkompartimenten eines Graslandökosystems sowie in Blatt-Cellulose erklärt werden kann. Ein Ziel war insbesondere, einen umfassenden Modellierungsansatz für die Prognose von Isotopensignaturen im Grasland zu erstellen.

Material und Methoden. Das physikalisch basierte ^{18}O-befähigte Boden-Pflanze-Atmosphäre Modell MuSICA wurde für ein trockenheitsanfälliges beweidetes Graslandökosystem parametrisiert. Die Modellprognosen der $\delta^{18}O$-Signaturen in den Wasserkompartimenten des Ökosystems, nämlich im Bodenwasser, im aufgenommenen Wasser und im Blattwasser ($\delta^{18}O_{soil}$, $\delta^{18}O_{source}$ and $\delta^{18}O_{leaf}$), und in der ^{18}O-Anreicherung des Blattwassers über dem aufgenommenen Wasser ($\Delta^{18}O_{leaf}$), wurden mit beobachteten ^{18}O-Daten verglichen. Die zugrunde liegenden Proben wurden etwa alle zwei Wochen in sieben aufeinanderfolgenden Vegetationsperioden (Jahre 2006 bis 2012) genommen. Um die $\delta^{18}O$-Signatur der Cellulose zu prognostizieren, wurde ein neues Allokations- und Wachstumsmodell entwickelt und zum MuSICA-Modell hinzugefügt. Mit dem kombinierten Modell wurden der assimilations- und allokationsgewichtete Einbau der Photo-Assimilate in die Cellulose der Blätter, das assoziierte Isotopensignal ($\delta^{18}O_{cellulose}$) sowie die Anreicherung der Cellulose gegenüber dem aufgenommenen Wasser ($\Delta^{18}O_{cellulose}$) prognostiziert. Modellprognosen der Kohlenstoffdynamik (Turnover des metabolischen Pools, Spross-Wurzel-Allokation) wurden mit Ergebnissen von ^{13}C-Tracer-basierten Studien auf derselben Weide validiert.

Ergebnisse und Diskussion. Die Variation der $\delta^{18}O$-Signaturen in den Wasserkompartimenten wurde durch das Modell realitätsnah wiedergegeben, was darauf schließen ließ, dass es die verschiedenen ökohydrologischen Eigenschaften des Graslandökosystems (einschließlich der Bodenwassergehalte und der Dynamik der Wasseraufnahme durch die Wurzeln) gut erfasste. Die beobachteten Isotopendaten des Bodenwassers und des aufgenommenen Wassers sowie die Modellprognosen zeigten, dass die Wasseraufnahme durch die Wurzeln vor allem aus der obersten Bodenschicht (d.h. aus den obersten 20 cm) erfolgte, unabhängig von deren Wassergehalt. Sowohl der Bodenwassergehalt als auch die relative Luftfeuchte beeinflussten $\Delta^{18}O_{leaf}$. Die Modellsimulationen indizierten, dass der Effekt der Bodentrockenheit mit trockenheitsinduziertem Stomataschluss in Verbindung stand. Die ^{18}O-Signale der Cellulose wurden mit dem neuen Allokations- und Wachstumsmodell und basierend auf den Prognosen von $\delta^{18}O_{source}$ und $\delta^{18}O_{leaf}$ simuliert. Die Modellprognosen von $\delta^{18}O_{cellulose}$ und $\Delta^{18}O_{cellulose}$ stimmten gut

mit den beobachteten Daten überein. Der beobachtete Zusammenhang zwischen $\Delta^{18}O_{cellulose}$ und relativer Luftfeuchte, Lufttemperatur und Bestandesleitfähigkeit wurde durch das Modell nur wiedergegeben, wenn der Modellierung ein feuchteabhängiger 'attenuation factor' ($p_{ex}\, p_x$) und eine temperaturabhängige biochemische Fraktionierung (ε_{bio}) zugrunde gelegt wurden. Die Bestandesleitfähigkeit korrelierte negativ mit $\Delta^{18}O_{cellulose}$ und $\delta^{18}O_{cellulose}$. Um die Kohärenz in den Modellprognosen zu verifizieren, wurde das Modell – in seiner Parametrisierung für $\delta^{18}O$ – verwendet, um die Wasserstoffisotopensignaturen ($\delta^{2}H$) der Wasserkompartimente des gleichen Standorts sowie die photosynthetische Kohlenstoffisotopendiskriminierung, abgeleitet aus der ^{13}C-Diskriminierung der Blattcellulose ($\Delta^{13}C_{cellulose}$), zu prognostizieren. Die zusätzliche Information aus der ^{13}C-Diskriminierung wies deutlich auf eine saisonale Änderung der Parameter der stomatären Leitfähigkeit und der Photosynthese hin, welche sich kaum auf die prognostizierte Cellulose-^{18}O-Anreicherung auswirkte. Schließlich wurde das Modell erfolgreich auf seine Befähigung getestet, die $\delta^{18}O_{cellulose}$-Variation in oberirdischer Biomasse des Park Grass Experiments wiederzugeben.

Schlussfolgerungen. In der vorliegenden Arbeit wurde aufgezeigt, wie ein mechanistisches ^{18}O-befähigtes Modell beitragen kann, die Ökohydrologie eines Ökosystems zu untersuchen und quantitativ zu analysieren. Die Beziehung zwischen Bestandesleitfähigkeit und Cellulose-^{18}O betont den Wert von $\delta^{18}O_{cellulose}$ für das Verständnis der durch den Klimawandel hervorgerufenen Änderungen in der Wassernutzungseffizienz von Grasland. Dieses Verständnis kann schließlich Vorhersagen über künftige Reaktionen von Graslandvegetation ermöglichen. Die aufgezeigten Lücken im aktuellen mechanistischen Verständnis des Zusammenhangs zwischen Blattwasser-^{18}O und Cellulose-^{18}O, insbesondere die Mechanismen, welche der Temperaturabhängigkeit von ε_{bio} und der Feuchteabhängigkeit von $p_{ex}\, p_x$ zugrunde liegen, dürften zukünftige theoretische und experimentelle Studien leiten können.

Contents

List of Figures

List of Tables

1. General Introduction

Rising atmospheric CO_2 concentrations throughout the past 250 years have provoked tremendous changes in the global climate system, with multiple feedbacks and amplifying effects among meteorological parameters that bring about climate and weather conditions (IPCC, 2013). Terrestrial vegetation and climate are strongly linked and interact dynamically in shaping the water and carbon cycle of ecosystems. Transpiration is thought to represent a large part of the total land-atmosphere evapotranspiration (e.g. Jasechko *et al.*, 2013; Good *et al.*, 2015b; Lian *et al.*, 2018), and hence terrestrial vegetation plays a key role in determining water fluxes. Water and carbon dynamics may not only be altered by changing climate, but also by morpho-physiological adaptations of plants to those changes (e.g. Poorter & Navas, 2003; Ainsworth & Long, 2005; Ainsworth & Rogers, 2007; Kimball, 2016). Plants that are exposed to elevated CO_2 often show higher net assimilation rates (A_n), lower stomatal conductance (g_s) (e.g. Ainsworth & Rogers, 2007; Leakey *et al.*, 2009), and hence higher intrinsic water-use efficiency (iWUE), which denotes the ratio of A_n to g_s (Ehleringer *et al.*, 1993). As monitoring of CO_2 and H_2O exchange in the soil-vegetation-atmosphere system has only started in recent decades, retrospective analyses that aimed to understand plants' responses to climate change have relied on plant-based proxies, such as the stable isotope composition in archived biomass. The oxygen, hydrogen and carbon isotope composition ($\delta^{18}O$, $\delta^{2}H$ and $\delta^{13}C$) in biological archives store a record of environmental conditions and changes, as well as of plant responses to environmental changes. Analysis of $\delta^{13}C$ in archived hay samples of the Rothamsted Park Grass Experiment (England) and in *Capra ibex* horns from Switzerland suggested that iWUE in temperate and alpine grasslands increased throughout the past decade, indicating that assimilation rates may have increased and/or that stomatal conductance may have decreased (Köhler *et al.*, 2010, 2012, 2016; Barbosa *et al.*, 2010). Increases in iWUE have also been reported for other taxa such as gymnosperm and angiosperm trees (e.g. Duquesnay *et al.*, 1998; Saurer *et al.*, 2004, 2014; Adams *et al.*, 2020). The $\delta^{18}O$ composition of plant cellulose or biomass has received considerable attention as it may complement the information derived from the $\delta^{13}C$ composition of plant biomass or cellulose. In particular, researchers have attempted to use $\delta^{18}O$ to constrain the interpretation of the $\delta^{13}C$ signal with regard to changes in stomatal conductance and/or assimilation rate (e.g. Scheidegger *et al.*, 2000; Grams *et al.*, 2007; Roden & Farquhar, 2012). Thus, $\delta^{18}O$ may help discern the cause(s) of observed changes in intrinsic water-use. Our incomplete understanding of the physiological mechanisms that have provoked the increase in iWUE in temperate grassland was one main starting point for the present work, which focused on enlarging our process-based knowledge of the formation of the stable oxygen isotope composition of cellulose ($\delta^{18}O_{cellulose}$) in grassland vegetation. In essence, cellulose extracted from plant biomass integrates the isotopic information recorded in source and leaf water; yet, our mechanistic understanding of the formation of $\delta^{18}O_{cellulose}$ is strongly limited. In particular, I investigated the $\delta^{18}O$ signal transfer from meteoric water through soil water, stem water and leaf water to $\delta^{18}O_{cellulose}$ in a temperate grassland ecosystem by making use of a process-based soil-vegetation-atmosphere transfer model. The current state of knowledge of the mechanisms operating along this process chain is presented in the following.

1.1 Isotopic imprint of meteoric water onto the soil water pool

Variation in isotopic abundances arises from fractionation against the heavy isotope in equilibrium reactions (α^+, equilibrium fractionation factor) and during diffusion (α_k, kinetic fractionation factor) (Mook, 2000). Molecules containing the light isotope ^{16}O (i.e. the light isotopologue $H_2{}^{16}O$) evaporate more easily and diffuse faster than the heavy isotopologue $H_2{}^{18}O$. Depending on the relative importance of the two fractionation factors, terrestrial and atmospheric water pools are either enriched or depleted in ^{18}O relative to oceanic water (Fig. 1.1a). The $^{18}O/^{16}O$ ratio of a sample (R_{sample}) is usually expressed as the ‰ deviation relative to the $^{18}O/^{16}O$ ratio of the V-SMOW (Vienna Standard Mean Ocean Water) standard ($R_{standard}$):

$$\delta^{18}O = R_{sample}/R_{standard} - 1 \quad (1.1)$$

The isotopic composition of precipitation (hereafter termed $\delta^{18}O_{rain}$) differs considerably between geographical locations (as characterised by latitude, continentality, altitude), seasons (Fig. 1.1a, b), and between heavy and light rains, with the differences largely governed by rainout and temperature effects (Dansgaard, 1964; Rozanski *et al.*, 1993; Gat, 1996; Araguás-Araguás *et al.*, 2000; Bowen *et al.*, 2019). During condensation and rain droplet formation, the heavy isotopologue preferentially passes into the liquid phase, leaving isotopically depleted water vapour behind. The temporal evolution of the isotopic composition of precipitation and vapour during continuous rainout is commonly described as a Rayleigh distillation process (Gat, 1996). Due to the lower vapour pressure of the heavier isotopologue $H_2{}^{18}O$, atmospheric vapour (with isotopic composition $\delta^{18}O_{vapour}$) is usually depleted compared to rain water. Under field conditions, water vapour is not always in equilibrium with precipitation (e.g. Fiorella *et al.*, 2019; Penchenat *et al.*, 2020), especially over vegetated surfaces (Lai *et al.*, 2008; Ueta *et al.*, 2013).

In principle, the isotopic fractionation theory outlined above also applies to deuterium (^2H), and the same standard is used for calculation of δ^2H values. Yet, equilibrium fractionation is higher and kinetic fractionation smaller for ^2H as compared to ^{18}O (Majoube, 1971; Luz *et al.*, 2009), leading to characteristic relations in the dual-isotope space (Fig. 1.1c). As this work mainly focused on the $\delta^{18}O$ signals in grassland, the following paragraphs are targeted to $\delta^{18}O$ and mention δ^2H only if relevant differences between the two isotopes are found.

During rainfall, meteoric water imparts its $\delta^{18}O$ to the soil water pool ($\delta^{18}O_{soil}$). The dynamics of infiltration, percolation and mixing of current precipitation with water stored in the soil depend on precipitation amount and intensity, on the physical properties of the soil as well as on the degree of water saturation prior to the precipitation event. In addition, vegetation exerts control on soil water dynamics and the spatio-temporal distribution of $\delta^{18}O_{soil}$ due to various effects: first, rain or snow interception on plant surfaces lead to a delayed water infiltration into the soil, and/or to a direct return of precipitation to the atmosphere via evaporation of intercepted water, which can make up almost 30 % of the total continental evapotranspiration (Good *et al.*, 2015b). Second, plants may direct infiltrating water towards their active root zones (Dubbert & Werner, 2019); and third, root water uptake and transpiration rates, as determined by canopy conductance, act upon the emptying and refilling dynamics of the soil

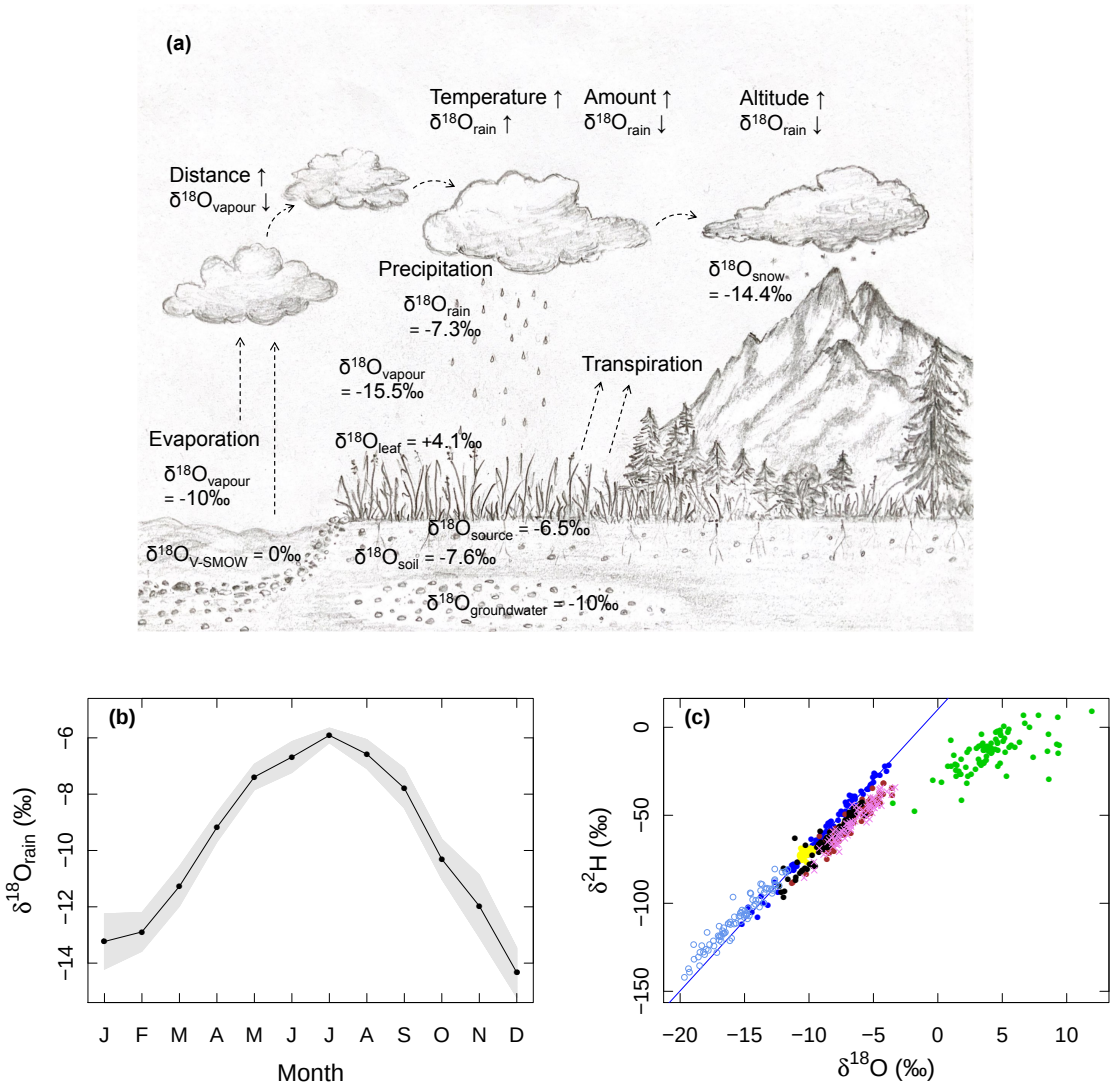

Figure 1.1: (a) δ^{18}O in the hydrological cycle, as determined by fractionation processes occurring along the path of water from the ocean to continental precipitation and terrestrial water pools. $\delta^{18}O_{vapour}$, $\delta^{18}O_{leaf}$, $\delta^{18}O_{source}$, $\delta^{18}O_{soil}$ and $\delta^{18}O_{groundwater}$ represent the average δ^{18}O values of atmospheric vapour, leaf water, pseudo-stem water, soil water (mean of soil water at 7 and 20 cm) and groundwater observed at pasture 8 of Grünschwaige Grassland Research Station during the growing seasons 2006–2012 (mid-April to end-October; see Hirl *et al.*, 2019). $\delta^{18}O_{rain}$ is the average amount-weighted δ^{18}O of precipitation as predicted by IsoGSM for the growing seasons 2006–2012, and $\delta^{18}O_{snow}$ is the average amount-weighted IsoGSM-predicted δ^{18}O for days with freezing temperature ($T_{air} < 0\,°C$) during November to mid-April 2006–2012. Both $\delta^{18}O_{rain}$ and $\delta^{18}O_{snow}$ were offset-corrected according to Hirl *et al.* (2019) (see panel (b)). (Drawing: Marianne Hirl) (b) Average seasonal cycle of $\delta^{18}O_{rain}$ at the study site, pasture no. 8 at Grünschwaige Grassland Research station, as predicted by the isotope-enabled nudged atmospheric general circulation model IsoGSM (Yoshimura *et al.*, 2011). Points and the grey band represent the mean and standard error for 2006 to 2012. The plotted data were corrected by the mean offset (1.3‰) between IsoGSM predictions and $\delta^{18}O_{rain}$ data observed at the study site (as in Hirl *et al.*, 2019, see their Figs. S2 and S3). (c) Dual isotope plot of rainwater (blue filled points), groundwater (yellow points), atmospheric water vapour (light blue open circles), soil water at 20 cm (black points) and 7 cm (brown points), stem water (pink crosses) and leaf water (green points), as observed at Grünschwaige during the study years 2006 to 2012. The blue line represents the global (and at the same time the local) meteoric water line: $\delta^2H = 8\,\delta^{18}O + 10‰$.

water pool and hence on the spatio-temporal distribution of $\delta^{18}O_{soil}$ (Brinkmann *et al.*, 2018; Hirl *et al.*, 2019).

The $\delta^{18}O$ of soil water is further altered due to soil evaporation, which often creates distinct isotopic profiles with high enrichment in the upper part and a decrease of $\delta^{18}O$ towards the lower part of the soil profile (e.g. Dubbert *et al.*, 2013). At dry sites, a characteristic local maximum $\delta^{18}O$ value is often found at the evaporation front, which marks the transition between the predominance of liquid water flux versus water vapour flux (Braud *et al.*, 2005a,b). Evaporative enrichment of soil water is usually less pronounced under vegetated surfaces than for bare soils (Dubbert *et al.*, 2013; Dubbert & Werner, 2019).

Apart from the vertical gradients in $\delta^{18}O_{soil}$ along the profile, there is indication now that pore-scale isotopic heterogeneity exists, which is related to isotopic depletion of water on organic surfaces (Chen *et al.*, 2016; Lin & Horita, 2016; Lin *et al.*, 2018). According to Chen *et al.* (2016), the 'surface effect' is much more pronounced for ^{2}H than for ^{18}O and for low soil water contents. That two different types of water may exist in, or pass through the soil-groundwater-streamwater-continuum has also been discussed in a slightly different context (called the "two water worlds" hypothesis): it was suggested that precipitation entering the soil may either be bound by the soil matrix and later supply plant water demand, or it may directly recharge groundwater and streams with little or no interaction with the soil-bound water (Brooks *et al.*, 2010; McDonnell, 2014). This limited 'hydrologic connectivity' between mobile and soil-bound water could explain isotopic differences between runoff and evapotranspiration at the global scale (Good *et al.*, 2015a).

In this work, 'soil water' is defined as the bulk water present in the soil at the time of sampling, as obtained by cryogenic vacuum distillation (see Hirl *et al.*, 2019). This is in line with the long-standing notion that water potential gradients between the soil and the atmosphere drive water uptake and transpiration, leaving little opportunity for roots to select between more mobile or less mobile water (Penna *et al.*, 2018).

1.2 Use of stable isotopes for determining plant water source

As pronounced isotopic gradients in $\delta^{18}O_{soil}$ from the top to the bottom of a soil profile are often found, comparison of $\delta^{18}O_{soil}$ with the $\delta^{18}O$ of water taken up by a plant (xylem water, termed $\delta^{18}O_{source}$ here) can give evidence on the depth of water uptake by plant roots (e.g. Kulmatiski *et al.*, 2006; Asbjornsen *et al.*, 2008; Moreno-Gutiérrez *et al.*, 2012; Rothfuss & Javaux, 2017). In grasses, unenriched water makes up the largest fraction of the water contained in the leaf growth and differentiation zone (LGDZ), the basal meristematic part of a vegetative grass tiller that is completely enclosed by the leaf sheaths of older leaves (Fig. 1.2; Kemp, 1980; Volenec & Nelson, 1981; Liu *et al.*, 2017a). The LGDZ and the older leaf sheaths together represent the pseudostem. LGDZ water was very close to source water in two C_3 and three C_4 grasses (Liu *et al.*, 2017a) and can thus be used for comparison with the $\delta^{18}O$ of soil water at different depths, to approximate the mean depth of root water uptake (see Hirl *et al.*, 2019). Furthermore, $\delta^{18}O_{source}$ can help differentiate between potential water sources such as soil water, stream

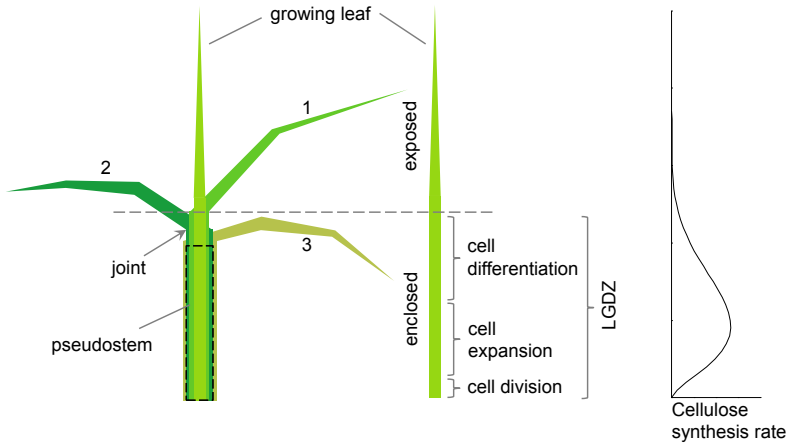

Figure 1.2: Scheme of a vegetative grass tiller (adapted from Liu *et al.*, 2017a). A vegetative tiller usually comprises three fully-expanded mature leaves, with leaf 1 the youngest and leaf 3 the oldest (senescing) leaf, plus one growing leaf. The joint marks the transition between leaf blade and leaf sheath. The pseudostem represents the basal part of the tiller and consists of the sheaths of the expanded leaves and the leaf growth and differentiation zone (LGDZ). The LGDZ comprises zones of cell division, expansion and differentiation, including cellulose synthesis and is completely enclosed inside the leaf sheaths of the next older leaf. The LGDZ is therefore not directly exposed to evaporative conditions in the surrounding air. Within a leaf, the tip of the leaf (blade) represents the oldest and the basal portion (of the sheath) the youngest part. The spatial distribution of the cellulose synthesis rate along the LGDZ is schematically displayed on the right (see Schnyder *et al.*, 1988; Maurice *et al.*, 1997; Schnyder *et al.*, 2000).

water and groundwater (e.g. Bowling *et al.*, 2017; Barbeta & Peñuelas, 2017). Both applications rely on the basic assumption that no fractionation against the heavy isotope occurs during root water uptake, which should at least be valid for oxygen (Walker & Richardson, 1991; Barnard *et al.*, 2006). Regarding hydrogen, isotopic offsets between xylem water and source (soil) water have been observed at xeric or halomorphic sites (Lin & Sternberg, 1993; Ellsworth & Williams, 2007), which has been interpreted as fractionation against the heavy isotope ^{2}H during root water uptake. Recent studies indicated that such isotopic offsets can also occur under well-watered and non-saline conditions (Liu *et al.*, 2017a; Vargas *et al.*, 2017; Barbeta *et al.*, 2020; von Freyberg *et al.*, 2020). Based on their results from a controlled experiment with *Fagus sylvatica* saplings, Barbeta *et al.* (2020) proposed that deuterium depletion of stem water relative to soil water might be the result of isotopically depleted water stored in non-conductive tissue of the stem rather than fractionation during water uptake. In that study, the differences between the $\delta^{18}O$ of soil and stem water were statistically not significant, indicating that in the presence of pronounced $\delta^{18}O$ gradients along the soil profile (see also Rothfuss & Javaux, 2017), comparison of $\delta^{18}O_{soil}$ and $\delta^{18}O_{source}$ should still allow for an identification of the zone of most active root water uptake and the temporal variation thereof. Furthermore, water storage in the pseudostem of grasses is very small compared to the amount of water possibly stored in non-conductive tissues of tree trunks.

Variation in root water uptake depth might be expected as a response to various factors, such as spatiotemporal variability of water and nutrient contents in the soil profile. Hitherto it was not clear whether edaphic drought arising from natural fluctuations of precipitation input and

transpiration systematically changes the depth of water uptake of C_3 grassland (Hirl *et al.*, 2019).

1.3 Leaf water enrichment

Leaves undergo an isotopic enrichment during transpiration, since the lighter isotopologues of water preferentially evaporate while the heavy isotopologues accumulate in the leaf (for a review see Cernusak *et al.*, 2016). The foundation for predicting leaf water ^{18}O enrichment was laid by (Craig & Gordon, 1965), who derived an equation for modelling the evaporative enrichment of a freely evaporating water body. The Craig-Gordon model was later adapted to leaves in order to predict the steady-state isotope ratio of water at the evaporative sites ($R_{e,ss}$) that line the stomatal cavities (Dongmann *et al.*, 1974; Flanagan *et al.*, 1991):

$$R_{e,ss} = \alpha^{+} \left(\alpha_{ks} R_{source} \frac{e_i - e_s}{e_i} + \alpha_{kb} R_{source} \frac{e_s - e_a}{e_i} + R_{vapour} \frac{e_a}{e_i} \right) \tag{1.2}$$

α^{+} is the equilibrium fractionation factor, and α_{ks} and α_{kb} denote the kinetic fractionation factors during water vapour diffusion through stomata and leaf boundary layer, respectively. R_{source} and R_{vapour} denote the isotope ratios of source (stem) water and atmospheric vapour, and e_i, e_s and e_a are the partial pressures of water vapour in the intercellular air space, at the leaf surface, and in the atmosphere. e_i is commonly assumed to correspond to saturation vapour pressure at leaf temperature; yet, recent findings indicate that this assumption may not always be valid (Cernusak *et al.*, 2018). As evident from Eqn 1.2, the isotopic enrichment at the evaporative site is determined by bidirectional water vapour exchange between the leaf and atmosphere, where the relative importance of the water vapour isotope ratio increases with increasing atmospheric relative humidity. While relative humidity is known to exert a strong control on leaf water enrichment, as yet only few studies have explored the role of edaphic drought (Yakir *et al.*, 1990a,b; Ferrio *et al.*, 2012; Hirl *et al.*, 2019).

In order to investigate and interpret the isotopic enrichment (or depletion) independently from variation in the source water signal, $R_{e,ss}$ and R_{vapour} are commonly expressed relative to R_{source}:

$$\Delta^{18}O_{sample} = \frac{R_{sample}}{R_{source}} - 1 = \frac{\delta^{18}O_{sample} - \delta^{18}O_{source}}{1 + \delta^{18}O_{source}} \tag{1.3}$$

where R_{sample} stands for $R_{e,ss}$, R_{leaf} (see below) or R_{vapour}. Thus, Eqn 1.2 becomes (Farquhar & Lloyd, 1993; Farquhar & Cernusak, 2005):

$$\Delta^{18}O_{e,ss} = \alpha^{+} \left(\alpha_k \left(1 - \frac{e_a}{e_i} \right) + \frac{e_a}{e_i} \left(\Delta^{18}O_{vapour} + 1 \right) \right) - 1 \tag{1.4}$$

α_k represents the weighted kinetic fractionation factor for the diffusion through stomata and boundary layer, with fractionations of 28‰ for molecular diffusion through stomates and 19‰ for laminar diffusion through the leaf boundary layer (Merlivat, 1978; Farquhar *et al.*, 2007):

$$\alpha_k = 1 + \frac{0.028\, g_s^{-1} + 0.019\, g_b^{-1}}{g_s^{-1} + g_b^{-1}} = 1 + \epsilon_k \tag{1.5}$$

where g_s and g_b are stomatal and boundary layer conductance to water vapour. The isotope fractionation factor during liquid-vapour equilibrium may be calculated from leaf temperature (T) according to Majoube (1971):

$$\alpha^+ = \exp\left(\frac{1137}{(273+T)^2} - \frac{0.4156}{273+T} - 0.0020667\right) = 1 + \epsilon^+ \tag{1.6}$$

Bulk leaf water ($\Delta^{18}O_{leaf}$) is often less enriched than Craig-Gordon predicted $\Delta^{18}O_{e,ss}$ (e.g. Yakir *et al.*, 1990a; Flanagan *et al.*, 1991; Lai *et al.*, 2008; Holloway-Phillips *et al.*, 2016; Hirl *et al.*, 2019). Two different concepts for explaining those observations are coexisting, namely the 'two-pool model' and the 'Péclet model'. The two-pool model assumes that water in veins and ground tissue is unenriched, while evaporatively enriched water resides mainly in mesophyll cells (Leaney *et al.*, 1985; Yakir *et al.*, 1994), yielding:

$$\Delta^{18}O_{leaf,ss} = (1-\varphi)\,\Delta^{18}O_{e,ss} \tag{1.7}$$

where $\Delta^{18}O_{leaf,ss}$ is the steady-state enrichment of bulk leaf water and φ denotes the proportion of unenriched water in bulk leaf water. In comparison, the Péclet model suggests that diffusion of enriched water from the evaporative sites to the xylem creates an exponential isotopic enrichment gradient in the leaf lamina, which is determined by the magnitude of the advective flux of source water relative to back diffusion (Farquhar & Lloyd, 1993). The leaf lamina Péclet model is given as (Farquhar & Lloyd, 1993; Farquhar *et al.*, 2007; Cuntz *et al.*, 2007):

$$\Delta^{18}O_{leaf,ss} = \Delta^{18}O_{e,ss}\,\frac{1-e^{-\wp}}{\wp} \tag{1.8}$$

with $\wp = EL/(CD)$ the Péclet number, E ($\mathrm{mol\,m^{-2}\,s^{-1}}$) leaf transpiration rate, L (m) the effective path length, $C = 55500\,\mathrm{mol\,m^{-3}}$ the molar density of liquid water, and D ($\mathrm{m^2\,s^{-1}}$) the diffusivity of $H_2{}^{18}O$ in liquid water (Farquhar & Lloyd, 1993; Cuntz *et al.*, 2007). The effective path length L is a fitted parameter that may be related to the pathway for water movement that predominates in the leaf under the specific environmental conditions (Barbour & Farquhar, 2004; Kahmen *et al.*, 2008; Song *et al.*, 2013; Barbour *et al.*, 2017). Farquhar & Gan (2003) extended the lamina Péclet model to account for separate Péclet effects in the xylem, veinlets and lamina mesophyll. While the Péclet model is conceptually realistic and supported by a range of observational datasets (e.g. Barbour *et al.*, 2000a, 2004; Ripullone *et al.*, 2008), various studies did not find evidence for a Péclet effect, suggesting that the use of the simpler two-pool model may be sufficient for predicting bulk leaf water enrichment (e.g. Roden *et al.*, 2015; Song *et al.*, 2015a; Hirl *et al.*, 2019). The principal difficulty with the regard to the evaluation of these models is that direct validation of the Craig-Gordon model would require micro-scale sampling and measurement of the thin water film that lines the stomatal cavity. Nevertheless, several researchers inferred the isotopic composition at the evaporative site by performing online measurements of transpiration and of the $\delta^{18}O$ of transpired vapour (e.g. Simonin *et al.*, 2013; Dubbert *et al.*, 2014; Song *et al.*, 2015b).

Under field conditions, a pronounced diurnal variation with maximum isotopic enrichment in the afternoon and minimum enrichment in the early morning is usually observed (Cernusak *et al.*, 2002, 2016; Lai *et al.*, 2008; Bögelein *et al.*, 2017; Hirl *et al.*, 2019). Steady-state

conditions are often not met due to dynamic variation of environmental conditions, meaning that the $\delta^{18}O$ of transpired vapour is not equal to $\delta^{18}O_{source}$ (e.g. Simonin *et al.*, 2013; Dubbert *et al.*, 2014). Non-steady state bulk leaf water enrichment ($\Delta^{18}O_{leaf}$) may be modelled as (Farquhar & Cernusak, 2005; Farquhar *et al.*, 2007):

$$\frac{\mathrm{d}(W\,\Delta^{18}O_{leaf})}{\mathrm{d}t} = -\frac{E}{\alpha_k\,\alpha^{+}\,(1-h)}\frac{\wp}{1-\mathrm{e}^{-\wp}}\left(\Delta^{18}O_{leaf} - \Delta^{18}O_{leaf,ss}\right) \tag{1.9}$$

where W ($\mathrm{mol\,m^{-2}}$) denotes leaf water content and the other parameters are defined as given above. Apart from those temporal dynamics, spatial variation in ^{18}O enrichment has been observed within single leaves. Enrichment was shown to increase from the base to the tip of grass leaf blades, the gradient being dependent on relative humidity (Helliker & Ehleringer, 2000, 2002a; Gan *et al.*, 2003; Ogée *et al.*, 2007). Also, small-scale spatial variation of leaf water, with a tendency to higher enrichment towards the edges was observed in dicot leaves (Wang & Yakir, 1995; Gan *et al.*, 2002; Šantrůček *et al.*, 2007; Gerlein-Safdi *et al.*, 2017). If combined with gradients in assimilation and sucrose synthesis rates, such spatial gradients of enrichment, and its dynamic response to external factors may lead to dynamic variation in the isotopic composition of sucrose exported from source leaves.

Of particular interest for plant physiological and paleoecological studies is the (theoretical) relationship between $\Delta^{18}O_{leaf}$ and stomatal conductance. Evaporative conditions (relative humidity or VPD) and other environmental factors (e.g. CO_2, irradiance, soil water status, O_3), as well as genetic and physiological properties act upon stomatal aperture and thereby affect leaf water evaporative enrichment: an increase in stomatal conductance 1) leads to a decrease in kinetic fractionation (ϵ_k; see Eqn 1.5), 2) increases transpiration, which decreases leaf temperature and increases the ratio of ambient to intercellular water vapour pressure (e_a/e_i) due to evaporative cooling, and 3) increases the Péclet number. Effects 1) to 3) all lead to a decrease of leaf water ^{18}O enrichment with increasing g_s (Eqns 1.2–1.8; Farquhar *et al.*, 2007). Although theoretically established, few studies have actually investigated a relation between leaf water ^{18}O enrichment (or the $\delta^{18}O$ of leaf water) and stomatal conductance (Pendall *et al.*, 2005, Ripullone *et al.*, 2008, Loucos *et al.*, 2015, Ellsworth *et al.*, 2017; see also Farquhar *et al.*, 2007). Thus, the relation between leaf water ^{18}O and g_s is actually not well characterized, and should depend strongly on the cause of variation in g_s. Once imprinted on leaf water enrichment, the stomatal conductance signal is expected to be transferred to photosynthates, phloem organic matter (Keitel *et al.*, 2003), and finally to cellulose.

1.4 $\delta^{18}O_{cellulose}$ – an integrator of assimilation and growth processes, and of environmental and ecohydrological dynamics

When cellulose is synthesized in the leaf growth and differentiation zone of grasses (see Fig. 1.2), in the meristematic tissue of growing dicot leaves, or in the cambium of trees, sucrose – the main transport sugar in plants (Lalonde *et al.*, 2003) and substrate for cellulose synthesis – is cleaved into hexose phosphates, allowing for isotopic exchange with water in the developing cell (see below; Barbour, 2007). Thus, the isotopic composition of cellulose ($\delta^{18}O_{cellulose}$) integrates

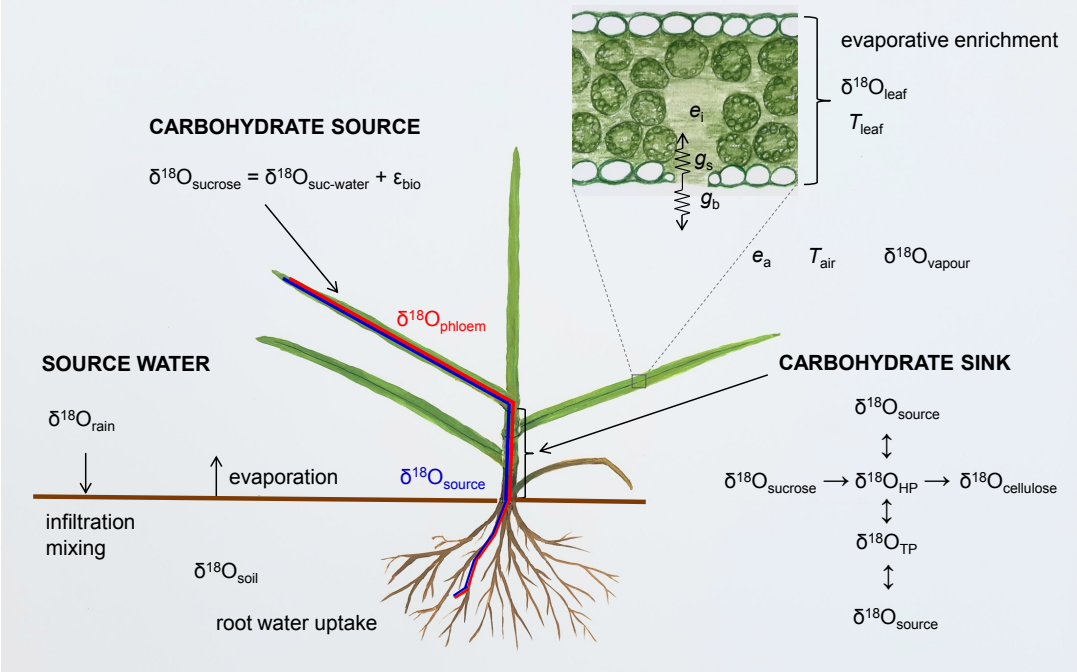

Figure 1.3: Overview of the main processes that affect the isotopic composition of cellulose. Precipitation (with isotopic composition $\delta^{18}O_{rain}$) infiltrates and mixes with water present in the soil ($\delta^{18}O_{soil}$). The water taken up by plant roots ($\delta^{18}O_{source}$) moves through the leaf growth and differentiation zone (LGDZ) to the leaf blades, where it becomes enriched in ^{18}O, the extent of enrichment being mainly dependent on the ratio of ambient (e_a) to intercellular partial pressure of water vapour (e_i), stomatal (g_s) and boundary layer conductance (g_b), leaf temperature (T_{leaf}) and water vapour isotopic composition ($\delta^{18}O_{vapour}$) (see Eqns 1.2–1.9). The isotopic composition of bulk leaf water ($\delta^{18}O_{leaf}$) may not always be identical to the isotopic composition of sucrose synthesis water ($\delta^{18}O_{suc\text{-}water}$, i.e. the water that is imprinted in leaf sucrose; see text). Sucrose (with $\delta^{18}O_{sucrose}$) is enriched compared to sucrose synthesis water due to biochemical fractionation (ε_{bio}). Sucrose is translocated via the phloem from leaf blades to the LGDZ (which represents a carbon sink), where it is cleaved and hexose phosphates (HP) are formed, which can be broken down into triose phosphates (TP). Carbonyl oxygen exchange with source water can occur for HP and TP molecules, leading to an attenuation of the leaf water enrichment signal. The resulting $\delta^{18}O_{cellulose}$ thus integrates leaf water enrichment and source water signals.

leaf and source water isotope signals (see Fig. 1.3 for an overview of the processes leading up to the cellulose isotope signal). $\delta^{18}O_{cellulose}$ and the enrichment of cellulose above source water ($\Delta^{18}O_{cellulose} = R_{cellulose}/R_{source} - 1$) can be modelled according to the Barbour-Farquhar equation (Barbour & Farquhar, 2000):

$$\delta^{18}O_{cellulose} = p_{ex}\, p_x\, (\delta^{18}O_{source} + \varepsilon_{bio}) + (1 - p_{ex}\, p_x)\, (\delta^{18}O_{leaf} + \varepsilon_{bio}) \tag{1.10a}$$

$$\Delta^{18}O_{cellulose} = \Delta^{18}O_{leaf}\, (1 - p_{ex}\, p_x) + \varepsilon_{bio} \tag{1.10b}$$

p_{ex} represents the proportion of oxygen in cellulose that exchanged with water at the site of cellulose synthesis, p_x is the proportion of unenriched water in the developing cell, and ε_{bio} denotes the average biochemical fractionation between water and oxygen in organic molecules used for cellulose synthesis. The product $p_{ex}\, p_x$ is termed 'attenuation factor' here, as in Liu *et al.* (2016). The state of knowledge and uncertainties regarding the parameters p_{ex}, p_x and ε_{bio} are discussed in detail below.

During CO_2 hydration and fixation, dark reaction and sucrose synthesis, the hydration of carbonyl groups and the formation of gem-diol intermediates allow for oxygen exchange between organic molecules and tissue water (Farquhar *et al.*, 1998; Sternberg *et al.*, 2006). Thus, leaf water ^{18}O enrichment is passed on to primary assimilates. It is supposed in Eqn 1.10 that sucrose synthesized in source leaves is in isotopic equilibrium with leaf lamina water, as suggested by two studies with castor bean (Barbour *et al.*, 2000a; Cernusak *et al.*, 2003). However, results from a recent study by Lehmann *et al.* (2017) on two C_3 grasses (*Lolium perenne* and *Dactylis glomerata*) indicated that this assumption may not always be valid. Thus, the question whether or not, or under which environmental conditions, sucrose is in equilibrium with lamina leaf water currently represents one major uncertainty regarding the ^{18}O signal transfer from leaf water to cellulose. In addition, the extent to which instantaneous values of $\Delta^{18}O_{leaf}$ are laid down in primary assimilates and finally in cellulose depends on assimilation and growth rates (Hemming *et al.*, 2001; Cernusak *et al.*, 2005; Ogée *et al.*, 2009; Hirl *et al.*, 2020). Under field conditions, the parameters of Eqn 1.10 as well as photosynthesis and growth rates may vary dynamically on a sub-hourly to daily timescale as a response to the dynamic variation in environmental and ecohydrological conditions. Especially the inert nature of leaf water isotopic enrichment (see above) limits the applicability of snapshot measurements of $\Delta^{18}O_{leaf}$ for the modelling and exploration of $\Delta^{18}O_{cellulose}$ or $\delta^{18}O_{cellulose}$. The temporal integration of cellulose represents an additional difficulty when it comes to the interpretation of the cellulose isotope signal (Hemming *et al.*, 2001; Damesin & Lelarge, 2003; Ogée *et al.*, 2009; Gessler *et al.*, 2009, 2014; Royles *et al.*, 2013; Liu *et al.*, 2017b; Hirl *et al.*, 2020). Process-based ecosystem models that generate continuous predictions of isotope signals and plant carbon fluxes can aid in the interpretation of $\delta^{18}O_{cellulose}$ from samples collected in natural (eco)systems (Roden *et al.*, 2000; Barbour *et al.*, 2002; Ogée *et al.*, 2009; Keel *et al.*, 2016; Ulrich *et al.*, 2019). Such models were hitherto unavailable for grassland (Hirl *et al.*, 2019, 2020). Also, in general, studies on the $\delta^{18}O$ of cellulose or biomass from grassland have been scarce (Flanagan & Farquhar, 2014; Webb & Longstaffe, 2006; Ramírez *et al.*, 2009; Hirl *et al.*, 2019, 2020).

As cellulose integrates source and leaf water isotopic signals, it also contains the environmental and physiological information imprinted in $\delta^{18}O_{source}$ and $\delta^{18}O_{leaf}$. In particular, $\delta^{18}O_{cellulose}$ is thought to represent an integrated proxy of stomatal conductance (Farquhar *et al.*, 1998; Scheidegger *et al.*, 2000; Barbour *et al.*, 2000b; Grams *et al.*, 2007) due to the association of leaf water ^{18}O enrichment and g_s (see sections 1.3 and 1.7). Also, the $\delta^{18}O_{cellulose}$ from tree-rings has been related to a range of meteorological/climatic parameters, such as temperature (e.g. Libby *et al.*, 1976; Labuhn *et al.*, 2014), sunshine duration (Hafner *et al.*, 2011), rainfall patterns and amounts as well as the $\delta^{18}O$ of rain (Treydte *et al.*, 2006; Schollaen *et al.*, 2013; Robertson *et al.*, 2001), and vapour pressure deficit (Kahmen *et al.*, 2011) or relative humidity (Shu *et al.*, 2005; Anderson *et al.*, 1998). Yet, the association of $\delta^{18}O_{cellulose}$ with climate is complex, owing to correlations among meteorological parameters and the dynamic nature of assimilation and growth under field conditions. Hence, teasing apart direct and indirect effects of climatic drivers on $\delta^{18}O_{cellulose}$ based on statistical correlations has proven to be difficult or even misleading, and necessitates the use of process-based models.

1.5 Biochemical fractionation between water and organic substrate

Carbohydrates are generally enriched in ^{18}O relative to the water in which they were formed, as isotopic exchange between carbonyl oxygen and water involves fractionation (Schmidt *et al.*, 2001). The average biochemical fractionation (ε_{bio}) between water and oxygen in organic molecules used for cellulose synthesis has long been taken as a constant of ≈27‰ (Epstein *et al.*, 1977; DeNiro & Epstein, 1981; Sternberg & DeNiro, 1983; Yakir & DeNiro, 1990). This notion was recently challenged by Sternberg & Ellsworth (2011), who heterotrophically generated cellulose from wheat seeds in the dark and found that ε_{bio} was inversely related to growth temperature, the effect being most pronounced for temperatures <20 °C (Fig. 1.4a). Importantly and interestingly, when the authors compiled $\Delta^{18}O_{cellulose}$ data from submerged aquatic plants and plotted those data against growing temperature, virtually the same polynomial relation between ε_{bio} (being represented by $\Delta^{18}O_{cellulose}$) and temperature was obtained. The finding of Sternberg & Ellsworth (2011) were controversially discussed in the recent past, with some authors suggesting that p_{ex} rather than ε_{bio} might be dependent on temperature (Zech *et al.*, 2014a,b; Sternberg, 2014).

One earlier examination of the potential temperature-dependency of ε_{bio} in a terrestrial ecosystem comes from Roden & Ehleringer (2000). Analysing the oxygen and hydrogen isotope ratios of xylem water, leaf water and cellulose of riparian cottonwood trees growing along an elevational gradient in Utah, these authors investigated whether there is indication for a temperature-dependent biochemical fractionation during wood cellulose formation in field-grown trees. Due to there being no significant variation in the isotopic composition of cellulose, leaf, xylem or stream water along the transect, the authors concluded that temperature did not exert control on biochemical fractionation. Yet, average growing season temperatures along the elevational transect lay between ca 23.5 °C and 28.5 °C, a range where the temperature sensitivity of ε_{bio} should be small according to Sternberg & Ellsworth (2011). Clearly, there is a great urgency for better empirical evidence for or against a temperature-dependent ε_{bio} in terrestrial vegetation.

1.6 The attenuation factor ($p_{ex}\, p_x$)

Although it is generally acknowledged that cellulose – at least leaf cellulose (see Cheesman & Cernusak, 2017; Voelker & Meinzer, 2017) – contains both a leaf water and a source water ^{18}O signal (Barbour & Farquhar, 2000, see above), uncertainties still remain regarding the degree of attenuation of the leaf water enrichment signal in sucrose along its way from source leaves to sink tissue. The proportion of unenriched water in the developing cell (p_x) is commonly calculated from a two-end-member mixing model (Liu *et al.*, 2017a; Cheesman & Cernusak, 2017):

$$p_x = \frac{\delta^{18}O_{cel\text{-}water} - \delta^{18}O_{suc\text{-}water}}{\delta^{18}O_{source} - \delta^{18}O_{suc\text{-}water}} = 1 - \frac{\Delta^{18}O_{cel\text{-}water}}{\Delta^{18}O_{suc\text{-}water}} \tag{1.11}$$

where 'cel-water' and 'suc-water' represent the water at the location of cellulose and sucrose synthesis, respectively. Depending on the experimental setting (controlled *vs.* field experiment)

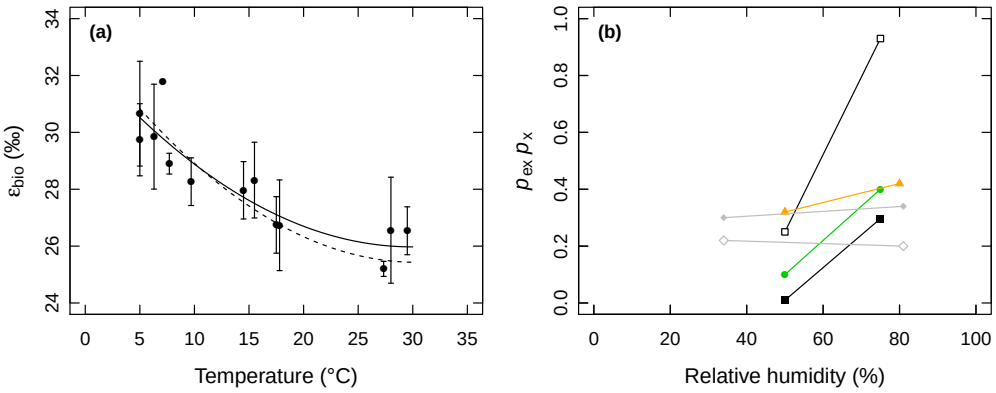

Figure 1.4: (a) Biochemical fractionation (ε_{bio}) as a function of temperature. ε_{bio} was estimated as the isotopic enrichment of cellulose in submerged aquatic plants relative to source water ($\Delta^{18}O_{cellulose}$; redrawn from Sternberg & Ellsworth, 2011). Error bars represent the standard deviation and the continuous line gives the best-fit polynomial regression, used for predicting $\Delta^{18}O_{cellulose}$ in Hirl *et al.* (2020). Original data come from DeNiro & Epstein (1981), Sauer *et al.* (2001) and Sternberg (1988). The dashed line represents ε_{bio} as a function of temperature as obtained in the wheat germination experiment of Sternberg & Ellsworth (2011). (b) Relation between relative air humidity and $p_{ex}\,p_x$ for various C_3 and C_4 grasses. $p_{ex}\,p_x$ was calculated from Eqn 1.10b, using $\Delta^{18}O_{leaf}$ and $\Delta^{18}O_{cellulose}$ data and a temperature-dependent ε_{bio}, computed from air temperature in the growth environment based on the polynomial regression for aquatic plants displayed in (b). Green points show data from a controlled environment experiment with *Lolium perenne* (ε_{bio} = 26.8‰; Juan C. Baca Cabrera, Regina T. Hirl, Jianjun Zhu, Hans Schnyder, unpublished data; see 2.2 and 3.4 and Baca Cabrera *et al.*, 2020). Closed and open squares show data from another controlled environment experiment conducted by Lehmann *et al.* (2017), where $p_{ex}\,p_x$ was either calculated using a temperature-dependent ε_{bio} = 25.5‰ (closed squares) or ε_{bio} = 27‰ (open squares; see Lehmann *et al.*, 2017, their Table 4). Orange triangles illustrate data for the C_4 grass *C. squarrosa*, with temperature-dependent ε_{bio} = 26.2‰ (Liu *et al.*, 2016; see 2.2 and 3.3). Diamonds show the relation between $p_{ex}\,p_x$ and relative humidity for C_3 (grey filled diamonds) and C_4 grasses (grey open diamonds) studied by Helliker & Ehleringer (2002a,b). Note that while relative humidity was constant throughout day and night in the experiments of Lehmann *et al.* (2017) and Liu *et al.* (2016), relative humidity differed between the dark and light period in the *L. perenne* experiment of JCBC, RTH, JZ and HS (unpublished). Relative humidity in panel (c) refers to daytime humidity. For the Helliker & Ehleringer (2002a) data, $p_{ex}\,p_x$ was plotted against relative humidity at midday, as given in their study.

and the plant functional type, $\delta^{18}O_{source}$ may be defined as the $\delta^{18}O$ of nutrient solution or tank water (e.g. Liu *et al.*, 2017a), soil water, or xylem water (Cernusak *et al.*, 2005). The defintion of 'source water' as being represented by one of those water compartments may be less critical for $\delta^{18}O$ than for $\delta^{2}H$ (Barbeta *et al.*, 2020), and if care is taken to prevent or minimize evaporation from soil or tank water in controlled experiments (Liu *et al.*, 2017a). The isotopic enrichment of sucrose synthesis water has been estimated as $\Delta^{18}O_{suc-water} = \Delta^{18}O_{sucrose} - \varepsilon_{bio}$, with $\Delta^{18}O_{sucrose}$ approximated by the ^{18}O enrichment of bulk phloem organic matter (Cernusak *et al.*, 2005). In the absence of direct measurements of $\Delta^{18}O_{sucrose}$, $\Delta^{18}O_{suc-water}$ was equated with the $\Delta^{18}O$ of bulk leaf water (Song *et al.*, 2014; Liu *et al.*, 2017a).

In the developing cells of tree trunks and in the leaf growth and differentiation zone (LGDZ) of grasses, p_x stayed close to 1 (Cernusak *et al.*, 2005; Liu *et al.*, 2017a, Fig. 1.2). As phloem water was only slightly enriched in ^{18}O as compared to xylem water (Cernusak *et al.*, 2005), and water in the LGDZ was close to source (irrigation) water (Liu *et al.*, 2017a), precise knowledge of $\Delta^{18}O_{suc-water}$ and the definition of $\delta^{18}O_{source}$ should only have a small effect on the estimation

of p_x for grasses and tree-rings. In contrast, considerable uncertainty exists with regard to putative spatio-temporal variation of p_x in the growing leaves of dicots.

The proportion of oxygen in cellulose that exchanged with water at the site of cellulose synthesis (p_{ex}) (Farquhar *et al.*, 1998; Barbour & Farquhar, 2000) is perhaps the most uncertain parameter of the Barbour-Farquhar model, at least for grasses and tree-rings where p_x is well constrained. The interpretation of observed variability in p_{ex} is complicated by the fact that p_{ex} is usually estimated from the Barbour-Farquhar model by inserting measured values of $\Delta^{18}O_{leaf}$ and $\Delta^{18}O_{cellulose}$ and literature-based estimates of ε_{bio} and p_x into that equation. As a consequence, the estimates obtained for p_{ex} integrate and reflect all kinds of errors and uncertainties: sampling and measurement errors (for $\delta^{18}O_{source}$, $\Delta^{18}O_{leaf}$, $\Delta^{18}O_{cellulose}$), as well as our incomplete understanding with regard to variation of the $\delta^{18}O$ of sucrose synthesis water and the relation between $\Delta^{18}O_{sucrose}$ and $\Delta^{18}O_{leaf}$. Also, unlike $\delta^{18}O_{cellulose}$, $\delta^{18}O_{source}$ and $\Delta^{18}O_{leaf}$ do not represent temporally-integrated signals.

Results from various studies indicated that p_{ex} is approximately 0.4 if cellulose is formed from carbohydrates (Sternberg *et al.*, 1986; Yakir & DeNiro, 1990; Roden & Ehleringer, 1999; Roden *et al.*, 2000; Sternberg *et al.*, 2003; Cernusak *et al.*, 2005). However, when sucrose is broken down into hexose monophosphates during cellulose formation in the growth zone, hexose monophosphates might undergo rapid 'futile' cycling with triose phosphates (Hill *et al.*, 1995). Variation in p_{ex} is commonly thought to arise from variation in the extent of futile cycling, as oxygen in carbonyl groups of dihydroxyacetonephosphate and 3-phosphoglyceraldehyde can be exchanged with local water, and triose phosphate isomerase additionally catalyses the rapid interconversion of the triose phosphates (Hill *et al.*, 1995). Theoretical estimates indicated that p_{ex} may range between 0.2 (if no futile cycling occurs and the only exchangeable oxygen appears in hexose phosphates) and 1 (if all hexose phosphates undergo futile cycling) (Farquhar *et al.*, 1998; Barbour & Farquhar, 2000):

$$p_{ex} = 0.2 + (0.6 + 0.2\,/\,(2 - y))\,y \tag{1.12}$$

with y the probability that a hexose phosphate molecule undergoes futile cycling. Assuming that a slower turnover of water-soluble carbohydrates or lower growth rates enhance the probability of substrate to undergo cycling through hexose and triose phosphates, several authors related the observed variation of p_{ex} to variation in the turnover time of carbohydrates, or to variation in the relation of sink to source strength (Barbour & Farquhar, 2000; Ellsworth & Sternberg, 2014; Song *et al.*, 2014; Cheesman & Cernusak, 2017; Szejner *et al.*, 2020). Thus, environmental parameters (e.g. light intensity, VPD or edaphic drought) may affect futile cycling rates and p_{ex} via their effect on plant growth rates or carbohydrate dynamics. Direct biochemical evidence for variation of p_{ex} *in vivo* and for the contribution of futile cycling to *in vivo* variation of p_{ex} is currently lacking.

Additional (apparent) variation in p_{ex} may arise from isotopic disequilibria between $\Delta^{18}O_{sucrose}$ and $\Delta^{18}O_{leaf}$ (Lehmann *et al.*, 2017), and from isotopic exchange potentially occurring when sucrose is transported from source leaves to sink tissue (Gessler *et al.*, 2013). A positive relation between relative humidity and $p_{ex}\,p_x$ was observed for a range of C_3 and C_4 grasses grown under controlled environment conditions when $p_{ex}\,p_x$ was calculated from observed $\Delta^{18}O_{leaf}$

and $\Delta^{18}O_{cellulose}$ based on Eqn 1.10b (Fig. 1.4b). Evidence for relative humidity-related variation of $p_{ex}\,p_x$ in plants grown under natural conditions in the field was hitherto lacking (Hirl *et al.*, 2020). As temperature and relative humidity vary simultaneously and dynamically in the field, disentangling the effects of temperature and humidity on ε_{bio} and $p_{ex}\,p_x$ requires the use of a mechanistic model.

1.7 Carbon isotopes, water-use efficiency and the dual isotope approach

As climate change alters both carbon and water dynamics of plants, water-use efficiency (WUE) is a parameter of great interest because it reflects the relationship between CO_2 assimilation and water loss. While instantaneous WUE represents the ratio of assimilation to transpiration, which is driven by atmospheric water deficit, plant physiological adaptations are reflected in intrinsic water-use efficiency (iWUE, also termed physiological WUE):

$$\text{iWUE} = \frac{A_n}{g_s} \tag{1.13a}$$

$$\text{iWUE} = \frac{c_a\left(1 - \frac{c_i}{c_a}\right)}{1.6} \tag{1.13b}$$

where A_n is leaf net assimilation rate, g_s is stomatal conductance to water vapour, c_i and c_a are intercellular and atmospheric CO_2 concentrations, and 1.6 represents the ratio of the conductances to water vapour and CO_2 (Farquhar *et al.*, 1989; Franks *et al.*, 2013). Information on c_i/c_a to retrospectively estimate iWUE can be obtained from analysis of the stable carbon isotope signature of cellulose or plant organic matter ($\delta^{13}C_p$) (Farquhar *et al.*, 1982, 1989):

$$\delta^{13}C_p = \delta^{13}C_a - a - (b - a)\,\frac{c_i}{c_a} \tag{1.14}$$

with a the fractionation during diffusion of CO_2 in air (4.4‰), b the fractionation during carboxylations (~27‰) (Farquhar *et al.*, 1989), and $\delta^{13}C_a$ the isotopic composition of atmospheric CO_2. $\delta^{13}C$ is defined on the lines of Eqn 1.1, with $R_{standard}$ the isotope ratio of the Vienna Pee Dee Belemnite standard. When physiological mechanisms are to be studied independently from $\delta^{13}C_a$, the ^{13}C discrimination ($\Delta^{13}C$) is commonly applied (Farquhar & Richards, 1984):

$$\Delta^{13}C = \frac{R_a}{R_p} - 1 = \frac{\delta^{13}C_a - \delta^{13}C_p}{1 + \delta^{13}C_p} \tag{1.15}$$

Together, Eqn 1.14 and 1.15 yield:

$$\Delta^{13}C = a + (b - a)\,\frac{c_i}{c_a} \tag{1.16}$$

Eqns 1.14 and 1.16 represent the simplified Farquhar model; a detailed version of the model, which accounts for the effects of diffusion through the boundary layer, stomata and mesophyll, as well as photorespiration and mitochondrial respiration, can be found in Farquhar *et al.* (1982, 1989) and Farquhar & Cernusak (2012). Recently, Ma *et al.* (2020) showed that if information on mesophyll conductance is lacking, ^{13}C based predictions of iWUE may be obtained by assuming a constant ratio of stomatal to mesophyll conductance.

The intercellular CO_2 concentration is the net result of CO_2 supply and demand and is thus determined both by stomatal conductance and photosynthetic capacity. Analysis of $\delta^{13}C$ (or $\Delta^{13}C$) alone does not allow to tease apart stomatal and photosynthetic effects on c_i and iWUE. It is thought that the $\delta^{18}O$ of cellulose or plant biomass may help interpret variation in $\Delta^{13}C$ and iWUE, as $\delta^{18}O_{cellulose}$ (or rather $\Delta^{18}O_{cellulose}$) may represent an integrated proxy of stomatal conductance (the 'dual isotope approach'; Farquhar *et al.*, 1998; Scheidegger *et al.*, 2000; Barbour *et al.*, 2000b; Grams *et al.*, 2007). Due to the expected negative relation between leaf water ^{18}O enrichment and g_s (see section 1.3), $\Delta^{18}O_{cellulose}$ is expected to decrease with increasing g_s. At the same time, increasing g_s causes an increase in c_i/c_a and $\Delta^{13}C$ (Eqn 1.16). Hence, a negative relationship between $\Delta^{18}O$ and $\Delta^{13}C$ may be expected if variation in $\Delta^{13}C$ is primarily caused by stomatal conductance changes (Grams *et al.*, 2007). Increases (or decreases) in $\delta^{18}O_{cellulose}$ in tree-rings have thus been interpreted to reflect decreases (or increases) in stomatal conductance (e.g. Sidorova *et al.*, 2009; Barnard *et al.*, 2012; Weigt *et al.*, 2018; Guerrieri *et al.*, 2019).

Several studies used $\delta^{18}O$ and $\delta^{13}C$ to discuss physiological responses to management practices such as thinning or fertilization, which act on limiting factors such as light, water or nutrients (Brooks & Coulombe, 2009; Brooks & Mitchell, 2011; Moreno-Gutiérrez *et al.*, 2011; Giuggiola *et al.*, 2016). Still, however, there remains significant uncertainty about the relation between cellulose-^{18}O and g_s which is complicated by the dynamic variation of stomatal or canopy conductance, growth and cellulose synthesis, and integration time and tissue life span in field conditions. In particular, it is challenging to obtain a time-integrated measure of stomatal conductance. As single or multiple snapshot measurements of g_s may be of limited value, mechanistic models that generate continuous predictions of g_s can aid in the evaluation of the $\delta^{18}O$-g_s relation.

1.8 Aims and outline of the thesis

The main aim of this thesis was to establish a comprehensive modelling framework for exploring the ^{18}O signal transfer from meteoric water to leaf cellulose of a grassland ecosystem. No such modelling framework has been in existence for grassland. In a first step, the process-based isotope-enabled soil-plant-atmosphere model MuSICA was parameterised for a temperate humid pasture ecosystem and then applied to track the transfer of the rainwater isotope signal through soil water, plant source water, as well as canopy leaf water and its enrichment above source water in samples collected at fortnightly intervals during the vegetation periods 2006–2012 (Hirl *et al.*, 2019). In doing so, the current system-scale ecohydrological understanding of the ^{18}O signal transfer was evaluated in detail. The aims were 1) to evaluate the effect of edaphic drought on the grassland community's root water uptake depth, 2) to disentangle the effects of soil and atmospheric moisture on canopy leaf water ^{18}O enrichment ($\Delta^{18}O_{leaf}$), 3) to assess the performance of the two-pool and the Péclet model in predicting $\Delta^{18}O_{leaf}$, and 4) to explore the role of plant morpho-physiological parameters and of isotopic input data in shaping the water and $\delta^{18}O$ dynamics of the ecosystem.

In a second step, a new allocation-and-growth module was devised and added to the process-based isotope-enabled model MuSICA (Hirl *et al.*, 2020). The combined model (termed MuSICAgrass in the following) generated continuous half-hourly predictions of the $\delta^{18}O$ of source water and of the plant metabolic pool, which allowed to make predictions of the cellulose isotopic signals. MuSICAgrass was tested for its ability to predict the $\delta^{18}O$ and $\Delta^{18}O$ of leaf cellulose from mixed-species collections of the co-dominant species of the studied grassland (growing seasons 2007–2012). Specifically, we examined two main uncertainties concerning the link of the leaf water and cellulose ^{18}O signals, namely 1) the sensitivity of the attenuation factor ($p_{ex}\,p_x$) to relative humidity, and 2) the temperature-sensitivity of ε_{bio}. These hypotheses have not been systematically tested in terrestrial ecosystems before. In addition, we explored whether $\Delta^{18}O_{cellulose}$ and $\delta^{18}O_{cellulose}$ of the grassland canopy were linked to canopy conductance.

Furthermore, this thesis contains the results of two controlled environment studies. In a first set of experiments, the effects of air vapour pressure deficit (VPD) and nitrogen supply on the $\Delta^{18}O$ of leaf water, the $\Delta^{18}O$ of cellulose, and on the attenuation factor ($p_{ex}\,p_x$) were examined (Liu *et al.*, 2016). That study used *Cleistogenes squarrosa*, a perennial C_4 grass from the Central Asia steppe. Additionally, we tested whether the $\delta^{18}O$ of air CO_2 had a measurable effect on the $\delta^{18}O$ of cellulose.

The second set of experiments set out to investigate the effect of air VPD and CO_2 concentration on diurnal growth patterns of the perennial C_3 grass *Lolium perenne* (Baca Cabrera *et al.*, 2020). Understanding how VPD and CO_2 affect growth patterns of grasses is of relevance for the modelling and potential use of $\delta^{18}O_{cellulose}$ for elucidating physiological adaptations of plants to changing atmospheric CO_2.

This thesis is organized as follows: Chapter 2 summarises the main components and features of the model, and provides an overview of the experimental site. In addition, the controlled environment experiments are presented in short. Chapter 3 contains the abstracts of the publications that emerged from this dissertation. In Chapter 4, major results are discussed and potential applications are presented. In particular, I evaluated the ability of MuSICAgrass to predict the $\delta^{2}H$ of ecosystem water pools at the temperate humid grassland ecosystem (section 4.2.1) and the $\Delta^{13}C$ of cellulose from the same samples that were analysed for their oxygen isotope ratios (section 4.2.2). In addition, I compared model predictions of $\delta^{18}O_{cellulose}$, made with the original parameterisation for Grünschwaige and meteorological forcing files for Rothamsted (1993–2010), with observations of $\delta^{18}O_{cellulose}$ in the Rothamsted Park Grass Experiment (section 4.2.3).

2. Synthesis of Materials and Methods

2.1 Process-based isotope-enabled modelling of grassland water and cellulose isotopes

The MuSICA model (Multi-layer Simulator of the Interactions between a vegetation Canopy and the Atmosphere) is an isotope-enabled soil-plant atmosphere transfer model that simulates ecosystem CO_2, energy and water fluxes, along with the $\delta^{18}O$ and $\delta^{2}H$ composition of ecosystem water pools (Ogée, 2000; Ogée *et al.*, 2003, 2009; Wingate *et al.*, 2010; Gangi *et al.*, 2015). MuSICA was originally devised for a maritime pine forest canopy and was for the first time applied to grassland in this work. Our study site was a temperate humid grazed *Lolio-Cynosuretum* grassland, pasture no. 8 at the former Grünschwaige Grassland Research Station of TUM near Munich (for details on site and management see Schnyder *et al.*, 2006). Vegetation was characterised by continuous and rapid leaf turnover and a short leaf lifespan (Schleip *et al.*, 2013). Due to the low water-holding capacity of the shallow topsoil, the site was prone to edaphic drought.

The model was forced by half-hourly meteorological and isotopic input data and predicted half-hourly values of latent and sensible heat flux, transpiration and evaporation, gross primary production and net ecosystem exchange, as well as the spatio-temporal dynamics of soil temperature, soil water content, and root water uptake. In addition, it simulated the spatio-temporal dynamics of $\delta^{18}O_{soil}$, as well as the temporal variation of $\delta^{18}O_{source}$ and the $\delta^{18}O$ of canopy leaf water (according to Eqns 1.2–1.9). Isotopic input data ($\delta^{18}O_{rain}$ and $\delta^{18}O_{vapour}$) collected at the study site were used whenever available, which were complemented with data from the general circulation model IsoGSM (Yoshimura *et al.*, 2011; see Hirl *et al.*, 2019 and section 4.1).

In the first part of this work, the model was parameterised for the study site and validated based on Eddy covariance data from the same site. Then, the model was tested for its ability to predict the spatio-temporal dynamics of the $\delta^{18}O$ of soil, pseudo-stem, and canopy leaf water, as well as root water uptake, thus describing, the '^{18}Oecohydrology' of the studied grassland ecosystem (Hirl *et al.*, 2019). $\delta^{18}O$ data for comparison with model predictions were obtained from fortnightly sampling of ecosystem water pools (groundwater, soil water at 7 and 20 cm depth, pseudo-stem and leaf samples, and atmospheric vapour) during the growing seasons 2006 to 2012. Pseudo-stem and leaf samples were mixed-species collections of the co-dominant species *Lolium perenne*, *Poa pratensis*, *Dactylis glomerata*, *Phleum pratense*, *Taraxacum officinale* and *Trifolium repens* present in the pasture plant community. Fortnightly sampling was complemented by collection of rainwater following rain events. Water was extracted from soil and leaf samples in a cryogenic vacuum distillation unit (see Liu *et al.*, 2016), and the isotopic composition of the water samples was determined using cavity ring-down spectroscopy or isotope ratio mass spectrometry (see Hirl *et al.*, 2019). In addition, cellulose was extracted from subsamples of dried leaf material according to Brendel *et al.* (2000) and Gaudinski *et al.* (2005) and analysed for its $\delta^{18}O$ and $\delta^{13}C$ composition (see Hirl *et al.*, 2020).

The soil was parameterised in terms of its structural and hydraulic characteristics (soil water retention and hydraulic conductivity, boundary conditions at the bottom of the soil profile), soil water vapour effective diffusivity, respiration, optical properties, as well as surface resistances, as described in detail in Hirl *et al.* (2019). The parameterisation of the vegetation included canopy structure and phenology, photosynthetic properties and leaf conductances, root distribution and hydraulics, as well as leaf optical properties. The same set of parameters was used for the entire 7-year study period.

In the second part, I constructed a new allocation-and-growth module and added this to the MuSICA model (Fig. 2.1). Based on a set of differential equations and proceeding from gross primary production and the isotope ratios of assimilates predicted by MuSICA, the allocation-and-growth module simulated maintenance and growth respiration, and shoot and root structural growth rates (Hirl *et al.*, 2020; 2.1). The salient features of that module are that it assumes a constant (target) size of the metabolic pool, which supplies substrate to growth only if the pool is filled and if gross primary production is larger than maintenance respiration. Thus, upkeep of maintenance respiration is prioritised over growth. Besides, in the model, resource partitioning between shoot and roots depends on xylem water potential, and hence on the soil water status. As such, the model predicts that leaf growth and cellulose synthesis predominantly occur under well-watered conditions, known to be a general feature of herbaceous vegetation (Boyer, 1970; Durand *et al.*, 1995). Cellulose synthesis was assumed proportional to aboveground growth rate.

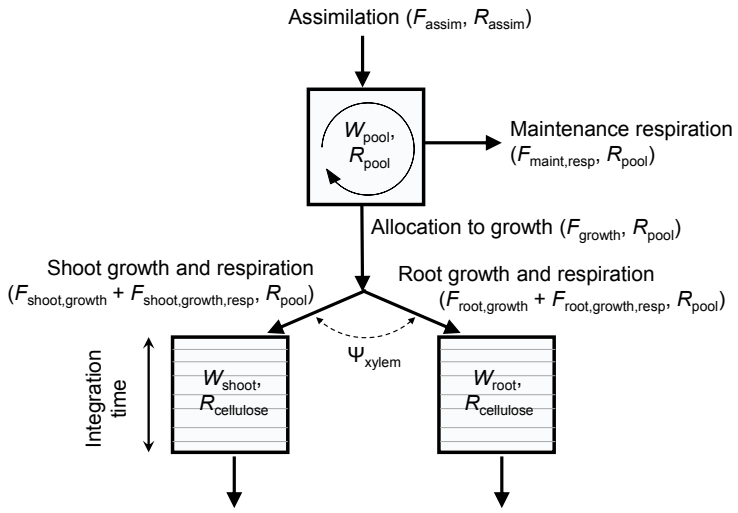

Figure 2.1: Schematic overview of the allocation-and-growth module devised for prediction of cellulose isotope signals (from Hirl *et al.*, 2020). W_{pool} denotes the size of the metabolic pool, and R_{assim}, R_{pool} and $R_{\mathrm{cellulose}}$ are the isotope ratios of the assimilates, the metabolic pool and cellulose. Ψ_{xylem} denotes xylem water potential, which determines the partitioning of assimilates between shoot and root growth. For details on model equations and parameterisation see Hirl *et al.* (2020).

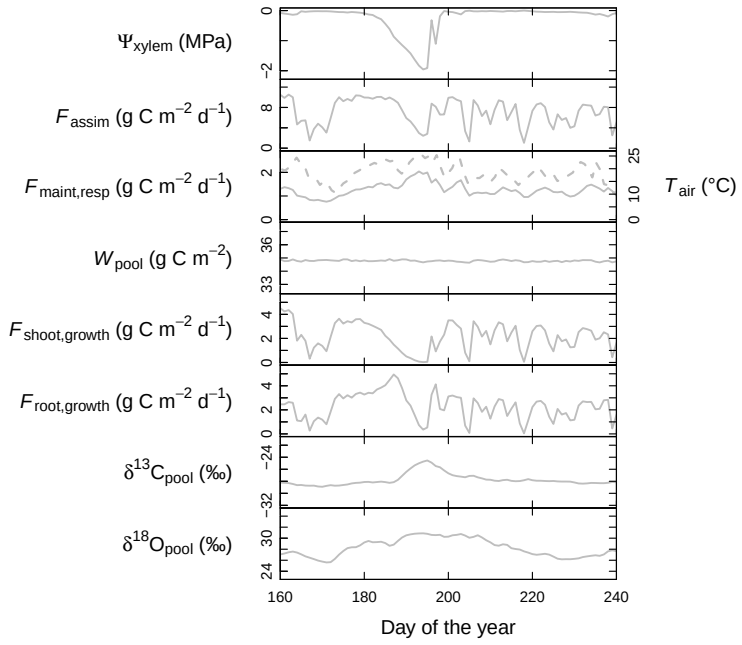

Figure 2.2: Predicted behaviour of carbon fluxes and of the isotope signatures of the metabolic pool during a dry period in summer 2010, as marked by a decline of xylem water potential (Ψ_{xylem}) around DOY 180: gross primary production (F_{assim}), maintenance respiration ($F_{\mathrm{maint,resp}}$), size of the metabolic pool (W_{pool}), shoot and root growth rates ($F_{\mathrm{shoot,growth}}$ and $F_{\mathrm{root,growth}}$), and the δ^{13}C and δ^{18}O of the metabolic pool ($\delta^{13}C_{\mathrm{pool}}$ and $\delta^{18}O_{\mathrm{pool}}$). Variation in $F_{\mathrm{maint,resp}}$ was assumed to be driven by air temperature (T_{air}, dashed line).

In the model, current assimilates mix with all non-structural carbohydrates that represent the plant metabolic carbon pool. Unlike previous versions of MuSICA (Ogée *et al.*, 2009), the isotope ratio of the assimilates is computed from the leaf water isotope ratio by assuming temperature-dependent biochemical fractionation (Fig. 1.4a; Sternberg & Ellsworth, 2011). The change of the sugar pool isotope ratio is then calculated based on the ratio of assimilation rate to the metabolic pool size and on the difference between the isotope ratios of the new assimilates and the metabolic pool. All fluxes out of the metabolic pool carry the isotopic signal of the metabolic pool, supposing that no fractionation during respiration or growth occurs (Cernusak *et al.*, 2004; Farquhar & Cernusak, 2012; but see Ogée *et al.*, 2009). Model parameterisation of soil, vegetation and of the allocation-and-growth module relied on measurements conducted at the experimental site (Schnyder *et al.*, 2006; Gamnitzer *et al.*, 2009, 2011; Schleip, 2013; Schleip *et al.*, 2013; Ostler *et al.*, 2016), supplemented by literature data on C_3 grassland.

Carbon fluxes and isotope signals of the metabolic pool simulated with MuSICAgrass, and in particular model behaviour during edaphic drought, are exemplified in Fig. 2.2 for the summer of 2010. Xylem water potential was predicted to decrease considerably around DOY 180 of 2010, causing GPP to decrease, while maintenance respiration still increased, in accordance with the increase of air temperature. Shoot growth rate decreased as predicted by the decrease of xylem water potential, while root growth was initially enhanced, but then decreased due to decreasing assimilate supply. Root growth recovered as soon as the metabolic pool was replenished. Throughout that period the size of the metabolic pool fluctuated around its target value, as prescribed by the model priorities. Shoot growth only re-started as soon as the xylem water potential relaxed. The δ^{13}C of the pool peaked concurrently with the decline in xylem water potential, while $\delta^{18}O_{\mathrm{pool}}$ was predicted to increase in a more dampened way.

The isotopic composition of cellulose was calculated from shoot growth rate-weighted isotope

ratios of xylem water and of the metabolic pool, with the relative contributions of xylem water and metabolic pool being determined by the attenuation factor $p_{ex}\,p_x$. In the standard simulation, $p_{ex}\,p_x$ was calculated from midday air relative humidity, and the biochemical fractionation occurring during sucrose breakdown and cellulose synthesis in the LGDZ was computed from daily mean air temperature (see Fig. 1.4a and Hirl *et al.*, 2020). Xylem water and metabolic pool isotope ratios were integrated over the assumed age of structural biomass in the samples (the integration time).

Finally, the deuterium isotope composition (δ^2H) of the water pools was calculated along the lines of δ^{18}O, but using isotope fractionation factors specific to deuterium (see e.g. Cernusak *et al.*, 2016). The carbon isotope discrimination (Δ^{13}C) of assimilates was computed based on the detailed Farquhar model (Farquhar *et al.*, 1982, 1989; with modifications following Wingate *et al.*, 2007).

2.2 Controlled environment experiments

Two different sets of controlled environment experiments were performed in order to explore the effects of air CO_2 concentration, vapour pressure deficit (VPD) and nitrogen (N) supply on the oxygen isotope composition of leaf water and cellulose, and on morpho-physiological parameters and growth processes that may influence the incorporation of the leaf water isotopic signal into cellulose (see Liu *et al.*, 2016; Baca Cabrera *et al.*, 2020). All experiments were performed in Conviron growth chambers with tightly controlled environmental conditions of relative humidity, temperature, irradiance, CO_2 concentration and C and O isotope composition of CO_2, nutrient supply and isotopic composition of the nutrient solution. These variables were surveyed throughout the duration of the experiment and adjusted if needed.

The first set of experiments aimed to investigate nitrogen supply and VPD effects on $\Delta^{18}O_{leaf}$ and $\Delta^{18}O_{cellulose}$ and on the relation between $\Delta^{18}O_{leaf}$ and $\Delta^{18}O_{cellulose}$ in the C_4 grass *Cleistogenes squarrosa*. The 2 x 2 factorial design included a low and a high N treatment (modified Hoagland nutrient solution with 7.5 or 22.5 mM nitrate-N, respectively) and low or high VPD (0.63 and 1.58 kPa throughout light and dark period). Moreover, we tested if the δ^{18}O of air CO_2 had a measureable effect on $\delta^{18}O_{cellulose}$.

The second set of experiments aimed at elucidating the effect of air CO_2 concentration and VPD on daily mean leaf elongation rate (LER) and day to night differences of LER (and thus, to a rough approximation, cellulose formation), final leaf dimensions, and epidermal cell length and number in the C_3 grass *Lolium perenne*. Perennial ryegrass was a major component of the mixed-species samples studied in Hirl *et al.* (2019, 2020) and constitutes one of the most important forage grasses in temperate climates. The mesocosm experiment consisted of a 3 x 2 factorial design with 200, 400 and 800 µmol mol^{-1} CO_2, and low (0.59 kPa) and high (1.17 kPa) VPD. Treatment effects on day-to-night differences in LER were related to leaf gas exchange characteristics and hydraulic controls (leaf water potential, osmotic potential, turgor pressure).

3. Summaries of manuscripts and contributions of the authors

This thesis comprises two first-author and two co-author papers. The abstracts and the authors' contributions are given below. Publications 1, 2 and 4 resulted from the DFG project SCHN 557/9-1 "The significance of cellulose-δ^{18}O for understanding water-use efficiency of grassland: Evidence from experimental, observational and process-based modeling studies". Hans Schnyder and I conceived and wrote the research proposal for that project together, and it provided funding for two doctoral students (Juan C. Baca Cabrera and me).

3.1 Publication 1: The ^{18}O ecohydrology of a grassland ecosystem – predictions and observations

Regina T. Hirl*, Hans Schnyder, Ulrike Ostler, Rudi Schäufele, Inga Schleip, Sylvia H. Vetter, Karl Auerswald, Juan C. Baca Cabrera, Lisa Wingate, Margaret M. Barbour, Jérôme Ogée

* Corresponding author

Published in Hydrology and Earth System Sciences: 23, 2581–2600, 2019. doi: 10.5194/hess-23-2581-2019

Abstract

The oxygen isotope composition (δ^{18}O) of leaf water ($\delta^{18}O_{leaf}$) is an important determinant of environmental and physiological information found in biological archives, but the system-scale understanding of the propagation of the δ^{18}O of rain through soil and xylem water to $\delta^{18}O_{leaf}$ has not been verified for grassland. Here we report a unique and comprehensive dataset of fortnightly δ^{18}O observations in soil, stem and leaf waters made over seven growing seasons in a temperate, drought-prone, mixed-species grassland. Using the ecohydrology part of a physically based, ^{18}O-enabled soil–plant–atmosphere transfer model (MuSICA), we evaluated our ability to predict the dynamics of δ^{18}O in soil water, the depth of water uptake, and the effects of soil and atmospheric moisture on ^{18}O enrichment of leaf water ($\Delta^{18}O_{leaf}$) in this ecosystem. The model accurately predicted the δ^{18}O dynamics of the different ecosystem water pools, suggesting that the model generated realistic predictions of the vertical distribution of soil water and root water uptake dynamics. Observations and model predictions indicated that water uptake occurred predominantly from shallow (<20 cm) soil depths throughout dry and wet periods in all years, presumably due (at least in part) to the effects of high grazing pressure on root system turnover and placement. $\Delta^{18}O_{leaf}$ responded to both soil and atmospheric moisture contents and was best described in terms of constant proportions of unenriched and evaporatively enriched water (two-pool model). The good agreement between model predictions and observations is remarkable as model parameters describing the relevant physical features or functional relationships of soil and vegetation were held constant with one single value for the entire mixed-species ecosystem.

Contributions

RTH, HS and JO designed the study. RTH analysed the data, parameterised the model and performed the modelling with guidance by JO. IS and UO designed the sampling scheme and set up, tested the water extraction unit and performed the diurnal water sampling. RS performed the isotope analyses. SHV analysed the eddy flux data. MMB performed the supplementary controlled environment experiments. RTH and HS wrote the paper, responded to the reviewers' comments and revised the manuscript accordingly after the initial submission. RTH, HS, UO, RS, IS, SHV, KA, JCBC, LW, MMB and JO contributed to the discussion and revision.

3.2 Publication 2:
Temperature-sensitive biochemical ^{18}O-fractionation and humidity-dependent attenuation factor are needed to predict δ^{18}O of cellulose from leaf water in a grassland ecosystem

Regina T. Hirl*, Jérôme Ogée*, Ulrike Ostler, Rudi Schäufele, Juan C. Baca Cabrera, Jianjun Zhu, Inga Schleip, Lisa Wingate, Hans Schnyder*

* Corresponding authors

Published in New Phytologist. doi: 10.1111/nph.17111

Abstract

We explore here our mechanistic understanding of the environmental and physiological processes that determine the oxygen isotope composition of leaf cellulose ($\delta^{18}O_{cellulose}$) in a drought-prone, temperate grassland ecosystem. A new allocation-and-growth model was designed and added to an ^{18}O-enabled soil–vegetation–atmosphere transfer model (MuSICA) to predict seasonal (April–October) and multi-annual (2007–2012) variation of $\delta^{18}O_{cellulose}$ and ^{18}O-enrichment of leaf cellulose ($\Delta^{18}O_{cellulose}$) based on the Barbour–Farquhar model. Modelled $\delta^{18}O_{cellulose}$ agreed best with observations when integrated over *c.* 400 growing-degree-days, similar to the average leaf lifespan observed at the site. Over the integration time, air temperature ranged from 7 to 22 °C and midday relative humidity from 47 to 73%. Model agreement with observations of $\delta^{18}O_{cellulose}$ ($R^2 = 0.57$) and $\Delta^{18}O_{cellulose}$ ($R^2 = 0.74$), and their negative relationship with canopy conductance, was improved significantly when both the biochemical ^{18}O-fractionation between water and substrate for cellulose synthesis (ε_{bio}, range 26–30‰) was temperature-sensitive, as previously reported for aquatic plants and heterotrophically-grown wheat seedlings, and the proportion of oxygen in cellulose reflecting leaf water ^{18}O-enrichment ($1 - p_{ex}\, p_x$, range 0.23–0.63) was dependent on air relative humidity, as observed in independent controlled experiments with grasses. Understanding physiological information in $\delta^{18}O_{cellulose}$ requires quantitative knowledge of climatic effects on $p_{ex}\, p_x$ and ε_{bio}.

Contributions

RTH, JO and HS conceptualized the research. RTH, UO and HS designed the allocation-and-growth module. RTH analyzed the data and performed the modelling with support by JO and UO. RS performed the isotope analysis. HS, UO and IS designed and UO and IS performed the tracer experiment. HS and RTH planned and RTH, JCBC and JZ performed the mesocosm experiment. RTH and HS wrote the paper, responded to the reviewers' comments and revised the manuscript accordingly after the initial submission. RTH, JO, UO, RS, JCBC, JZ, IS, LW and HS contributed to relevant parts of the discussion and the revision of the manuscript.

3.3 Publication 3:
Nitrogen fertilization and δ^{18}O of CO_2 have no effect on ^{18}O-enrichment of leaf water and cellulose in *Cleistogenes squarrosa* (C_4) – is VPD the sole control?

Hai Tao Liu, Xiao Ying Gong, Rudi Schäufele, Fang Yang, Regina Theresia Hirl, Anja Schmidt, Hans Schnyder

Published in Plant, Cell & Environment: 39, 2701–2712, 2016. doi: 10.1111/pce.12824

Abstract

The oxygen isotope composition of cellulose ($\delta^{18}O_{Cel}$) archives hydrological and physiological information. Here, we assess previously unexplored direct and interactive effects of the δ^{18}O of CO_2 ($\delta^{18}O_{CO2}$), nitrogen (N) fertilizer supply and vapour pressure deficit (VPD) on $\delta^{18}O_{Cel}$, ^{18}O-enrichment of leaf water ($\Delta^{18}O_{LW}$) and cellulose ($\Delta^{18}O_{Cel}$) relative to source water, and $p_{ex}\,p_x$, the proportion of oxygen in cellulose that exchanged with unenriched water at the site of cellulose synthesis, in a C_4 grass (*Cleistogenes squarrosa*). $\delta^{18}O_{CO2}$ and N supply, and their interactions with VPD, had no effect on $\delta^{18}O_{Cel}$, $\Delta^{18}O_{LW}$, $\Delta^{18}O_{Cel}$ and $p_{ex}\,p_x$. $\Delta^{18}O_{Cel}$ and $\Delta^{18}O_{LW}$ increased with VPD, while $p_{ex}\,p_x$ decreased. That VPD-effect on $p_{ex}\,p_x$was supported by sensitivity tests to variation of $\Delta^{18}O_{LW}$ and the equilibrium fractionation factor between carbonyl oxygen and water. N supply altered growth and morphological features, but not ^{18}O relations; conversely, VPD had no effect on growth or morphology, but controlled ^{18}O relations. The work implies that reconstructions of VPD from $\Delta^{18}O_{Cel}$ would overestimate amplitudes of VPD variation, at least in this species, if the VPD-effect on $p_{ex}\,p_x$ is ignored. Progress in understanding the relationship between $\Delta^{18}O_{LW}$ and $\Delta^{18}O_{Cel}$ will require separate investigations of p_{ex} and p_x and of their responses to environmental conditions.

Contributions

HS and HTL designed and planned the research. HTL, XYG and FY performed the experiment. HTL analysed the data. HTL, HS, RTH, XYG, FY, and RS discussed the results. HTL and HS wrote the manuscript. All authors contributed to the revision.

3.4 Publication 4:
Atmospheric CO_2 and VPD alter the diel oscillation of leaf elongation in perennial ryegrass: compensation of hydraulic limitation by stored-growth

Juan C. Baca Cabrera, Regina T. Hirl, Jianjun Zhu, Rudi Schäufele, Hans Schnyder

Published in New Phytologist: 227, 1776-1789, 2020. doi: 10.1111/nph.16639

Abstract

We explored the effects of atmospheric CO_2 concentration (C_a) and vapor pressure deficit (VPD) on putative mechanisms controlling leaf elongation in perennial ryegrass. Plants were grown in stands at a C_a of 200, 400 or 800 µmol mol^{-1} combined with high (1.17 kPa) or low (0.59 kPa) VPD during the 16 h-day in well-watered conditions with reduced nitrogen supply. We measured day : night-variation of leaf elongation rate ($LER_{day} : LER_{night}$), final leaf length and width, epidermal cell number and length, stomatal conductance, transpiration, leaf water potential and water-soluble carbohydrates and osmotic potential in the leaf growth-and-differentiation zone (LGDZ). Daily mean LER or morphometric parameters did not differ between treatments, but LER_{night} strongly exceeded LER_{day}, particularly at low C_a and high VPD. Across treatments LER_{day} was negatively related to transpiration ($R^2 = 0.75$) and leaf water potential ($R^2 = 0.81$), while LER_{night} was independent of leaf water potential or turgor. Enhancement of LER_{night} over LER_{day} was proportional to the turgor-change between day and night ($R^2 = 0.93$). LGDZ sugar concentration was high throughout diel cycles, providing no evidence of source limitation in any treatment. Our data indicate a mechanism of diel cycling between daytime hydraulic and night-time stored-growth controls of LER, buffering C_a and daytime VPD effects on leaf elongation.

Contributions

HS, JCBC, RTH and RS designed the experiment. RTH, JCBC and HS set up the protocols for leaf elongation, leaf area and leaf gas exchange measurements and for harvests for carbohydrate analyses. The study consisted of five experimental runs. The experiments and measurements were carried out by RTH, JCBC, JZ and RS. RTH performed a first analysis of leaf gas exchange data. JCBC analysed the data and wrote the first draft. All authors contributed to discussions and to the revision of the manuscript.

4. General and summarising discussion

4.1 General and summarising discussion of publications

This thesis focused on the mechanistic understanding of the processes leading up to the formation of the ^{18}O signal in leaf cellulose from grassland vegetation. In the first part of the modelling work (Hirl *et al.*, 2019), I evaluated our system-scale understanding of the ^{18}O signal transfer from rainwater to soil water, source (pseudo-stem) water and leaf water in a temperate humid grassland ecosystem. The process-based soil-vegetation-atmosphere model MuSICA was used to predict the $\delta^{18}O$ composition of the relevant water pools of the ecosystem, which were compared with fortnightly observations of the isotopic signals. The model produced realistic predictions of the $\delta^{18}O$ composition of soil, xylem and leaf water and of leaf water enrichment relative to source water, indicating that the relevant ecohydrological and ecophysiological processes were described in adequate detail in the model. In particular, I explored the effects of edaphic drought on the grassland community's depth of root water uptake, investigated and disentangled the role of atmospheric and soil moisture on leaf water ^{18}O enrichment, and assessed carry-over effects of plant morpho-physiological parameters on water fluxes and on the dynamics of $\delta^{18}O$ of soil, source and leaf water.

This detailed mechanistic evaluation of the '^{18}O ecohydrology' of the studied grassland then allowed to test hypotheses concerning the propagation of the water isotope signals from leaf and source water to cellulose in grasses. To this end, a new allocation-and-growth module for predicting grass leaf growth and isotope signals was devised and appended to the MuSICA model (Hirl *et al.*, 2020). The allocation-and-growth model predicted the temporal dynamics of maintenance and growth respiration, allocation to shoot and root growth, and the isotopic composition of the plant metabolic pool and of cellulose. Predicted carbon dynamics were validated based on measurements of the metabolic pool turnover, allocation, and leaf life span, obtained from previous investigations at the study site (Gamnitzer *et al.*, 2009; Schleip, 2013; Schleip *et al.*, 2013). Predictions of $\delta^{18}O_{cellulose}$ and $\Delta^{18}O_{cellulose}$ generated by MuSICAgrass were again compared with fortnightly data. The model reproduced well the observed interannual dynamics and conspicuous short-term and seasonal patterns, as well as the relationship between meteorological parameters and cellulose ^{18}O signals. Thereby it lended itself as a well-grounded tool to test hypotheses concerning the attenuation factor ($p_{ex}\,p_x$), biochemical fractionation (ε_{bio}), and stomatal conductance signals in cellulose-^{18}O.

Significance of shallow soil water for root water uptake of grassland vegetation

It was shown in this work that root water uptake at the Grünschwaige grassland site was mainly confined to the uppermost part (<20 cm) of the shallow mineral topsoil for both dry and moist soil conditions (Hirl *et al.*, 2019). No indication for a systematic shift of root water uptake to deeper soil layers was previously reported for other grasslands or savannas (Nippert & Knapp, 2007a,b; Kulmatiski & Beard, 2013; Prechsl *et al.*, 2015). In the present study, the depth of root water uptake was inferred by comparing the $\delta^{18}O$ of pseudo-stem water with the $\delta^{18}O$ of soil water from two depths (7 and 20 cm). Due to the limited spatial resolution of the observed $\delta^{18}O_{soil}$ data, we additionally harnessed the MuSICA model to corroborate the conclusions drawn from the observed data. In particular, we used MuSICA 1) to generate continuous predictions of $\delta^{18}O_{soil}$ along the profile, and thus to interpolate between observed depth positions, 2) to predict the mean (uptake-weighted) root water uptake depth, independently from observed $\delta^{18}O_{soil}$, and 3) to assess the agreement between predicted and observed data for different scenarios of root distributions (see sensitivity analysis in Hirl *et al.*, 2019). The latter analysis showed that model-data agreement deteriorated if roots were supposed to be located in the lower part of the mineral topsoil, as compared to the standard simulation in which most roots were assumed to be located in the upper part (Fig. S8 in Hirl *et al.*, 2019). MuSICA predicted a mean uptake-weighted root water uptake depth above 15 cm in most cases, and a near-monotonous decrease of $\delta^{18}O_{soil}$ from the upper to the lower depth position for many of the sampling dates (see Fig. S13 in Hirl *et al.*, 2019). If $\delta^{18}O_{soil}$ displayed no or little gradients along the soil profile, the information obtained from the comparison between xylem and soil water would be very limited, irrespective of the approach that is adopted to infer the depth of water uptake (e.g. graphical inference, two-end member mixing model or the Bayesian multi-source linear mixing model; see Rothfuss & Javaux, 2017 for a review).

Our conclusions on the main root water uptake zone relied on the oxygen isotope composition. It is worth noting that the same results were obtained if the $\delta^{2}H$ of stem water was compared with the $\delta^{2}H$ of soil water at the two soil depth positions (not shown). This is interesting given the fact that discrepancies between the $\delta^{2}H$ of soil and stem water have been observed in trees, pointing to the existence of isotopically-depleted water storage pools in stems (Barbeta *et al.*, 2019, 2020). Also, Liu *et al.* (2017a) noticed a deuterium depletion of leaf growth zone water as compared to source (nutrient solution or pot) in various grasses grown under controlled and well-watered conditions in climate chambers.Yet, the comparison of pseudo-stem water and soil water at 7 cm observed at Grünschwaige did not provide evidence for deuterium depletion in the pseudo-stems.

The dominant role of air relative humidity for ^{18}O enrichment of leaf water and cellulose

Moreover, I investigated the role of soil and atmospheric moisture status on the ^{18}O signals in leaf water and cellulose, and the implications for the potential use of cellulose-^{18}O as an indicator of stomatal conductance. While relative humidity exerted strong control on $\Delta^{18}O_{leaf}$ and $\Delta^{18}O_{cellulose}$ in samples from the Grünschwaige pasture, a significant effect of edaphic

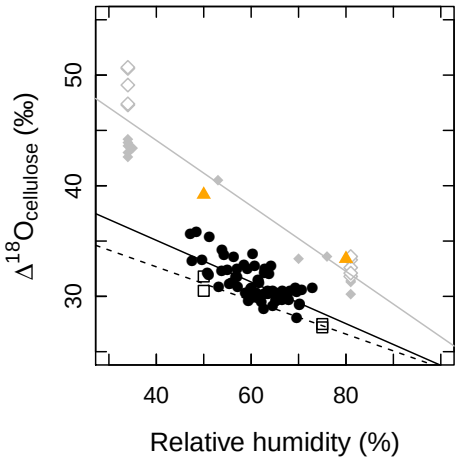

Figure 4.1: Relationship between relative humidity and $\Delta^{18}O_{cellulose}$ from different studies that investigated grass (or grassland) leaf cellulose isotope signals. Black points show the data observed at Grünschwaige (Hirl *et al.*, 2020), open squares represent the data from the two C_3 grasses *Lolium perenne* and *Dactylis glomerata* investigated by Lehmann *et al.* (2017), orange triangles represent $\Delta^{18}O_{cellulose}$ in *Cleistogenes squarrosa* (Liu *et al.*, 2016), grey filled diamonds show $\Delta^{18}O_{cellulose}$ in five C_3 grasses and grey open diamonds $\Delta^{18}O_{cellulose}$ in five C_4 grasses studied by Helliker & Ehleringer (2002a,b). The data from Hirl *et al.* (2020) show the observed $\Delta^{18}O_{cellulose}$ data regressed against midday (± 3 hours around noon) relative humidity. In the experiments of Lehmann *et al.* (2017) and Liu *et al.* (2016), relative humidity was constant throughout day and night. The $\Delta^{18}O_{cellulose}$ data from Helliker & Ehleringer (2002a) and Helliker & Ehleringer (2002b) is plotted against midday and daytime relative humidity, respectively, as reported in the two studies. The grey line indicates the regression line through the pooled data of Helliker & Ehleringer (2002a,b) and Liu *et al.* (2016); the black continuous and the black dashed line display the regression lines for the $\Delta^{18}O_{cellulose}$ data from Hirl *et al.* (2020) and from Lehmann *et al.* (2017), respectively. Regarding the Helliker & Ehleringer (2002b) study, the data from the high (>90%) relative humidity treatment was excluded in the above Figure (as in Helliker & Ehleringer 2002b, their Fig. 7).

drought was detected for $\Delta^{18}O_{leaf}$ but not for $\Delta^{18}O_{cellulose}$ (Hirl *et al.*, 2019, 2020). In line with that, $\Delta^{18}O_{leaf}$ and $\Delta^{18}O_{cellulose}$ in the C_4 grass *Cleistogenes squarrosa* responded strongly to relative humidity (Liu *et al.*, 2016). The *C. squarrosa* dataset did not allow to investigate the role of soil water status on $\Delta^{18}O_{cellulose}$, as all plants were well watered in that experimental setting.

The humidity sensitivity of $\Delta^{18}O_{cellulose}$ in *C. squarrosa* was very similar to the humidity sensitivity of various C_3 and C_4 grasses investigated by Helliker & Ehleringer (2002a,b) (-0.3‰ $\%^{-1}$, calculated as the slope of the linear regression of the pooled data from Helliker & Ehleringer, 2002a,b and Liu *et al.*, 2016), and higher than the humidity sensitivity of the Grünschwaige pasture data (-0.19‰ $\%^{-1}$), and of $\Delta^{18}O_{cellulose}$ data for *Lolium perenne* and *Dactylis glomerata* from Lehmann *et al.* (2017) (-0.15‰ $\%^{-1}$) (Fig. 4.1). Differences in absolute values of $\Delta^{18}O_{cellulose}$ and in its humidity sensitivity may have arisen from differences in $\delta^{18}O_{vapour}$ between studies, from differences in morpho-physiological properties that affect leaf water enrichment, or from deviations between the $\Delta^{18}O$ of bulk leaf water and the $\Delta^{18}O$ of sucrose synthesis water.

Overall, the relations between relative humidity and $\Delta^{18}O_{leaf}$ (Fig. 4 in Hirl *et al.*, 2019) and $\Delta^{18}O_{cellulose}$ (Fig. S3 in Hirl *et al.*, 2020) were well reproduced by the MuSICA model. The model was also used to differentiate between direct and indirect effects of meteorological variables on $\Delta^{18}O_{cellulose}$ of grassland vegetation. In particular, model sensitivity analysis indicated that short-wave radiation did not have a direct effect on $\Delta^{18}O_{cellulose}$, but was correlated with $\Delta^{18}O_{cellulose}$ due to the correlation between short-wave radiation, relative humidity and temperature. Similarly, sensitivity analysis demonstrated that the effect of wind speed on $\Delta^{18}O_{cellulose}$ was not causal. Altogether, the results from this work underline the importance of relative humidity in shaping the ^{18}O enrichment of leaf water and cellulose.

Humidity sensitivity of the attenuation factor

Furthermore, model-data comparison demonstrated the need to include a humidity-dependent attenuation factor ($p_{ex}\,p_x$) when predicting cellulose ^{18}O signals in the Grünschwaige grassland vegetation. Specifically, the pronounced relationship between observed $\Delta^{18}O_{cellulose}$ and relative humidity (see above) was only reproduced by MuSICAgrass if the attenuation factor $p_{ex}\,p_x$ was assumed sensitive to relative humidity. We ascribed this sensitivity to humidity-dependent isotopic imbalances between bulk leaf water and sucrose in grass blades (Hirl *et al.*, 2020). Longitudinal leaf water ^{18}O enrichment gradients from the base to the tip have been reported for grass blades, which are particularly strong at low relative humidity (Helliker & Ehleringer, 2000, 2002a; Gan *et al.*, 2003). If these gradients combine with sucrose synthesis gradients (Williams *et al.*, 1993), it may not be valid to simply predict the $\delta^{18}O$ of sucrose from the $\delta^{18}O$ of bulk leaf water. Data from Lehmann *et al.* (2017) for two C_3 grasses (*L. perenne* and *D. glomerata*) indicated that the $\delta^{18}O$ of sucrose was more sensitive to relative humidity than the $\delta^{18}O$ of leaf water. Then, if $p_{ex}\,p_x$ is calculated from $\Delta^{18}O_{cellulose}$ and $\Delta^{18}O_{leaf}$, the resulting $p_{ex}\,p_x$ will be positively related to relative humidity. Such relative humidity-dependent variation of $p_{ex}\,p_x$ was observed in the controlled environment study with *C. squarrosa* (Liu *et al.*, 2016), and for a range of other C_3 and C_4 grasses (Fig. 1.4b).

Evaporative enrichment gradients may also be found in basipetally growing needles of conifer trees, in which an increasing leaf water enrichment from base to tips has also been observed (Kannenberg *et al.*, 2020). Thus, the results of the present study may have implications for the interpretation of cellulose ^{18}O signals in vegetation and ecosystems other than grassland.

Apart from the uncertainties regarding the $\delta^{18}O$ of sucrose synthesis water, several authors suggested that variation in $p_{ex}\,p_x$ may arise from variation in the rate of futile cycling, which has been related to growth rates or turnover rates of substrate (Barbour & Farquhar, 2000; Ellsworth & Sternberg, 2014; Song *et al.*, 2014; Cheesman & Cernusak, 2017; Szejner *et al.*, 2020). Yet, in the present study, p_{ex} was neither related to the residence time of substrate in the metabolic pool, nor to integration time, which is a function of growth and senescence rates (Hirl *et al.*, 2020). Furthermore, oxygen isotope exchange during phloem loading and transport was discussed as a potential mechanism explaining the lower ^{18}O enrichment of phloem organic matter as compared to leaf organic matter in two coniferous and one broadleaf tree species (Gessler *et al.*, 2013). Whether or not the isotopic composition of sucrose is altered

along its way from the leaf blades of grasses to the leaf growth and differentiation zone is currently unknown.

Temperature sensitivity of biochemical fractionation

In addition, the results from this modelling study demonstrated the importance of including a temperature-sensitive biochemical fractionation (ε_{bio}) for predicting ^{18}O signals in cellulose from grassland vegetation (Hirl *et al.*, 2020). We thus provided first general field-based evidence for a temperature effect on ε_{bio} in terrestrial vegetation. The temperature-sensitivity of ε_{bio} accounted for almost two thirds of the temperature sensitivity of $\Delta^{18}O_{cellulose}$ and counterbalanced the temperature-sensitivity of $\delta^{18}O_{rain}$, which lead to a lack of correlation between $\delta^{18}O_{cellulose}$ and temperature (Hirl *et al.*, 2020). Until then, indication for a temperature-dependent ε_{bio} only came from a compilation of $\Delta^{18}O$ data from aquatic plants and from heterotrophic tissue culture with wheat (Sternberg & Ellsworth, 2011), from a compilation of Sphagnum moss $\delta^{18}O$ data (Xia & Yu, 2020), and from a laboratory experiment with acetone (Sternberg & DeNiro, 1983). Sternberg & DeNiro (1983) experimentally determined the fractionation factors between acetone and water at three different temperatures (15, 25 and 35 °C) and observed that ε_{bio} was higher at 15 and 25 °C than at 35 °C (15 and 25 °C: 28‰; 35 °C: 26‰). For the comparison between 15 and 35 °C, the magnitude and direction of that change of ε_{bio} with temperature parallels with the temperature-sensitivity of ε_{bio} derived by Sternberg & Ellsworth (2011) for aquatic plants: the ε_{bio} estimated from the Sternberg & Ellsworth (2011) function are 27.6‰ for 15 °C and 26.2‰ for 35 °C.

Together, the above results point to the need to consider the effect of temperature on ε_{bio} when interpreting cellulose ^{18}O signals especially from cold, e.g. boreal or temperate biomes, and are of paramount importance for palaeoclimatological or palaeoecological studies. Also, ε_{bio} may affect cellulose-^{18}O in aquatic plants laid down in lacustrine or river sediments, which have been harnessed to infer past $\delta^{18}O$ of lake water (e.g. Mayr *et al.*, 2015) or rain (e.g. Hepp *et al.*, 2015), therewith trying to derive changes in hydrological, climatic or atmospheric circulation patterns (e.g. Mayr *et al.*, 2013; Zhu *et al.*, 2014; Heyng *et al.*, 2015). Besides, cellulose from antarctic moss banks or other peatlands have been frequently used for palaeoclimatic reconstructions (e.g. Royles & Griffiths, 2015; Royles *et al.*, 2016; Roland *et al.*, 2015).

Canopy conductance signal in cellulose-^{18}O

Of note, a significant negative relationship between the $\Delta^{18}O$ (or $\delta^{18}O$) of leaf water and instantaneous canopy conductance, and between the $\Delta^{18}O$ (or $\delta^{18}O$) of leaf cellulose and midday canopy conductance (averaged over the integration time) was found for the data observed at Grünschwaige and for the predicted data (Fig. 4.2). The relation between leaf water ^{18}O enrichment and conductance obviously arose from the effect of stomatal aperture on kinetic fractionation and leaf temperature, since evidence for a Péclet effect was not found for the vegetation at Grünschwaige (Hirl *et al.*, 2019). Considerable scatter was observed in the leaf water ^{18}O vs. canopy conductance plots when conductance was $<300\,mmol\,m^{-2}\,s^{-1}$, coinciding with low soil water contents at 7 cm (Fig. 4.2). Leaf water ^{18}O enrichment was generally enhanced

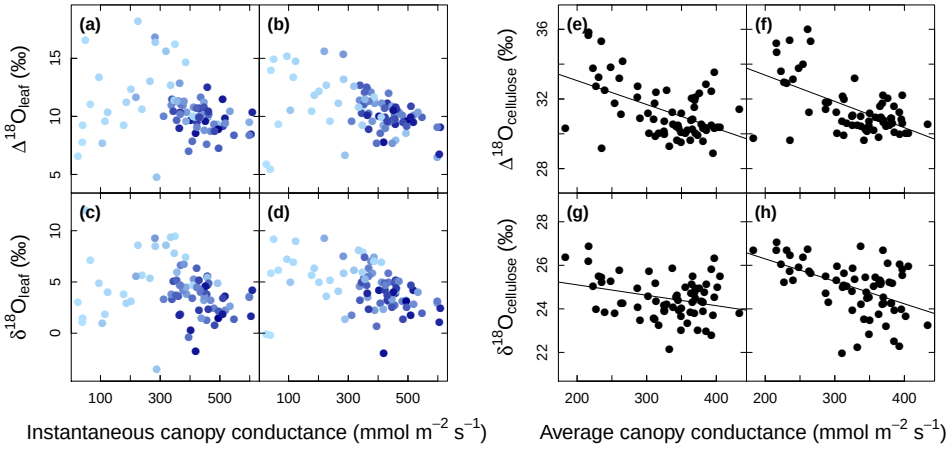

Figure 4.2: Relation between instantaneous canopy conductance and (a) observed and (b) predicted isotopic enrichment of leaf water relative to source water ($\Delta^{18}O_{leaf}$) and (c) observed and (d) predicted isotopic composition of leaf water ($\delta^{18}O_{leaf}$) at Grünschwaige pasture no. 8. Light and dark blue values show soil water contents close to the permanent wilting point and close to field capacity (as in Hirl *et al.*, 2019). Relation between midday canopy conductance averaged over the integration time and (e) observed and (f) predicted isotopic enrichment of cellulose relative to source water ($\Delta^{18}O_{cellulose}$) and (g) observed and (h) predicted isotopic composition of cellulose ($\delta^{18}O_{cellulose}$). Panels (e) to (h) are adapted from Hirl *et al.* (2020). Solid lines indicate the linear regression lines, with regression equations as given in Fig. 8 of Hirl *et al.* (2020).

under dry soil conditions, which was connected to a decrease canopy conductance (Fig. 5 in Hirl *et al.*, 2019). This edaphic drought signal in $\Delta^{18}O_{leaf}$ was not retrieved in $\Delta^{18}O_{cellulose}$ (Fig. S6 in Hirl *et al.*, 2020). Still, we did detect a clear relationship between $\Delta^{18}O_{cellulose}$ and g_s, which lends support to ^{18}O-based interpretations of g_s, $\Delta^{13}C$ and iWUE in grassland ecosystems such as the long-term Park Grass Experiment at Rothamsted (see section 4.2.3). In fact, as sucrose used for cellulose synthesis may be more strongly linked to evaporative conditions than bulk leaf water, the stomatal conductance signal in $\Delta^{18}O_{cellulose}$ may actually be more pronounced than expected from the g_s signal in bulk leaf water enrichment.

Although numerous studies have applied $\delta^{18}O$ to interpret variation in $\delta^{13}C$ (e.g. Sidorova *et al.*, 2009; Barnard *et al.*, 2012; Weigt *et al.*, 2018; Guerrieri *et al.*, 2019), comparably few studies investigated a relation between the $\delta^{18}O$ (or $\Delta^{18}O$) of cellulose or bulk organic matter and stomatal conductance, or reported data that allow to derive such a relation. Those studies are compiled in Table 4.1. g_s values come from single or repeated leaf gas exchange or porometer measurements. Overall, the sensitivities of ^{18}O to g_s ranged between -3.2 and -82.8 ‰ $(mol\,m^{-2}\,s^{-1})^{-1}$. In comparison, the sensitivities of observed (predicted) $\Delta^{18}O_{cellulose}$ and $\delta^{18}O_{cellulose}$ to canopy conductance for the samples from Grünschwaige pasture were -14 (-15) and -5 (-10) ‰ $(mol\,m^{-2}\,s^{-1})^{-1}$. Regarding the studies that analysed both cellulose and bulk organic matter, the sensitivity to alterations of stomatal conductance was higher for bulk organic matter than for cellulose in one study on bread wheat (Barbour *et al.*, 2000b) and in another study on arctic willow (Sullivan & Welker, 2007). In contrast, Barbour & Farquhar (2000) observed an offset between the $\Delta^{18}O$ of cellulose and the $\Delta^{18}O$ of whole leaf tissue, indicating that the sensitivity to stomatal conductance was the same for these two components.

Table 4.1: Overview of studies that reported a relation between $\delta^{18}O_{cellulose}$ or $\Delta^{18}O_{cellulose}$ in leaf cellulose or bulk leaf tissue and stomatal conductance. The sensitivity of ^{18}O to g_s is given in ‰ $(\mathrm{mol\,m^{-2}\,s^{-1}})^{-1}$.

Plant species	Growth conditions	Tissue	Sensitivity	Main cause of g_s variation
Barbour & Farquhar (2000)				
Gossypium hirsutum L.	controlled	$\Delta^{18}O$ bulk leaf	-3.3; $R^2 = 0.92$	abscisic acid
Barbour *et al.* (2000b)				
Triticum aestivum L.	field	$\delta^{18}O$ leaf cellulose	-5.7; $R^2 = 0.79$	genetic (8 cultivars)
Triticum aestivum L.	field	$\delta^{18}O$ bulk leaf	-13.4; $R^2 = 0.86$	genetic (8 cultivars)
Triticum aestivum L.	field	$\delta^{18}O$ bulk grain	-6.2; $R^2 = 0.71$	genetic (8 cultivars)
Chairi *et al.* (2016)				
Zea mays L.	controlled	$\delta^{18}O$ bulk shoot	-20.2; $R^2 = 0.93$	genetic; water availability
Grams *et al.* (2007)				
Fagus sylvatica L. seedlings	controlled	$\delta^{18}O$ leaf cellulose	-28.2; $R^2 = 0.73$	CO_2 O_3; plant competition
Picea abies L. seedlings	controlled	$\delta^{18}O$ leaf cellulose	-20.5; $R^2 = 0.67$	CO_2 O_3; plant competition
Moreno-Gutiérrez *et al.* (2012)				
10 coexisting species	field	$\Delta^{18}O$ leaf cellulose	-82.8; $R^2 = 0.92$	species
Scheidegger *et al.* (2000)				
Festuca rubra L., *Potentilla aurea* L., *Achillea millefolium* L.	field	$\delta^{18}O$ bulk leaf	-5.6; $R^2 = 0.56$	species; land-use intensity
Siegwolf *et al.* (2001)				
Populus × *euramericana*	controlled	$\delta^{18}O$ bulk leaf	-18.6; $R^2 = 0.88$	soil nitrogen supply; air NO_2
Sullivan & Welker (2007)				
Salix arctica Pall.	field	$\Delta^{18}O$ leaf cellulose	-11.5; $R^2 = 0.83$	soil temperature; soil water content
Salix arctica Pall.	field	$\Delta^{18}O$ bulk leaf	-17.9; $R^2 = 0.62$	soil temperature; soil water content
Tankari *et al.* (2019)				
Vigna unguiculata L. Walp.	controlled	$\Delta^{18}O$ bulk leaf	-3.2; $R^2 = 0.83$	water availability; inoculation with rhizobia
Thompson *et al.* (2007)				
Solanum lycopersicum L.	controlled	$\Delta^{18}O$ bulk leaf	-1.6; $R^2 = 0.92$	abscisic acid

While bulk leaf organic matter may contain structural and non-structural carbohydrates, secondary plant metabolites, proteins, lipids and waxes, in likely varying proportions, cellulose is chemically uniform and inert (Haigler *et al.*, 2001). Whether cellulose or bulk organic matter should be used as a proxy for stomatal conductance depends on the scope of the study. The data aggregated in Table 4.1 did not allow to explore systematic differences in the ^{18}O-sensitivity to g_s between plant funtional groups (such as monocots and dicots, or woody and herbaceous plants), or due to different causes of variation in g_s, as the studies reported different measures ($\delta^{18}O$ or $\Delta^{18}O$) in different compartments (cellulose or bulk tissue). In order to detect possible systematic differences between functional groups, one would need to conduct experiments in which only one factor that drives variation in g_s is varied.

Effect of isotopic input data

It was further shown in this work that the prediction accuracy of the seasonal variation of the $\delta^{18}O$ of soil water at the shallower depth and of stem water was higher for 2007 to 2012, when local rainwater $\delta^{18}O$ data were available, as compared to 2006 (see Table 2 in Hirl *et al.*, 2019). Also, model-data agreement for soil, stem and leaf water was worse if IsoGSM $\delta^{18}O_{rain}$ and $\delta^{18}O_{vapour}$ data – once corrected by the mean offset between local and IsoGSM data – were used for 2007 to 2012 (not shown). Regarding cellulose, the agreement between observed $\delta^{18}O_{cellulose}$ and model predictions that were based on offset-corrected IsoGSM data was lower than for the standard simulation, but still relatively high ($R^2 = 0.45$, MBE = 0.7, MAE = 0.9; as compared to $R^2 = 0.57$, MBE = 0.5, MAE = 0.8 in the standard simulation). Besides, IsoGSM based predictions of $\delta^{18}O_{cellulose}$ agreed well with predictions from the standard simulation ($R^2 = 0.86$; Fig. 4.3). This result is encouraging, given the fact that studies exploring $\delta^{18}O_{cellulose}$ from natural ecosystem often have to rely on model predictions of $\delta^{18}O_{rain}$ as local rainwater data are very often missing.

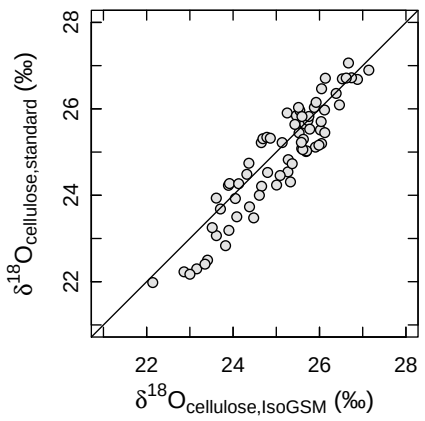

Figure 4.3: Relation between standard predictions of $\delta^{18}O_{cellulose}$ for the Grünschwaige site (shown in Hirl *et al.*, 2020) and model predictions based on IsoGSM $\delta^{18}O_{rain}$ and $\delta^{18}O_{vapour}$ data (each corrected by the mean offset between local rainwater and vapour data and IsoGSM data; see Fig. S3 and S4 in Hirl *et al.*, 2019). The linear regression equation relating standard predictions of $\delta^{18}O_{cellulose}$ to IsoGSM predictions was: $\delta^{18}O_{cellulose,standard} = 1.09\,\delta^{18}O_{cellulose,IsoGSM} - 2.36$; $R^2 = 0.86$; $P < 0.001$ (note that the slope was not significantly different from 1).

Modelling ^{18}O signals in grass cellulose grown in sub-ambient or elevated CO_2 environments: knowledge from controlled environment experiments and future prospects

In the present work, the simulation of cellulose isotope signals was based on predicted daily sums of shoot growth, daily mean values of the isotope ratios of xylem water and the metabolic pool, midday means of the attenuation factor ($p_{ex}\, p_x$), and daily means of ε_{bio} (see Eqn S7 in Hirl *et al.*, 2020). ε_{bio} was calculated from air temperature using the function for aquatic plants reported by Sternberg & Ellsworth (2011). Potential diurnal variation in leaf growth rates was not accounted for in the simulations (e.g. Schnyder & Nelson, 1988; Baca Cabrera *et al.*, 2020). In our controlled environment experiments with *Lolium perenne*, we observed that day-night differences in leaf growth rates were most pronounced under high vapour pressure deficit and half-ambient CO_2 concentration, with leaf elongation rates (given in mm h^{-1}) being approximately twice as high during the night as compared to the day (Baca Cabrera *et al.*, 2020). While diurnal variations in the $\delta^{18}O$ of xylem water and in the $\delta^{18}O$ of the metabolic pool predicted for the Grünschwaige pasture were generally small (<0.5‰ for most days), considerable day to night differences in air temperature were found for that site (10 °C on average for the growing seasons 2007 to 2012). If leaf growth and cellulose synthesis rates are actually higher during the night than during the day, the temperature which is relevant for ε_{bio} might be lower than daily mean temperature, and thus ε_{bio} may in fact be higher. Thus, a diurnally resolved instead of a daily mean ε_{bio} may need to be applied for predictions of $\Delta^{18}O_{cellulose}$ and $\delta^{18}O_{cellulose}$ under high evaporative demand and low atmospheric CO_2 concentration. Also, the data from our controlled environment experiments indicated that the leaf life span was lower at elevated CO_2 (800 ppm) as compared to sub-ambient and ambient CO_2 (200 and 400 ppm) (Juan C. Baca Cabrera, Regina T. Hirl, Jianjun Zhu, Hans Schnyder, unpublished data). Thus, the integration time, which represents the maximum age of structural biomass in a sample, may need to be adjusted if we want to model $\delta^{18}O_{cellulose}$ in plants grown under elevated CO_2.

4.2 Applications of MuSICAgrass

In the following, MuSICAgrass as parameterised in Hirl *et al.* (2019, 2020) is used to predict the deuterium isotopic signatures (δ^2H) of the water pools that had been analyzed for δ^{18}O in Hirl *et al.* (2019). δ^2H was measured concurrently with δ^{18}O using Picarro CRDS. Enlarging knowledge on the δ^2H of ecosystem water pools is of interest with regard to the interpretation of the δ^2H signals in leaf cuticular waxes, which have been used for paleoclimate reconstructions (e.g. Sachse *et al.*, 2012; Kahmen *et al.*, 2013a,b; Gamarra *et al.*, 2016).

The model was further tested for its ability to predict the ^{13}C discrimination of cellulose ($\Delta^{13}C_{cellulose}$), obtained from the same samples that had been analysed for δ^{18}O in Hirl *et al.* (2020) (for details on mass spectrometric analysis of δ^{13}C see Ostler *et al.*, 2016 and Liu *et al.*, 2017b). Finally, the model was used to simulate the δ^{18}O signatures of cellulose in samples from the Park Grass Experiment, located at the Rothamsted Agricultural Research Station in Harpenden (UK). Understanding the formation of $\delta^{18}O_{cellulose}$ from the Park Grass Experiment may help interpret the cause of the increase in intrinsic water-use efficiency observed at that site during the past century (Köhler *et al.*, 2010, 2012, 2016).

4.2.1 Prediction of δ^2H of water pools at Grünschwaige

Observed and predicted soil water at 20 and 7 cm, pseudo-stem water and leaf water are plotted in dual-isotope space in 4.4. All water compartments scattered below the meteoric water line. While predicted and observed soil water at 20 cm depth and leaf water agreed well in the dual-isotope space, predicted soil water at 7 cm and pseudo-stem water lay closer to the meteoric water line than the observed data. This shift of the predicted data towards the meteoric water line may be related to ^{2}H depletion on organic surfaces (Chen *et al.*, 2016), which is currently unaccounted for in MuSICA, and is also reflected in a relatively stronger overestimation of δ^2H relative to δ^{18}O for soil water at 7 cm and stem water (Table 4.2). Also, Chen *et al.* (2020) recently proposed that deuterium depletion of stem water may result from isotopic exchange of organic hydrogen with water during cryogenic vacuum distillation. Thus, the mechanism underlying the ^{2}H depletion is currently under debate and still needs to be resolved.

Table 4.2: Mean bias error (MBE, calculated as described in Hirl *et al.*, 2019) for the comparison between predicted and observed δ^{18}O and δ^2H of ecosystem water pools, along with the ratio of the two MBE values. All entries are given in ‰.

	Soil water 20 cm	Soil water 7 cm	Stem water	Leaf water
MBE δ^{18}O	0.48	0.77	0.37	0.30
MBE δ^2H	4.54	10.30	7.98	0.27
MBE δ^2H : MBE δ^{18}O	9.46	13.38	21.57	0.90

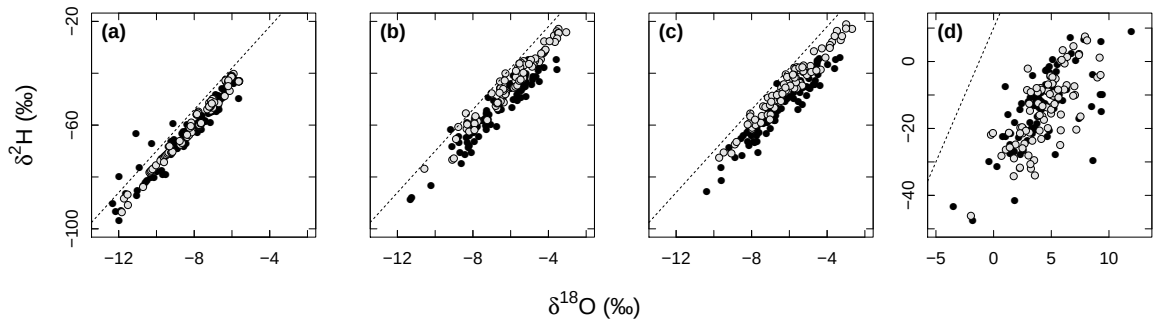

Figure 4.4: Relationship between the δ^2H and δ^{18}O of (a) soil water at 20 cm depth, (b) soil water at 7 cm, (c) pseudo-stem water, and (d) leaf water. Black points depict the data observed at the Grünschwaige pasture and grey points represent the predicted data. The dashed line in each panel represents the Global Meteoric Water Line ($\delta^2\mathrm{H} = 8\,\delta^{18}\mathrm{O} + 10‰$), which corresponds to the local meteoric water line at the study site.

4.2.2 Prediction of $\Delta^{13}\mathbf{C_{cellulose}}$ and of the relation between $\Delta^{13}\mathbf{C_{cellulose}}$ and $\Delta^{18}\mathbf{O_{cellulose}}$

Predictions of $\Delta^{13}\mathrm{C_{cellulose}}$ made with the standard parameterisation from Hirl *et al.* (2019, 2020) qualitatively reproduced the observed $\Delta^{13}\mathrm{C_{cellulose}}$ patterns (Fig. 4.5a). However, considerable discrepancies between predicted and observed data were found particularly early in the growing season (2007, 2008, 2011), and in late summer (mainly 2009 and 2011), which led to a relatively poor quantitative agreement for the pooled data ($R^2 = 0.12$; Fig. 4.6a). Model-data agreement for $\Delta^{13}\mathrm{C_{cellulose}}$ was improved dramatically when seasonally-adjusted values of stomatal and photosynthetic parameters were applied ($R^2 = 0.64$; Fig. 4.5a and 4.6b). This adjustment included a lower slope of the Ball-Woodrow-Berry (BWB) stomatal conductance model (m_{gs}; Ball *et al.*, 1987) in spring and a higher value in summer/autumn, as well as decreased photosynthetic capacity in late summer and autumn (Table 4.3). Alteration of the slope of the BWB model changes the responsiveness of stomatal conductance to assimilation rate, and thus the ratio of assimilation to stomatal conductance, i.e. intrinsic water-use efficiency (Ball *et al.*, 1987; Miner *et al.*, 2017). Lower photosynthetic capacity in late summer/autumn is in accordance with a lower sink capacity and poor light penetration into a vegetative canopy in autumn as compared to reproductive swards in spring (Deinum, 1976). Importantly, the change of these parameters had a very minor effect on the prediction of $\Delta^{18}\mathrm{O_{cellulose}}$ (Fig. 4.5b), and did not change the conclusions from Hirl *et al.* (2020) concerning the relative humidity-dependence of $p_{\mathrm{ex}}\,p_{\mathrm{x}}$ and the temperature-sensitivity of $\varepsilon_{\mathrm{bio}}$. Furthermore, the modified model (Table 4.3) replicated well the observed positive relation between$\Delta^{18}\mathrm{O_{cellulose}}$ and -$\Delta^{13}\mathrm{C_{cellulose}}$ (Fig. 4.7), which is indicative of strong stomatal control of the ^{13}C signal (Scheidegger *et al.*, 2000; Grams *et al.*, 2007).

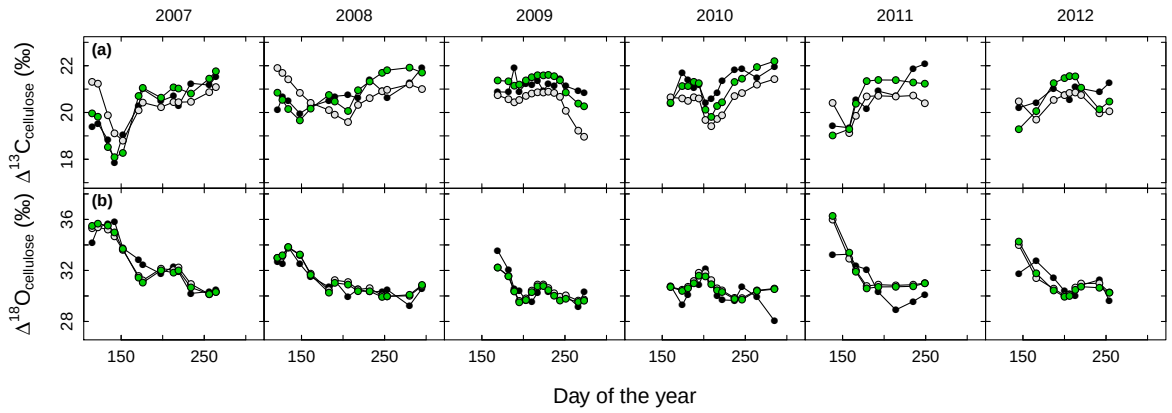

Figure 4.5: Time courses of $\Delta^{13}C_{cellulose}$ and $\Delta^{18}O_{cellulose}$ from samples collected at pasture no. 8 of Grünschwaige Grassland Research station. Black points illustrate the observed data and light grey points the data predicted with the standard parameterisation of Hirl *et al.* (2019, 2020). Green points show model predictions made with adjusted stomatal and photosynthetic parameters as explained in the main text (see also Table 4.3).

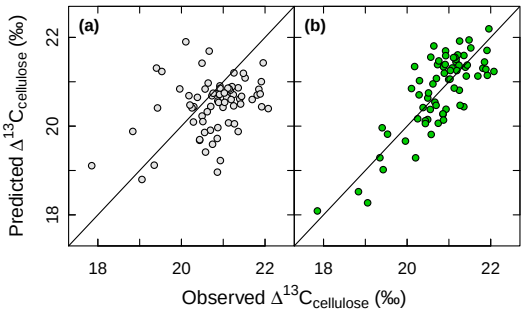

Figure 4.6: Scatter plots showing the relationships between $\Delta^{13}C_{cellulose}$ observed at pasture no. 8 of Grünschwaige Grassland Research station and $\Delta^{13}C_{cellulose}$ predicted (a) with the standard parameterisation of (Hirl *et al.*, 2019, 2020), and (b) based on adjusted stomatal and photosynthetic parameters (see Table 4.3).

Table 4.3: Parameter values for stomatal responsiveness (m_{gs}), maximum rate of carboxylation at 25 °C (V_{cmax}) and potential rate of electron transport at 25 °C (J_{max}) applied in the standard simulation and in the adjusted simulation. For equations on stomatal and photosynthetic submodels, the reader is referred to Hirl *et al.* (2019) and Ogée (2000).

	m_{gs}	V_{cmax} (µmol m^{-2} s^{-1})	J_{max} (µmol m^{-2} s^{-1})
Standard simulation			
whole year	10	60	100
Adjusted			
1 January – 15 May	7	60	100
16 May –15 August	12	60	100
16 August – 31 December	12	30	50

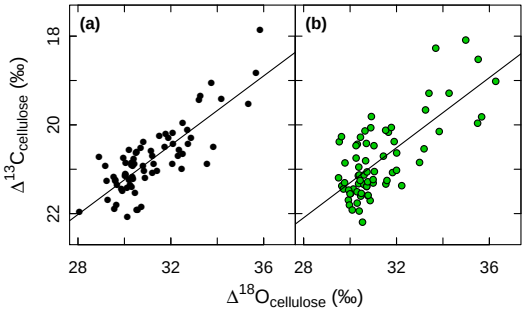

Figure 4.7: Relationship between $\Delta^{13}C_{cellulose}$ and $\Delta^{18}O_{cellulose}$ (a) for the data observed at Grünschwaige pasture no. 8, and (b) for data predicted based on the adjusted parameterisation (Table 4.3). Note that the y-axis is inverted (as in Grams *et al.*, 2007). The slopes of the above regressions were not significantly different from each other.

4.2.3 Prediction of $\delta^{18}O_{cellulose}$ in samples from the Rothamsted Park Grass Experiment

As one aim of the project was to understand the significance of $\delta^{18}O_{cellulose}$ for the interpretation of last century water-use efficiency changes at the Park Grass experiment, I used MuSICAgrass in its standard parameterisation (for pasture no. 8 of Grünschwaige Grassland Research station) to compare model predictions and observations of $\delta^{18}O_{cellulose}$ in samples from the Park Grass Experiment (PGE), using forcing files that were available for an 18 years-long period (1993–2010). Established in 1856 as a fertilization trial, the Park Grass Experiment is now the world's oldest experiment on permanent grassland (for an overview see Silvertown *et al.*, 2006; Storkey *et al.*, 2015). The individual plots of the PGE receive different amounts and combinations of inorganic fertilizer (including N, P, K, Mg, Na, S) or manure, and various amounts of chalk. Additionally, the experiment also runs unfertilized control plots. Treatments differ profoundly in soil pH, botanical composition, species diversity, and yield (e.g. Jenkinson *et al.*, 1994; Crawley *et al.*, 2005). All plots are cut each year in June, and dried bulk aboveground biomass samples from each plot and harvest have been stored in the Rothamsted sample archive since the inception of the experiment. Hay samples from that archive were analysed for $\delta^{18}O_{cellulose}$ following the procedures described in Hirl *et al.* (2020).

The observed data presented in Fig. 4.8 represent average $\delta^{18}O$ values of samples from the limed and unlimed control plots, and from the limed subplots of the PK, N1, N*1 and N*1PK plots (see description in the legend of Fig. 4.8). In the simulation, the integration time was set to two months, assuming that cellulose samples integrate cellulose synthesized in May and June until the yearly cut. Model predictions reproduced relatively well the observed patterns, in particular the year-to-year variation in $\delta^{18}O_{cellulose}$. This is encouraging given the fact that the model parameterisation was not adjusted to the Park Grass site, and suggests that meteorological drivers have similar effects at the Grünschwaige and Rothamsted grassland sites. In going forward it will be necessary to reparameterise MuSICAgrass using soil and vegetation properties at the Rothamsted site.

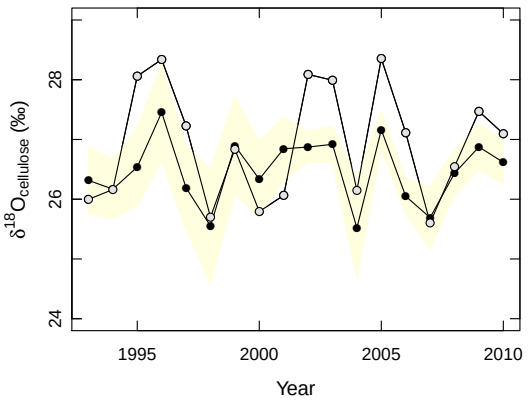

Figure 4.8: Time course of the oxygen isotope composition of cellulose ($\delta^{18}O_{cellulose}$) observed in mixed-species grassland samples of the Park Grass Experiment at Rothamsted Research Station, UK (black points, with 95% confidence band displayed in yellow). Model predictions obtained with the standard parameterisation for pasture 8 at Grünschwaige Grassland Research Station are illustrated in grey. Predicted isotope ratios of xylem water and of the metabolic pool (see Eqn S7 in Hirl *et al.*, 2020) were averaged over a two-month period (May and June). The observed data are average values of $\delta^{18}O_{cellulose}$ from plots 2/2a and 3a (limed control plots), 2/2d and 3d (unlimed control plots), 7a and 15a (limed PK plots), 1a (limed N1 plot, receiving 48 kg N as ammonium sulphate), 17a (limed N*1 plot, receiving 48 kg N as sodium nitrate), and 16a (limed N*1PK plot, receiving 48 kg N as sodium nitrate, plus P and K).

4.3 Conclusions and perspective

This work provided a mechanistic framework for simulating isotope signals in water pools and cellulose of a grassland ecosystem. Overall, the model performed well in predicting $\delta^{18}O$ signals. Model predictions of the ecohydrology of the system were utilized to explore the effect of edaphic drought on leaf water ^{18}O enrichment and root water uptake depth. Application of the model to deuterium revealed offsets between predicted and observed source water and predicted and observed soil water at 7 cm, when $\delta^{18}O$ and $\delta^{2}H$ were plotted in dual-isotope space. The mechanisms underlying these offsets still need to be clarified. Then, a mechanistic description of deuterium depletion will need to be implemented in ecosystem models like MuSICA.

The use of the combined model (MuSICAgrass) allowed separation of the effects of temperature and relative humidity on biochemical fractionation and the attenuation factor. Thus, this work provided first field-based evidence for the temperature-sensitivity of ε_{bio} and the humidity-sensitivity of $p_{ex}\,p_x$ in a terrestrial ecosystem, with the latter effect potentially linked to humidity-dependent evaporative enrichment gradients and sucrose synthesis gradients along grass leaf blades. Future studies should be directed at testing two major steps of the ^{18}O signal transfer from leaf water to leaf cellulose of grassland vegetation: 1) the relationship between the $\Delta^{18}O$ of leaf water and the $\Delta^{18}O$ of sucrose extracted from leaves, and variation of this relation as a response to environmental conditions, and 2) isotopic differences between the $\Delta^{18}O$ of sucrose extracted from leaves and the $\Delta^{18}O$ of sucrose extracted from the phloem or growth zone. Clarification of these steps will allow significantly better understanding of the $\delta^{18}O$ signal in cellulose. Also, it will help to quantify the effect of futile cycling in developing cells on in vivo variation of p_{ex}. Furthermore, the biochemical mechanisms and their associated

isotope effects that underlie the temperature effect on biochemical fractionation remain to be elucidated.

Reasonable prediction of ^{13}C discrimination in cellulose samples based on MuSICAgrass required seasonally variable stomatal and photosynthetic parameters, an adjustment that had a negligible effect on the prediction of ^{18}O signals. How seasonal variation in stomatal and photosynthetic properties is related to water use efficiency and water use strategies of grassland might be explored in future work.

Bibliography

Adams MA, Buckley TN, Turnbull TL (2020) Diminishing CO_2-driven gains in water-use efficiency of global forests. *Nature Climate Change* **10**: 466–471.

Ainsworth EA, Long SP (2005) What have we learned from 15 years of free-air CO_2 enrichment (FACE)? A meta-analytic review of the responses of photosynthesis, canopy properties and plant production to rising CO_2. *New Phytologist* **165**: 351–372.

Ainsworth EA, Rogers A (2007) The response of photosynthesis and stomatal conductance to rising [CO_2]: mechanisms and environmental interactions. *Plant, Cell & Environment* **30**: 258–270.

Anderson WT, Bernasconi SM, McKenzie JA, Saurer M (1998) Oxygen and carbon isotopic record of climatic variability in tree ring cellulose (*Picea abies*): An example from central Switzerland (1913–1995). *Journal of Geophysical Research: Atmospheres* **103**: 31,625–31,636.

Araguás-Araguás L, Froehlich K, Rozanski K (2000) Deuterium and oxygen-18 isotope composition of precipitation and atmospheric moisture. *Hydrological Processes* **14**: 1341–1355.

Asbjornsen H, Shepherd G, Helmers M, Mora G (2008) Seasonal patterns in depth of water uptake under contrasting annual and perennial systems in the Corn Belt Region of the Midwestern U.S. *Plant and Soil* **308**: 69–92.

Baca Cabrera JC, Hirl RT, Zhu J, Schäufele R, Schnyder H (2020) Atmospheric CO_2 and VPD alter the diel oscillation of leaf elongation in perennial ryegrass: compensation of hydraulic limitation by stored-growth. *New Phytologist* **227**: 1776–1789.

Ball JT, Woodrow IE, Berry JA (1987) A model predicting stomatal conductance and its contribution to the control of photosynthesis under different environmental conditions. In: Biggins J (ed) Progress in Photosynthesis Research (vol. 4), Martinus Nijhoff Publishers, Dordrecht, the Netherlands, pp 221–224.

Barbeta A, Peñuelas J (2017) Relative contribution of groundwater to plant transpiration estimated with stable isotopes. *Scientific reports* **7**: 1–10.

Barbeta A, Jones SP, Clavé L, Wingate L, Gimeno TE, Fréjaville B, Wohl S, Ogée J (2019) Unexplained hydrogen isotope offsets complicate the identification and quantification

of tree water sources in a riparian forest. *Hydrology and Earth System Sciences* **23**: 2129–2146.

Barbeta A, Gimeno TE, Clavé L, Fréjaville B, Jones SP, Delvigne C, Wingate L, Ogée J (2020) An explanation for the isotopic offset between soil and stem water in a temperate tree species. *New Phytologist* **227**: 766–779.

Barbosa ICR, Köhler IH, Auerswald K, Lüps P, Schnyder H (2010) Last-century changes of alpine grassland water-use efficiency: a reconstruction through carbon isotope analysis of a time-series of *Capra ibex* horns. *Global Change Biology* **16**: 1171–1180.

Barbour MM (2007) Stable oxygen isotope composition of plant tissue: a review. *Functional Plant Biology* **34**: 83–94.

Barbour MM, Farquhar GD (2000) Relative humidity- and ABA-induced variation in carbon and oxygen isotope ratios of cotton leaves. *Plant, Cell & Environment* **23**: 473–485.

Barbour MM, Farquhar GD (2004) Do pathways of water movement and leaf anatomical dimensions allow development of gradients in $H_2{}^{18}O$ between veins and the sites of evaporation within leaves? *Plant, Cell & Environment* **27**: 107–121.

Barbour MM, Schurr U, Henry BK, Wong SC, Farquhar GD (2000a) Variation in the oxygen isotope ratio of phloem sap sucrose from castor bean. Evidence in support of the Péclet effect. *Plant Physiology* **123**: 671–679.

Barbour MM, Fischer RA, Sayre KD, Farquhar GD (2000b) Oxygen isotope ratio of leaf and grain material correlates with stomatal conductance and grain yield in irrigated wheat. *Australian Journal of Plant Physiology* **27**: 625–637.

Barbour MM, Walcroft AS, Farquhar GD (2002) Seasonal variation in $\delta^{13}C$ and $\delta^{18}O$ of cellulose from growth rings of *Pinus radiata*. *Plant, Cell & Environment* **25**: 1483–1499.

Barbour MM, Roden JS, Farquhar GD, Ehleringer JR (2004) Expressing leaf water and cellulose oxygen isotope ratios as enrichment above source water reveals evidence of a Péclet effect. *Oecologia* **138**: 426–435.

Barbour MM, Farquhar GD, Buckley TN (2017) Leaf water stable isotopes and water transport outside the xylem. *Plant, Cell & Environment* **40**: 914–920.

Barnard HR, Brooks JR, Bond BJ (2012) Applying the dual-isotope conceptual model to interpret physiological trends under uncontrolled conditions. *Tree Physiology* **32**: 1183–1198.

Barnard RL, de Bello F, Gilgen AK, Buchmann N (2006) The $\delta^{18}O$ of root crown water best reflects source water $\delta^{18}O$ in different types of herbaceous species. *Rapid Communications in Mass Spectrometry* **20**: 3799–3802.

Bögelein R, Thomas FM, Kahmen A (2017) Leaf water ^{18}O and ^{2}H enrichment along vertical canopy profiles in a broadleaved and a conifer forest tree. *Plant, Cell & Environment* **40**: 1086–1103.

Bowen GJ, Cai Z, Fiorella RP, Putman AL (2019) Isotopes in the water cycle: Regional- to global-scale patterns and applications. *Annual Review of Earth and Planetary Sciences* **47**: 453–479.

Bowling DR, Schulze ES, Hall SJ (2017) Revisiting streamside trees that do not use stream water: can the two water worlds hypothesis and snowpack isotopic effects explain a missing water source? *Ecohydrology* **10**: e1771, e1771 ECO-16-0104.R1.

Boyer JS (1970) Leaf enlargement and metabolic rates in corn, soybean, and sunflower at various leaf water potentials. *Plant Physiology* **46**: 233–235.

Braud I, Bariac T, Gaudet JP, Vauclin M (2005a) SiSPAT-Isotope, a coupled heat, water and stable isotope (HDO and $H_2{}^{18}O$) transport model for bare soil. Part I. Model description and first verifications. *Journal of Hydrology* **309**: 277–300.

Braud I, Bariac T, Vauclin M, Boujamlaoui Z, Gaudet JP, Biron P, Richard P (2005b) SiSPAT-Isotope, a coupled heat, water and stable isotope (HDO and $H_2{}^{18}O$) transport model for bare soil. Part II. Evaluation and sensitivity tests using two laboratory data sets. *Journal of Hydrology* **309**: 301–320.

Brendel O, Iannetta PPM, Stewart D (2000) A rapid and simple method to isolate pure alpha-cellulose. *Phytochemical Analysis* **11**: 7–10.

Brinkmann N, Seeger S, Weiler M, Buchmann N, Eugster W, Kahmen A (2018) Employing stable isotopes to determine the residence times of soil water and the temporal origin of water taken up by *Fagus sylvatica* and *Picea abies* in a temperate forest. *New Phytologist* **219**: 1300–1313.

Brooks JR, Coulombe R (2009) Physiological responses to fertilization recorded in tree rings: isotopic lessons from a long-term fertilization trial. *Ecological Applications* **19**: 1044–1060.

Brooks JR, Mitchell AK (2011) Interpreting tree responses to thinning and fertilization using tree-ring stable isotopes. *New Phytologist* **190**: 770–782.

Brooks JR, Barnard HR, Coulombe R, McDonnell JJ (2010) Ecohydrologic separation of water between trees and streams in a Mediterranean climate. *Nature Geoscience* **3**: 100–104.

Cernusak LA, Pate JS, Farquhar GD (2002) Diurnal variation in the stable isotope composition of water and dry matter in fruiting *Lupinus angustifolius* under field conditions. *Plant, Cell & Environment* **25**: 893–907.

Cernusak LA, Wong SC, Farquhar GD (2003) Oxygen isotope composition of phloem sap in relation to leaf water in *Ricinus communis*. *Functional Plant Biology* **30**: 1059–1070.

Cernusak LA, Farquhar GD, Wong SC, Stuart-Williams H (2004) Measurement and interpretation of the oxygen isotope composition of carbon dioxide respired by leaves in the dark. *Plant Physiology* **136**: 3350–3363.

Cernusak LA, Farquhar GD, Pate JS (2005) Environmental and physiological controls over oxygen and carbon isotope composition of Tasmanian blue gum, *Eucalyptus globulus*. *Tree Physiology* **25**: 129–146.

Cernusak LA, Barbour MM, Arndt SK, Cheesman AW, English NB, Feild TS, Helliker BR, Holloway-Phillips MM, Holtum JAM, Kahmen A, McInerney FA, Munksgaard NC, Simonin KA, Song X, Stuart-Williams H, West JB, Farquhar GD (2016) Stable isotopes in leaf water of terrestrial plants. *Plant, Cell & Environment* **39**: 1087–1102.

Cernusak LA, Ubierna N, Jenkins MW, Garrity SR, Rahn T, Powers HH, Hanson DT, Sevanto S, Wong SC, McDowell NG, Farquhar GD (2018) Unsaturation of vapour pressure inside leaves of two conifer species. *Scientific reports* **8**: 1–7.

Chairi F, Elazab A, Sanchez-Bragado R, Araus JL, Serret MD (2016) Heterosis for water status in maize seedlings. *Agricultural Water Management* **164**: 100–109.

Cheesman AW, Cernusak LA (2017) Infidelity in the outback: climate signal recorded in $\Delta^{18}O$ of leaf but not branch cellulose of eucalypts across an Australian aridity gradient. *Tree Physiology* **37**: 554–564.

Chen G, Auerswald K, Schnyder H (2016) ^{2}H and ^{18}O depletion of water close to organic surfaces. *Biogeosciences* **13**: 3175–3186.

Chen Y, Helliker BR, Tang X, Li F, Zhou Y, Song X (2020) Stem water cryogenic extraction biases estimation in deuterium isotope composition of plant source water. *Proceedings of the National Academy of Sciences*. https://doi.org/10.1073/pnas.2014422117.

Craig H, Gordon LI (1965) Deuterium and oxygen 18 variations in the ocean and the marine atmosphere. In: Tongiorgi E (ed) Stable isotopes in oceanographic studies and paleotemperatures, Consiglio Nazionale Delle Ricerche, Laboratorio di Geologia Nucleare, Pisa, Italy, pp 9–130.

Crawley MJ, Johnston AE, Silvertown J, Dodd M, de Mazancourt C, Heard MS, Henman DF, Edwards GR (2005) Determinants of species richness in the Park Grass Experiment. *The American Naturalist* **165**: 179–192.

Cuntz M, Ogée J, Farquhar GD, Peylin P, Cernusak LA (2007) Modelling advection and diffusion of water isotopologues in leaves. *Plant, Cell & Environment* **30**: 892–909.

Damesin C, Lelarge C (2003) Carbon isotope composition of current-year shoots from *Fagus sylvatica* in relation to growth, respiration and use of reserves. *Plant, Cell & Environment* **26**: 207–219.

Dansgaard W (1964) Stable isotopes in precipitation. *Tellus* **16**: 436–468.

Deinum B (1976) Photosynthesis and sink size: An explanation for the low productivity of grass swards in autumn. *Netherlands Journal of Agricultural Science* **24**: 238–246.

DeNiro MJ, Epstein S (1981) Isotopic composition of cellulose from aquatic organisms. *Geochimica et Cosmochimica Acta* **45**: 1885–1894.

Dongmann G, Nürnberg HW, Förstel H, Wagener K (1974) On the enrichment of $h_2{}^{18}o$ in the leaves of transpiring plants. *Radiation and Environmental Biophysics* **11**: 41–52.

Dubbert M, Werner C (2019) Water fluxes mediated by vegetation: emerging isotopic insights at the soil and atmosphere interfaces. *New Phytologist* **221**: 1754–1763.

Dubbert M, Cuntz M, Piayda A, Maguás C, Werner C (2013) Partitioning evapotranspiration – Testing the Craig and Gordon model with field measurements of oxygen isotope ratios of evaporative fluxes. *Journal of Hydrology* **496**: 142–153.

Dubbert M, Cuntz M, Piayda A, Werner C (2014) Oxygen isotope signatures of transpired water vapor: the role of isotopic non-steady-state transpiration under natural conditions. *New Phytologist* **203**: 1242–1252.

Duquesnay A, Bréda N, Stievenard M, Dupouey JL (1998) Changes of tree-ring $\delta^{13}C$ and water-use efficiency of beech (*Fagus sylvatica* L.) in north-eastern France during the past century. *Plant, Cell & Environment* **21**: 565–572.

Durand JL, Onillon B, Schnyder H, Rademacher I (1995) Drought effects on cellular and spatial parameters of leaf growth in tall fescue. *Journal of Experimental Botany* **46**: 1147–1155.

Ehleringer JR, Hall AE, Farquhar GD (eds) (1993) Stable isotopes and plant carbon-water relations. Academic Press, San Diego, California, USA.

Ellsworth PV, Sternberg LSL (2014) Biochemical effects of salinity on oxygen isotope fractionation during cellulose synthesis. *New Phytologist* **202**: 784–789.

Ellsworth PZ, Williams DG (2007) Hydrogen isotope fractionation during water uptake by woody xerophytes. *Plant and Soil* **291**: 93–107.

Ellsworth PZ, Ellsworth PV, Cousins AB (2017) Relationship of leaf oxygen and carbon isotopic composition with transpiration efficiency in the C_4 grasses *Setaria viridis* and *Setaria italica*. *Journal of Experimental Botany* **68**: 3513–3528.

Epstein S, Thompson P, Yapp CJ (1977) Oxygen and hydrogen isotopic ratios in plant cellulose. *Science* **198**: 1209–1215.

Farquhar GD, Cernusak LA (2005) On the isotopic composition of leaf water in the non-steady state. *Functional Plant Biology* **32**: 293–303.

Farquhar GD, Cernusak LA (2012) Ternary effects on the gas exchange of isotopologues of carbon dioxide. *Plant, Cell & Environment* **35**: 1221–1231.

Farquhar GD, Gan KS (2003) On the progressive enrichment of the oxygen isotopic composition of water along a leaf. *Plant, Cell & Environment* **26**: 1579–1597.

Farquhar GD, Lloyd J (1993) Carbon and oxygen isotope effects in the exchange of carbon dioxide between terrestrial plants and the atmosphere. In: Ehleringer JR, Hall AE, Farquhar GD (eds) Stable isotopes and plant carbon-water relations, Academic Press, San Diego, California, USA, pp 47–70.

Farquhar GD, Richards RA (1984) Isotopic composition of plant carbon correlates with water-use efficiency of wheat genotypes. *Australian Journal of Plant Physiology* **11**: 539–552.

Farquhar GD, O'Leary MH, Berry JA (1982) On the relationship between carbon isotope discrimination and the intercellular carbon dioxide concentration in leaves. *Functional Plant Biol* **9**: 121–137.

Farquhar GD, Ehleringer JR, Hubick KT (1989) Carbon isotope discrimination and photosynthesis. *Annual Review of Plant Physiology and Plant Molecular Biology* **40**: 503–537.

Farquhar GD, Barbour MM, Henry BK (1998) Interpretation of oxygen isotope composition of leaf material. In: Griffiths H (ed) Stable isotopes: integration of biological, ecological and geochemical processes, BIOS Scientific Publishers, Oxford, UK, pp 27–61.

Farquhar GD, Cernusak LA, Barnes B (2007) Heavy water fractionation during transpiration. *Plant Physiology* **143**: 11–18.

Ferrio JP, Pou A, Florez-Sarasa I, Gessler A, Kodama N, Flexas J, Ribas-Carbó M (2012) The Péclet effect on leaf water enrichment correlates with leaf hydraulic conductance and mesophyll conductance for CO_2. *Plant, Cell & Environment* **35**: 611–625.

Fiorella RP, West JB, Bowen GJ (2019) Biased estimates of the isotope ratios of steady-state evaporation from the assumption of equilibrium between vapour and precipitation. *Hydrological Processes* **33**: 2576–2590.

Flanagan LB, Farquhar GD (2014) Variation in the carbon and oxygen isotope composition of plant biomass and its relationship to water-use efficiency at the leaf- and ecosystem-scales in a northern Great Plains grassland. *Plant, Cell & Environment* **37**: 425–438.

Flanagan LB, Comstock JP, Ehleringer JR (1991) Comparison of modeled and observed environmental influences on the stable oxygen and hydrogen isotope composition of leaf water in *Phaseolus vulgaris* L. *Plant Physiology* **96**: 588–596.

Franks PJ, Adams MA, Amthor JS, Barbour MM, Berry JA, Ellsworth DS, Farquhar GD, Ghannoum O, Lloyd J, McDowell N, Norby RJ, Tissue DT, von Caemmerer S (2013) Sensitivity of plants to changing atmospheric CO_2 concentration: from the geological past to the next century. *New Phytologist* **197**: 1077–1094.

von Freyberg J, Allen ST, Grossiord C, Dawson TE (2020) Plant and root-zone water isotopes are difficult to measure, explain, and predict: Some practical recommendations for determining plant water sources. *Methods in Ecology and Evolution* **11**: 1352–1367.

Gamarra B, Sachse D, Kahmen A (2016) Effects of leaf water evaporative ^{2}H-enrichment and biosynthetic fractionation on leaf wax *n*-alkane δ^{2}H values in C3 and C4 grasses. *Plant, Cell & Environment* **39**: 2390–2403.

Gamnitzer U, Schäufele R, Schnyder H (2009) Observing ^{13}C labelling kinetics in CO_2 respired by a temperate grassland ecosystem. *New Phytologist* **184**: 376–386.

Gamnitzer U, Moyes AB, Bowling DR, Schnyder H (2011) Measuring and modelling the isotopic composition of soil respiration: insights from a grassland tracer experiment. *Biogeosciences* **8**: 1333–1350.

Gan KS, Wong SC, Yong JWH, Farquhar GD (2002) ^{18}O spatial patterns of vein xylem water, leaf water, and dry matter in cotton leaves. *Plant Physiology* **130**: 1008–1021.

Gan KS, Wong SC, Yong JWH, Farquhar GD (2003) Evaluation of models of leaf water ^{18}O enrichment using measurements of spatial patterns of vein xylem water, leaf water and dry matter in maize leaves. *Plant, Cell & Environment* **26**: 1479–1495.

Gangi L, Rothfuss Y, Ogée J, Wingate L, Vereecken H, Brüggemann N (2015) A new method for in situ measurements of oxygen isotopologues of soil water and carbon dioxide with high time resolution. *Vadose Zone Journal* **14**, vzj2014.11.0169.

Gat JR (1996) Oxygen and hydrogen isotopes in the hydrologic cycle. *Annual Review of Earth and Planetary Sciences* **24**: 225–262.

Gaudinski JB, Dawson TE, Quideau S, Schuur EAG, Roden JS, Trumbore SE, Sandquist DR, Oh SW, Wasylishen RE (2005) Comparative analysis of cellulose preparation techniques for use with ^{13}C, ^{14}C, and ^{18}O isotopic measurements. *Analytical Chemistry* **77**: 7212–7224.

Gerlein-Safdi C, Gauthier PPG, Sinkler CJ, Caylor KK (2017) Leaf water ^{18}O and ^{2}H maps show directional enrichment discrepancy in *Colocasia esculenta*. *Plant, Cell & Environment* **40**: 2095–2108.

Gessler A, Brandes E, Buchmann N, Helle G, Rennenberg H, Barnard RL (2009) Tracing carbon and oxygen isotope signals from newly assimilated sugars in the leaves to the tree-ring archive. *Plant, Cell & Environment* **32**: 780–795.

Gessler A, Brandes E, Keitel C, Boda S, Kayler ZE, Granier A, Barbour M, Farquhar GD, Treydte K (2013) The oxygen isotope enrichment of leaf-exported assimilates – does it always reflect lamina leaf water enrichment? *New Phytologist* **200**: 144–157.

Gessler A, Ferrio JP, Hommel R, Treydte K, Werner RA, Monson RK (2014) Stable isotopes in tree rings: towards a mechanistic understanding of isotope fractionation and mixing processes from the leaves to the wood. *Tree Physiology* **34**: 796–818.

Giuggiola A, Ogée J, Rigling A, Gessler A, Bugmann H, Treydte K (2016) Improvement of water and light availability after thinning at a xeric site: which matters more? A dual isotope approach. *New Phytologist* **210**: 108–121.

Good SP, Noone D, Kurita N, Benetti M, Bowen GJ (2015a) D/H isotope ratios in the global hydrologic cycle. *Geophysical Research Letters* **42**: 5042–5050.

Good SP, Noone D, Bowen G (2015b) Hydrologic connectivity constrains partitioning of global terrestrial water fluxes. *Science* **349**: 175–177.

Grams TEE, Kozovits AR, Häberle KH, Matyssek R, Dawson TE (2007) Combining δ^{13}C and δ^{18}O analyses to unravel competition, CO_2 and O_3 effects on the physiological performance of different-aged trees. *Plant, Cell & Environment* **30**: 1023–1034.

Guerrieri R, Belmecheri S, Ollinger SV, Asbjornsen H, Jennings K, Xiao J, Stocker BD, Martin M, Hollinger DY, Bracho-Garrillo R, Clark K, Dore S, Kolb T, Munger JW, Novick K, Richardson AD (2019) Disentangling the role of photosynthesis and stomatal conductance on rising forest water-use efficiency. *Proceedings of the National Academy of Sciences* **116**: 16,909–16,914.

Hafner P, Robertson I, McCarroll D, Loader NJ, Gagen M, Bale RJ, Jungner H, Sonninen E, Hilasvuori E, Levanič T (2011) Climate signals in the ring widths and stable carbon, hydrogen and oxygen isotopic composition of *Larix decidua* growing at the forest limit in the southeastern European Alps. *Trees* **25**: 1141–1154.

Haigler CH, Ivanova-Datcheva M, Hogan PS, Salnikov VV, Hwang S, Martin K, Delmer DP (2001) Carbon partitioning to cellulose synthesis. *Plant Molecular Biology* **47**: 29–51.

Helliker BR, Ehleringer JR (2000) Establishing a grassland signature in veins: ^{18}O in the leaf water of C_3 and C_4 grasses. *Proceedings of the National Academy of Sciences* **97**: 7894–7898.

Helliker BR, Ehleringer JR (2002a) Differential ^{18}O enrichment of leaf cellulose in C_3 *versus* C_4 grasses. *Functional Plant Biology* **29**: 435–442.

Helliker BR, Ehleringer JR (2002b) Grass blades as tree rings: environmentally induced changes in the oxygen isotope ratio of cellulose along the length of grass blades. *New Phytologist* **155**: 417–424.

Hemming D, Fritts H, Leavitt S, Wright W, Long A, Shashkin A (2001) Modelling tree-ring δ^{13}C. *Dendrochronologia* **19**: 23–38.

Hepp J, Tuthorn M, Zech R, Mügler I, Schlütz F, Zech W, Zech M (2015) Reconstructing lake evaporation history and the isotopic composition of precipitation by a coupled δ^{18}O–δ^{2}H biomarker approach. *Journal of Hydrology* **529**: 622–631.

Heyng AM, Mayr C, Lücke A, Moschen R, Wissel H, Striewski B, Bauersachs T (2015) Middle and Late Holocene paleotemperatures reconstructed from oxygen isotopes and GDGTs of sediments from Lake Pupuke, New Zealand. *Quaternary International* **374**: 3–14.

Hill SA, Waterhouse JS, Field EM, Switsur VR, Ap Rees T (1995) Rapid recycling of triose phosphates in oak stem tissue. *Plant, Cell & Environment* **18**: 931–936.

Hirl RT, Schnyder H, Ostler U, Schäufele R, Schleip I, Vetter SH, Auerswald K, Baca Cabrera JC, Wingate L, Barbour MM, Ogée J (2019) The ^{18}O ecohydrology of a grassland ecosystem – predictions and observations. *Hydrology and Earth System Sciences* **23**: 2581–2600.

Hirl RT, Ogée J, Ostler U, Schäufele R, Baca Cabrera JC, Zhu J, Schleip I, Wingate L, Schnyder H (2020) Temperature-sensitive biochemical ^{18}O-fractionation and humidity-dependent attenuation factor are needed to predict δ^{18}O of cellulose from leaf water in a grassland ecosystem. *New Phytologist*. https://doi.org/10.1111/nph.17111.

Holloway-Phillips M, Cernusak LA, Barbour M, Song X, Cheesman A, Munksgaard N, Stuart-Williams H, Farquhar GD (2016) Leaf vein fraction influences the Péclet effect and ^{18}O enrichment in leaf water. *Plant, Cell & Environment* **39**: 2414–2427.

IPCC (2013) Climate Change 2013: The Physical Science Basis. Contribution of Working Group I to the Fifth Assessment Report of the Intergovernmental Panel on Climate Change [Stocker TF, Qin D, Plattner G-K, Tignor M, Allen SK, Boschung J, Nauels A, Xia Y, Bex V, Midgley PM (eds)]. Cambridge University Press, Cambridge, United Kingdom and New York, NY, USA.

Jasechko S, Sharp ZD, Gibson JJ, Birks SJ, Yi Y, Fawcett PJ (2013) Terrestrial water fluxes dominated by transpiration. *Nature* **496**: 347–350.

Jenkinson DS, Potts JM, Perry JN, Barnett V, Coleman K, Johnston AE (1994) Trends in herbage yields over the last century on the Rothamsted Long-term Continuous Hay Experiment. *The Journal of Agricultural Science* **122**: 365–374.

Kahmen A, Simonin K, Tu KP, Merchant A, Callister A, Siegwolf R, Dawson TE, Arndt SK (2008) Effects of environmental parameters, leaf physiological properties and leaf water relations on leaf water δ^{18}O enrichment in different *Eucalyptus* species. *Plant, Cell & Environment* **31**: 738–751.

Kahmen A, Sachse D, Arndt SK, Tu KP, Farrington H, Vitousek PM, Dawson TE (2011) Cellulose δ^{18}O is an index of leaf-to-air vapor pressure difference (VPD) in tropical plants. *Proceedings of the National Academy of Sciences* **108**: 1981–1986.

Kahmen A, Schefuß E, Sachse D (2013a) Leaf water deuterium enrichment shapes leaf wax *n*-alkane δD values of angiosperm plants I: Experimental evidence and mechanistic insights. *Geochimica et Cosmochimica Acta* **111**: 39–49.

Kahmen A, Hoffmann B, Schefuß E, Arndt SK, Cernusak LA, West JB, Sachse D (2013b) Leaf water deuterium enrichment shapes leaf wax *n*-alkane δD values of angiosperm plants II: Observational evidence and global implications. *Geochimica et Cosmochimica Acta* **111**: 50–63.

Kannenberg SA, Fiorella RP, Anderegg WRL, Monson RK, Ehleringer JR (2020) Seasonal and diurnal trends in progressive isotope enrichment along needles in two pine species. *Plant, Cell & Environment*. https://doi.org/10.1111/pce.13915.

Keel SG, Joos F, Spahni R, Saurer M, Weigt RB, Klesse S (2016) Simulating oxygen isotope ratios in tree ring cellulose using a dynamic global vegetation model. *Biogeosciences* **13**: 3869–3886.

Keitel C, Adams MA, Holst T, Matzarakis A, Mayer H, Rennenberg H, Geßler A (2003) Carbon and oxygen isotope composition of organic compounds in the phloem sap provides a short-term measure for stomatal conductance of European beech (*Fagus sylvatica* L.). *Plant, Cell & Environment* **26**: 1157–1168.

Kemp DR (1980) The location and size of the extension zone of emerging wheat leaves. *New Phytologist* **84**: 729–737.

Köhler IH, Poulton PR, Auerswald K, Schnyder H (2010) Intrinsic water-use efficiency of temperate seminatural grassland has increased since 1857: an analysis of carbon isotope discrimination of herbage from the Park Grass Experiment. *Global Change Biology* **16**: 1531–1541.

Köhler IH, Macdonald A, Schnyder H (2012) Nutrient supply enhanced the increase in intrinsic water-use efficiency of a temperate seminatural grassland in the last century. *Global Change Biology* **18**: 3367–3376.

Köhler IH, Macdonald AJ, Schnyder H (2016) Last-century increases in intrinsic water-use efficiency of grassland communities have occurred over a wide range of vegetation composition, nutrient inputs, and soil pH. *Plant Physiology* **170**: 881–890.

Kimball BA (2016) Crop responses to elevated CO_2 and interactions with H_2O, N, and temperature. *Current Opinion in Plant Biology* **31**: 36–43.

Kulmatiski A, Beard KH (2013) Root niche partitioning among grasses, saplings, and trees measured using a tracer technique. *Oecologia* **171**: 25–37.

Kulmatiski A, Beard KH, Stark JM (2006) Exotic plant communities shift water-use timing in a shrub-steppe ecosystem. *Plant and Soil* **288**: 271–284.

Labuhn I, Daux V, Pierre M, Stievenard M, Girardclos O, Féron A, Genty D, Masson-Delmotte V, Mestre O (2014) Tree age, site and climate controls on tree ring cellulose $\delta^{18}O$: A case study on oak trees from south-western France. *Dendrochronologia* **32**: 78–89.

Lai CT, Ometto JPHB, Berry JA, Martinelli LA, Domingues TF, Ehleringer JR (2008) Life form-specific variations in leaf water oxygen-18 enrichment in Amazonian vegetation. *Oecologia* **157**: 197–210.

Lalonde S, Tegeder M, Throne-Holst M, Frommer WB, Patrick JW (2003) Phloem loading and unloading of sugars and amino acids. *Plant, Cell & Environment* **26**: 37–56.

Leakey ADB, Ainsworth EA, Bernacchi CJ, Rogers A, Long SP, Ort DR (2009) Elevated CO_2 effects on plant carbon, nitrogen, and water relations: six important lessons from FACE. *Journal of Experimental Botany* **60**: 2859–2876.

Leaney FW, Osmond CB, Allison GB, Ziegler H (1985) Hydrogen-isotope composition of leaf water in C_3 and C_4 plants: its relationship to the hydrogen-isotope composition of dry matter. *Planta* **164**: 215–220.

Lehmann MM, Gamarra B, Kahmen A, Siegwolf RTW, Saurer M (2017) Oxygen isotope fractionations across individual leaf carbohydrates in grass and tree species. *Plant, Cell & Environment* **40**: 1658–1670.

Lian X, Piao S, Huntingford C, Li Y, Zeng Z, Wang X, Ciais P, McVicar TR, Peng S, Ottlé C, Yang H, Yang Y, Zhang Y, Wang T (2018) Partitioning global land evapotranspiration using CMIP5 models constrained by observations. *Nature Climate Change* **8**: 640–646.

Libby LM, Pandolfi LJ, Payton PH, Marshall J, Becker B, Giertz-Sienbenlist V (1976) Isotopic tree thermometers. *Nature* **261**: 284–288.

Lin G, Sternberg LdSL (1993) Hydrogen isotopic fractionation by plant roots during water uptake in coastal wetland plants. In: Ehleringer JR, Hall AE, Farquhar GD (eds) Stable isotopes and plant carbon-water relations, Academic Press, San Diego, California, USA, pp 497–510.

Lin Y, Horita J (2016) An experimental study on isotope fractionation in a mesoporous silica-water system with implications for vadose-zone hydrology. *Geochimica et Cosmochimica Acta* **184**: 257–271.

Lin Y, Horita J, Abe O (2018) Adsorption isotope effects of water on mesoporous silica and alumina with implications for the land-vegetation-atmosphere system. *Geochimica et Cosmochimica Acta* **223**: 520–536.

Liu HT, Gong XY, Schäufele R, Yang F, Hirl RT, Schmidt A, Schnyder H (2016) Nitrogen fertilization and $\delta^{18}O$ of CO_2 have no effect on ^{18}O-enrichment of leaf water and cellulose in *Cleistogenes squarrosa* (C_4) – is VPD the sole control? *Plant, Cell & Environment* **39**: 2701–2712.

Liu HT, Schäufele R, Gong XY, Schnyder H (2017a) The $\delta^{18}O$ and $\delta^{2}H$ of water in the leaf growth-and-differentiation zone of grasses is close to source water in both humid and dry atmospheres. *New Phytologist* **214**: 1423–1431.

Liu HT, Yang F, Gong XY, Schäufele R, Schnyder H (2017b) An oxygen isotope chronometer for cellulose deposition: the successive leaves formed by tillers of a C_4 perennial grass. *Plant, Cell & Environment* **40**: 2121–2132.

Loucos KE, Simonin KA, Song X, Barbour MM (2015) Observed relationships between leaf $H_2{}^{18}O$ Péclet effective length and leaf hydraulic conductance reflect assumptions in Craig-Gordon model calculations. *Tree Physiology* **35**: 16–26.

Luz B, Barkan E, Yam R, Shemesh A (2009) Fractionation of oxygen and hydrogen isotopes in evaporating water. *Geochimica et Cosmochimica Acta* **73**: 6697–6703.

Ma WT, Tcherkez G, Wang XM, Schäufele R, Schnyder H, Yang Y, Gong XY (2020) Accounting for mesophyll conductance substantially improves ^{13}C-based estimates of intrinsic water-use efficiency. *New Phytologist*. https://doi.org/10.1111/nph.16958.

Majoube M (1971) Fractionnement en oxygène 18 et en deutérium entre l'eau et sa vapeur. *Journal de Chimie Physique* **68**: 1423–1436.

Maurice I, Gastal F, Durand JL (1997) Generation of form and associated mass deposition during leaf development in grasses: a kinematic approach for non-steady growth. *Annals of Botany* **80**: 673–683.

Mayr C, Lücke A, Wagner S, Wissel H, Ohlendorf C, Haberzettl T, Oehlerich M, Schäbitz F, Wille M, Zhu J, Zolitschka B (2013) Intensified southern hemisphere westerlies regulated atmospheric CO_2 during the last deglaciation. *Geology* **41**: 831–834.

Mayr C, Laprida C, Lücke A, Martín RS, Massaferro J, Ramón-Mercau J, Wissel H (2015) Oxygen isotope ratios of chironomids, aquatic macrophytes and ostracods for lake-water isotopic reconstructions – Results of a calibration study in Patagonia. *Journal of Hydrology* **529**: 600–607, advances in Paleohydrology Research and Applications.

McDonnell JJ (2014) The two water worlds hypothesis: ecohydrological separation of water between streams and trees? *WIREs Water* **1**: 323–329.

Merlivat L (1978) Molecular diffusivities of $H_2{}^{16}O$, $HD^{16}O$, and $H_2{}^{18}O$ in gases. *The Journal of Chemical Physics* **69**: 2864–2871.

Miner GL, Bauerle WL, Baldocchi DD (2017) Estimating the sensitivity of stomatal conductance to photosynthesis: a review. *Plant, Cell & Environment* **40**: 1214–1238.

Mook WG (2000) Environmental isotopes in the hydrological cycle. Principles and applications, Vol. I, Introduction: Theory, Methods, Review. UNESCO, IHP-V, Technical Documents in Hydrology, 39, Paris, France.

Moreno-Gutiérrez C, Barberá GG, Nicolás E, De Luis M, Castillo VM, Martínez-Fernández F, Querejeta JI (2011) Leaf δ^{18}O of remaining trees is affected by thinning intensity in a semiarid pine forest. *Plant, Cell & Environment* **34**: 1009–1019.

Moreno-Gutiérrez C, Dawson TE, Nicolás E, Querejeta JI (2012) Isotopes reveal contrasting water use strategies among coexisting plant species in a Mediterranean ecosystem. *New Phytologist* **196**: 489–496.

Nippert JB, Knapp AK (2007a) Linking water uptake with rooting patterns in grassland species. *Oecologia* **153**: 261–272.

Nippert JB, Knapp AK (2007b) Soil water partitioning contributes to species coexistence in tallgrass prairie. *Oikos* **116**: 1017–1029.

Ogée J (2000) Développement et applications du modèle MuSICA: étude des échanges gazeux d'eau et de carbone entre une pinède landaise et l'atmosphère. PhD thesis, Université Paul Sabatier – Toulouse III, Toulouse.

Ogée J, Brunet Y, Loustau D, Berbigier P, Delzon S (2003) *MuSICA*, a CO_2, water and energy multilayer, multileaf pine forest model: evaluation from hourly to yearly time scales and sensitivity analysis. *Global Change Biology* **9**: 697–717.

Ogée J, Cuntz M, Peylin P, Bariac T (2007) Non-steady-state, non-uniform transpiration rate and leaf anatomy effects on the progressive stable isotope enrichment of leaf water along monocot leaves. *Plant, Cell & Environment* **30**: 367–387.

Ogée J, Barbour MM, Wingate L, Bert D, Bosc A, Stievenard M, Lambrot C, Pierre M, Bariac T, Loustau D, Dewar RC (2009) A single-substrate model to interpret intra-annual stable isotope signals in tree-ring cellulose. *Plant, Cell & Environment* **32**: 1071–1090.

Ostler U, Schleip I, Lattanzi FA, Schnyder H (2016) Carbon dynamics in aboveground biomass of co-dominant plant species in a temperate grassland ecosystem: same or different? *New Phytologist* **210**: 471–484.

Penchenat T, Vimeux F, Daux V, Cattani O, Viale M, Villalba R, Srur A, Outrequin C (2020) Isotopic equilibrium between precipitation and water vapor in Northern Patagonia and its consequences on $\delta^{18}O_{cellulose}$ estimate. *Journal of Geophysical Research: Biogeosciences* **125**: e2019JG005,418.

Pendall E, Williams DG, Leavitt SW (2005) Comparison of measured and modeled variations in piñon pine leaf water isotopic enrichment across a summer moisture gradient. *Oecologia* **145**: 605–618.

Penna D, Hopp L, Scandellari F, Allen ST, Benettin P, Beyer M, Geris J, Klaus J, Marshall JD, Schwendenmann L, Volkmann THM, von Freyberg J, Amin A, Ceperley N, Engel M, Frentress J, Giambastiani Y, McDonnell JJ, Zuecco G, Llorens P, Siegwolf RTW, Dawson TE, Kirchner JW (2018) Ideas and perspectives: Tracing terrestrial ecosystem water fluxes using hydrogen and oxygen stable isotopes – challenges and opportunities from an interdisciplinary perspective. *Biogeosciences* **15**: 6399–6415.

Poorter H, Navas ML (2003) Plant growth and competition at elevated CO_2: on winners, losers and functional groups. *New Phytologist* **157**: 175–198.

Prechsl UE, Burri S, Gilgen AK, Kahmen A, Buchmann N (2015) No shift to a deeper water uptake depth in response to summer drought of two lowland and sub-alpine C_3-grasslands in Switzerland. *Oecologia* **177**: 97–111.

Ramírez DA, Querejeta JI, Bellot J (2009) Bulk leaf $\delta^{18}O$ and $\delta^{13}C$ reflect the intensity of intraspecific competition for water in a semi-arid tussock grassland. *Plant, Cell & Environment* **32**: 1346–1356.

Ripullone F, Matsuo N, Stuart-Williams H, Wong SC, Borghetti M, Tani M, Farquhar G (2008) Environmental effects on oxygen isotope enrichment of leaf water in cotton leaves. *Plant Physiology* **146**: 729–736.

Robertson I, Waterhouse JS, Barker AC, Carter AHC, Switsur VR (2001) Oxygen isotope ratios of oak in east England: implications for reconstructing the isotopic composition of precipitation. *Earth and Planetary Science Letters* **191**: 21–31.

Roden J, Kahmen A, Buchmann N, Siegwolf R (2015) The enigma of effective path length for ^{18}O enrichment in leaf water of conifers. *Plant, Cell & Environment* **38**: 2551–2565.

Roden JS, Ehleringer JR (1999) Hydrogen and oxygen isotope ratios of tree-ring cellulose for riparian trees grown long-term under hydroponically controlled environments. *Oecologia* **121**: 467–477.

Roden JS, Ehleringer JR (2000) There is no temperature dependence of net biochemical fractionation of hydrogen and oxygen isotopes in tree-ring cellulose. *Isotopes in Environmental and Health Studies* **36**: 303–317.

Roden JS, Farquhar GD (2012) A controlled test of the dual-isotope approach for the interpretation of stable carbon and oxygen isotope ratio variation in tree rings. *Tree Physiology* **32**: 490–503.

Roden JS, Lin G, Ehleringer JR (2000) A mechanistic model for interpretation of hydrogen and oxygen isotope ratios in tree-ring cellulose. *Geochimica et Cosmochimica Acta* **64**: 21–35.

Roland TP, Daley TJ, Caseldine CJ, Charman DJ, Turney CSM, Amesbury MJ, Thompson GJ, Woodley EJ (2015) The 5.2 ka climate event: Evidence from stable isotope and multi-proxy palaeoecological peatland records in Ireland. *Quaternary Science Reviews* **124**: 209–223.

Rothfuss Y, Javaux M (2017) Reviews and syntheses: Isotopic approaches to quantify root water uptake: a review and comparison of methods. *Biogeosciences* **14**: 2199–2224.

Royles J, Griffiths H (2015) Invited review: climate change impacts in polar regions: lessons from Antarctic moss bank archives. *Global Change Biology* **21**: 1041–1057.

Royles J, Ogée J, Wingate L, Hodgson DA, Convey P, Griffiths H (2013) Temporal separation between CO_2 assimilation and growth? Experimental and theoretical evidence from the desiccation-tolerant moss *Syntrichia ruralis*. *New Phytologist* **197**: 1152–1160.

Royles J, Amesbury MJ, Roland TP, Jones GD, Convey P, Griffiths H, Hodgson DA, Charman DJ (2016) Moss stable isotopes (carbon-13, oxygen-18) and testate amoebae reflect environmental inputs and microclimate along a latitudinal gradient on the Antarctic Peninsula. *Oecologia* **181**: 931–945.

Rozanski K, Araguás-Araguás L, Gonfiantini R (1993) Isotopic patterns in modern global precipitation. In: Swart PK, Lohmann KC, Mckenzie J, Savin S (eds) Climate change in continental isotopic records, American Geophysical Union (AGU), pp 1–36.

Sachse D, Billault I, Bowen GJ, Chikaraishi Y, Dawson TE, Feakins SJ, Freeman KH, Magill CR, McInerney FA, van der Meer MTJ, Polissar P, Robins RJ, Sachs JP, Schmidt HL, Sessions AL, White JWC, West JB, Kahmen A (2012) Molecular paleohydrology: interpreting the hydrogen-isotopic composition of lipid biomarkers from photosynthesizing organisms. *Annual Review of Earth and Planetary Sciences* **40**: 221–249.

Šantrůček J, Květoň J, Šetlík J, Bulíčková L (2007) Spatial variation of deuterium enrichment in bulk water of snowgum leaves. *Plant Physiology* **143**: 88–97.

Sauer PE, Miller GH, Overpeck JT (2001) Oxygen isotope ratios of organic matter in arctic lakes as a paleoclimate proxy: field and laboratory investigations. *Journal of Paleolimnology* **25**: 43–64.

Saurer M, Siegwolf RTW, Schweingruber FH (2004) Carbon isotope discrimination indicates improving water-use efficiency of trees in northern Eurasia over the last 100 years. *Global Change Biology* **10**: 2109–2120.

Saurer M, Spahni R, Frank DC, Joos F, Leuenberger M, Loader NJ, McCarroll D, Gagen M, Poulter B, Siegwolf RTW, Andreu-Hayles L, Boettger T, Dorado Liñán I, Fairchild IJ, Friedrich M, Gutierrez E, Haupt M, Hilasvuori E, Heinrich I, Helle G, Grudd H, Jalkanen R, Levanič T, Linderholm HW, Robertson I, Sonninen E, Treydte K, Waterhouse JS, Woodley EJ, Wynn PM, Young GHF (2014) Spatial variability and temporal trends in water-use efficiency of European forests. *Global Change Biology* **20**: 3700–3712.

Scheidegger Y, Saurer M, Bahn M, Siegwolf R (2000) Linking stable oxygen and carbon isotopes with stomatal conductance and photosynthetic capacity: a conceptual model. *Oecologia* **125**: 350–357.

Schleip I (2013) Carbon residence time in above-ground and below-ground biomass of a grazed grassland community. PhD thesis, Technische Universität München, Munich.

Schleip I, Lattanzi FA, Schnyder H (2013) Common leaf life span of co-dominant species in a continuously grazed temperate pasture. *Basic and Applied Ecology* **14**: 54–63.

Schmidt HL, Werner RA, Roßmann A (2001) ^{18}O Pattern and biosynthesis of natural plant products. *Phytochemistry* **58**: 9–32.

Schnyder H, Nelson CJ (1988) Diurnal growth of tall fescue leaf blades I. Spatial distribution of growth, deposition of water, and assimilate import in the elongation zone. *Plant Physiology* **86**: 1070–1076.

Schnyder H, Nelson CJ, Spollen WG (1988) Diurnal growth of tall fescue leaf blades II. Dry matter partitioning and carbohydrate metabolism in the elongation zone and adjacent expanded tissue. *Plant Physiology* **86**: 1077–1083.

Schnyder H, Schäufele R, Visser Rd, Nelson CJ (2000) An integrated view of C and N uses in leaf growth zones of defoliated grasses. In: Lemaire G, Hodgson J, Moraes A, Cavalho PC, Nabinger C (eds) Grassland ecophysiology and grazing ecology, CAB International, Cambridge, UK, pp 41–60.

Schnyder H, Schwertl M, Auerswald K, Schäufele R (2006) Hair of grazing cattle provides an integrated measure of the effects of site conditions and interannual weather variability on δ^{13}C of temperate humid grassland. *Global Change Biology* **12**: 1315–1329.

Schollaen K, Heinrich I, Neuwirth B, Krusic PJ, D'Arrigo RD, Karyanto O, Helle G (2013) Multiple tree-ring chronologies (ring width, δ^{13}C and δ^{18}O) reveal dry and rainy season signals of rainfall in Indonesia. *Quaternary Science Reviews* **73**: 170–181.

Shu Y, Feng X, Gazis C, Anderson D, Faiia AM, Tang K, Ettl GJ (2005) Relative humidity recorded in tree rings: A study along a precipitation gradient in the Olympic Mountains, Washington, USA. *Geochimica et Cosmochimica Acta* **69**: 791–799.

Sidorova OV, Siegwolf RTW, Saurer M, Shashkin AV, Knorre AA, Prokushkin AS, Vaganov EA, Kirdyanov AV (2009) Do centennial tree-ring and stable isotope trends of *Larix gmelinii* (Rupr.) Rupr. indicate increasing water shortage in the Siberian north? *Oecologia* **161**: 825–835.

Siegwolf RTW, Matyssek R, Saurer M, Maurer S, Günthardt-Goerg MS, Schmutz P, Bucher JB (2001) Stable isotope analysis reveals differential effects of soil nitrogen and nitrogen dioxide on the water use efficiency in hybrid poplar leaves. *New Phytologist* **149**: 233–246.

Silvertown J, Poulton P, Johnston E, Edwards G, Heard M, Biss PM (2006) The Park Grass Experiment 1856–2006: its contribution to ecology. *Journal of Ecology* **94**: 801–814.

Simonin KA, Roddy AB, Link P, Apodaca R, Tu KP, Hu J, Dawson TE, Barbour MM (2013) Isotopic composition of transpiration and rates of change in leaf water isotopologue storage in response to environmental variables. *Plant, Cell & Environment* **36**: 2190–2206.

Song X, Barbour MM, Farquhar GD, Vann DR, Helliker BR (2013) Transpiration rate relates to within- and across-species variations in effective path length in a leaf water model of oxygen isotope enrichment. *Plant, Cell & Environment* **36**: 1338–1351.

Song X, Farquhar GD, Gessler A, Barbour MM (2014) Turnover time of the non-structural carbohydrate pool influences δ^{18}O of leaf cellulose. *Plant, Cell & Environment* **37**: 2500–2507.

Song X, Loucos KE, Simonin KA, Farquhar GD, Barbour MM (2015a) Measurements of transpiration isotopologues and leaf water to assess enrichment models in cotton. *New Phytologist* **206**: 637–646.

Song X, Simonin KA, Loucos KE, Barbour MM (2015b) Modelling non-steady-state isotope enrichment of leaf water in a gas-exchange cuvette environment. *Plant, Cell & Environment* **38**: 2618–2628.

Sternberg L, Ellsworth PFV (2011) Divergent biochemical fractionation, not convergent temperature, explains cellulose oxygen isotope enrichment across latitudes. *PloS one* **6**: e28,040.

Sternberg L, Pinzon MC, Anderson WT, Jahren AH (2006) Variation in oxygen isotope fractionation during cellulose synthesis: intramolecular and biosynthetic effects. *Plant, Cell & Environment* **29**: 1881–1889.

Sternberg LdSL (1988) D/H ratios of environmental water recorded by D/H ratios of plant lipids. *Nature* **333**: 59–61.

Sternberg LdSL (2014) Comment on "Oxygen isotope ratios ($^{18}O/^{16}O$) of hemicellulose-derived sugar biomarkers in plants, soils and sediments as paleoclimate proxy I: Insight from a climate chamber experiment" by Zech et al. (2014). *Geochimica et Cosmochimica Acta* **141**: 677–679.

Sternberg LDSL, DeNiro MJ, Savidge RA (1986) Oxygen isotope exchange between metabolites and water during biochemical reactions leading to cellulose synthesis. *Plant Physiology* **82**: 423–427.

Sternberg LdSL, Anderson WT, Morrison K (2003) Separating soil and leaf water ^{18}O isotopic signals in plant stem cellulose. *Geochimica et Cosmochimica Acta* **67**: 2561–2566.

Sternberg LdSLO, DeNiro MJD (1983) Biogeochemical implications of the isotopic equilibrium fractionation factor between the oxygen atoms of acetone and water. *Geochimica et Cosmochimica Acta* **47**: 2271–2274.

Storkey J, Macdonald AJ, Poulton PR, Scott T, Köhler IH, Schnyder H, Goulding KWT, Crawley MJ (2015) Grassland biodiversity bounces back from long-term nitrogen addition. *Nature* **528**: 401–404.

Sullivan PF, Welker JM (2007) Variation in leaf physiology of *Salix arctica* within and across ecosystems in the High Arctic: test of a dual isotope ($\Delta^{13}C$ and $\Delta^{18}O$) conceptual model. *Oecologia* **151**: 372–386.

Szejner P, Clute T, Anderson E, Evans MN, Hu J (2020) Reduction in lumen area is associated with the $\delta^{18}O$ exchange between sugars and source water during cellulose synthesis. *New Phytologist* **226**: 1583–1593.

Tankari M, Wang C, Zhang X, Li L, Soothar R, Ma H, Xing H, Yan C, Zhang Y, Liu F, Wang Y (2019) Leaf gas exchange, plant water relations and water use efficiency of *Vigna unguiculata* L. Walp. inoculated with rhizobia under different soil water regimes. *Water* **11**: 498.

Thompson AJ, Andrews J, Mulholland BJ, McKee JMT, Hilton HW, Horridge JS, Farquhar GD, Smeeton RC, Smillie IRA, Black CR, Taylor IB (2007) Overproduction of abscisic acid in tomato increases transpiration efficiency and root hydraulic conductivity and influences leaf expansion. *Plant Physiology* **143**: 1905–1917.

Treydte KS, Schleser GH, Helle G, Frank DC, Winiger M, Haug GH, Esper J (2006) The twentieth century was the wettest period in northern Pakistan over the past millennium. *Nature* **440**: 1179–1182.

Ueta A, Sugimoto A, Iijima Y, Yabuki H, Maximov TC, Velivetskaya TA, Ignatiev AV (2013) Factors controlling diurnal variation in the isotopic composition of atmospheric water vapour observed in the taiga, eastern Siberia. *Hydrological Processes* **27**: 2295–2305.

Ulrich DEM, Still C, Brooks JR, Kim Y, Meinzer FC (2019) Investigating old-growth ponderosa pine physiology using tree-rings, δ^{13}C, δ^{18}O, and a process-based model. *Ecology* **100**: e02,656.

Vargas AI, Schaffer B, Yuhong L, Sternberg LdSL (2017) Testing plant use of mobile vs immobile soil water sources using stable isotope experiments. *New Phytologist* **215**: 582–594.

Voelker SL, Meinzer FC (2017) Where and when does stem cellulose δ^{18}O reflect a leaf water enrichment signal? *Tree Physiology* **37**: 551–553.

Volenec JJ, Nelson CJ (1981) Cell dynamics in leaf meristems of contrasting tall fescue genotypes. *Crop Science* **21**: 381–385.

Walker CD, Richardson SB (1991) The use of stable isotopes of water in characterising the source of water in vegetation. *Chemical Geology* **94**: 145–158.

Wang XF, Yakir D (1995) Temporal and spatial variations in the oxygen-18 content of leaf water in different plant species. *Plant, Cell & Environment* **18**: 1377–1385.

Webb EA, Longstaffe FJ (2006) Identifying the δ^{18}O signature of precipitation in grass cellulose and phytoliths: Refining the paleoclimate model. *Geochimica et Cosmochimica Acta* **70**: 2417–2426.

Weigt RB, Streit K, Saurer M, Siegwolf RTW (2018) The influence of increasing temperature and CO_2 concentration on recent growth of old-growth larch: contrasting responses at leaf and stem processes derived from tree-ring width and stable isotopes. *Tree Physiology* **38**: 706–720.

Williams JHH, Collis BE, Pollock CJ, Williams ML, Farrar JF (1993) Variability in the distribution of photoassimilates along leaves of temperate Gramineae. *New Phytologist* **123**: 699–703.

Wingate L, Seibt U, Moncrieff JB, Jarvis PG, Lloyd J (2007) Variations in ^{13}C discrimination during CO_2 exchange by *Picea sitchensis* branches in the field. *Plant, Cell & Environment* **30**: 600–616.

Wingate L, Ogée J, Burlett R, Bosc A, Devaux M, Grace J, Loustau D, Gessler A (2010) Photosynthetic carbon isotope discrimination and its relationship to the carbon isotope signals of stem, soil and ecosystem respiration. *New Phytologist* **188**: 576–589.

Xia Z, Yu Z (2020) Temperature-dependent oxygen isotope fractionation in plant cellulose biosynthesis revealed by a global dataset of peat mosses. *Frontiers in Earth Science* **8**: 307.

Yakir D, DeNiro MJ (1990) Oxygen and hydrogen isotope fractionation during cellulose metabolism in *Lemna gibba* L. *Plant Physiology* **93**: 325–332.

Yakir D, DeNiro MJ, Gat JR (1990a) Natural deuterium and oxygen-18 enrichment in leaf water of cotton plants grown under wet and dry conditions: evidence for water compartmentation and its dynamics. *Plant, Cell & Environment* **13**: 49–56.

Yakir D, DeNiro MJ, Ephrath JE (1990b) Effects of water stress on oxygen, hydrogen and carbon isotope ratios in two species of cotton plants. *Plant, Cell & Environment* **13**: 949–955.

Yakir D, Berry JA, Giles L, Osmond CB (1994) Isotopic heterogeneity of water in transpiring leaves: identification of the component that controls the $\delta^{18}O$ of atmospheric O_2 and CO_2. *Plant, Cell & Environment* **17**: 73–80.

Yoshimura K, Frankenberg C, Lee J, Kanamitsu M, Worden J, Röckmann T (2011) Comparison of an isotopic atmospheric general circulation model with new quasi-global satellite measurements of water vapor isotopologues. *Journal of Geophysical Research: Atmospheres* **116**: D19,118.

Zech M, Mayr C, Tuthorn M, Leiber-Sauheitl K, Glaser B (2014a) Oxygen isotope ratios ($^{18}O/^{16}O$) of hemicellulose-derived sugar biomarkers in plants, soils and sediments as paleoclimate proxy I: Insight from a climate chamber experiment. *Geochimica et Cosmochimica Acta* **126**: 614–623.

Zech M, Mayr C, Tuthorn M, Leiber-Sauheitl K, Glaser B (2014b) Reply to the comment of Sternberg on "Zech et al. (2014) Oxygen isotope ratios ($^{18}O/^{16}O$) of hemicellulose-derived sugar biomarkers in plants, soils and sediments as paleoclimate proxy I: Insight from a climate chamber experiment. GCA 126, 614–623.". *Geochimica et Cosmochimica Acta* **141**: 680–682.

Zhu J, Lücke A, Wissel H, Mayr C, Enters D, Ja Kim K, Ohlendorf C, Schäbitz F, Zolitschka B (2014) Climate history of the Southern Hemisphere Westerlies belt during the last glacial-interglacial transition revealed from lake water oxygen isotope reconstruction of Laguna Potrok Aike (52° S, Argentina). *Climate of the Past* **10**: 2153–2169.

Danksagung

Zum Schluss gilt mein Dank all denjenigen, die zu meiner Dissertation beigetragen und mich unterstützt haben.

Allen voran möchte ich mich bei Ihnen, Herr Schnyder, bedanken, dass Sie mir die Möglichkeit gegeben haben, bei Ihnen am Lehrstuhl zu promovieren. Durch die Projekte, die ich während des Studiums unter Ihrer Betreuung durchführen durfte, haben Sie mein Interesse an der Wissenschaft geweckt und ich habe unglaublich viel von Ihnen gelernt! Vielen Dank für Ihre Unterstützung, die vielen Diskussionen, Ihre Begeisterung und Ihren Zuspruch!

I would like to thank Jérôme Ogée and Lisa Wingate for their advice and support during the past years, and for giving me the opportunity to come to Bordeaux. En particulier, je remercie Jérôme pour être mon deuxième encadrant de thèse et pour donner la possibilité de travailler avec MuSICA!

Mein Dank geht auch an alle Kollegen des Lehrstuhls für Grünlandlehre, die mich in meiner Zeit am Lehrstuhl unterstützt und begleitet haben. Ulli, vielen Dank für deine Hilfsbereitschaft und deine konstruktive Unterstützung! Juan and Jianjun, I will always remember the good time we had working together in the lab, growing, measuring and harvesting plants. Rudi, vielen Dank für deine Hilfsbereitschaft und die vielen Diskussionen. Auch allen anderen aktuellen und ehemaligen Kollegen gilt mein Dank.

5. Appendix A: Publications

The following articles are included in this thesis:

Publication 1:
Hirl RT, Schnyder H, Ostler U, Schäufele R, Schleip I, Vetter SH, Auerswald K, Baca Cabrera JC, Wingate L, Barbour MM, Ogée J (2019) The ^{18}O ecohydrology of a grassland ecosystem – predictions and observations. *Hydrology and Earth System Sciences* **23**: 2581–2600.

Publication 2:
Hirl RT, Ogée J, Ostler U, Schäufele R, Baca Cabrera JC, Zhu J, Schleip I, Wingate L, Schnyder H (2020) Temperature-sensitive biochemical ^{18}O-fractionation and humidity-dependent attenuation factor are needed to predict $\delta^{18}O$ of cellulose from leaf water in a grassland ecosystem. *New Phytologist.* https://doi.org/10.1111/nph.17111.

Publication 3:
Liu HT, Gong XY, Schäufele R, Yang F, Hirl RT, Schmidt A, Schnyder H (2016) Nitrogen fertilization and $\delta^{18}O$ of CO_2 have no effect on ^{18}O-enrichment of leaf water and cellulose in *Cleistogenes squarrosa* (C_4) – is VPD the sole control? *Plant, Cell & Environment* **39**: 2701–2712.

Publication 4:
Baca Cabrera JC, Hirl RT, Zhu J, Schäufele R, Schnyder H (2020) Atmospheric CO_2 and VPD alter the diel oscillation of leaf elongation in perennial ryegrass: compensation of hydraulic limitation by stored-growth. *New Phytologist* **227**: 1776–1789.